

UC San Diego

UC San Diego Electronic Theses and Dissertations

Title

Improving Clinical Practices in the Neonatal Intensive Care Unit: A Bioengineering Approach

Permalink

<https://escholarship.org/uc/item/1sm3w42b>

Author

Sinha, Mridu Bhashini

Publication Date

2017

Peer reviewed|Thesis/dissertation

UNIVERSITY OF CALIFORNIA, SAN DIEGO

**Improving Clinical Practices in the Neonatal Intensive Care Unit: A
Bioengineering Approach**

A dissertation submitted in partial satisfaction of the
requirements for the degree
Doctor of Philosophy

in

Bioengineering

by

Mridu Bhashini Sinha

Committee in charge:

Professor Todd P. Coleman, Chair
Professor Pedro J. Cabrales Arevalo
Professor Stephanie I. Fraley
Professor Shelly Lawrence
Professor Lawrence Prince
Professor Anita Raj

2017

Copyright
Mridu Bhashini Sinha, 2017
All rights reserved.

The dissertation of Mridu Bhashini Sinha is approved,
and it is acceptable in quality and form for publication
on microfilm and electronically:

Chair

University of California, San Diego

2017

DEDICATION

To my Family.

To my mother, who taught me that life is not about being the best, but being *your* very best. To my father, who has taught me perseverance, to love and live.

To my bother and sister, for being my role models and my best friends. To my husband, for keeping me grounded. To my grandparents and my entire extended family. Everyday, your love, support and blessings drive me to be a better human being and to contribute to our world.

EPIGRAPH

Mind is everything, you become what you think

–Buddha

TABLE OF CONTENTS

Signature Page	iii
Dedication	iv
Epigraph	v
Table of Contents	vi
List of Figures	viii
List of Tables	ix
Acknowledgements	x
Vita	xi
Abstract of the Dissertation	xii
Chapter 1	
Introduction	1
1.1 Neonatal Mortality: Overview	1
1.2 Understanding Hypoxic-Ischemic Encephalopathy(HIE)	2
1.2.1 Challenges in proving Therapeutic Hypothermia for HIE	3
1.3 Understating Sepsis	4
1.3.1 Sepsis: Challenges in the Clinics	6
1.3.2 Limitation of Gold Standard Diagnostic Blood Cul- ture Methodologies	7
1.4 Thesis	9
1.5 Acknowledgements	10
Chapter 2	
Web-Based Decision Support Tool for Identification of poten- tial candidates for Neonatal Hypothermia	11
2.1 Introduction	11
2.2 Methodology	13
2.2.1 Prototype Development	13
2.2.2 Design Consideration	14
2.2.3 Surveying Intent for Adoption	14
2.3 Results	15
2.3.1 Interface Design	15
2.3.2 Early Adoption Survey Results	18
2.4 Discussion	21

	2.5	Future work	23
	2.6	Acknowledgements	24
Chapter 3		Emerging Technologies for Sepsis Diagnostics	25
	3.1	Abstract	25
	3.2	Ideal Sepsis Diagnostics	26
	3.3	Detection from whole blood	26
	3.3.1	Modern Nucleic Acid Amplification Technologies	28
	3.3.2	Host-targeted technologies	44
	3.3.3	Amplification-Free Technology	46
	3.3.4	Machine Learning Applied to Molecular Detection Patterns and Clinical Data for Diagnosis	47
	3.4	Conclusion	49
	3.5	Acknowledgements	50
Chapter 4		Development of Universal Digital High-Resolution Melt Device	51
	4.1	Abstract	51
	4.2	Introduction	52
	4.3	Results	55
	4.4	Materials and Methods	67
	4.5	Discussion	71
	4.6	Acknowledgements	75
Chapter 5		5 Software Platform for Classification and Anomaly Detection	76
	5.1	Abstract	76
	5.2	Introduction	77
	5.3	Results	78
	5.3.1	Ramp rate dependent melt curves for enhanced classification	78
	5.3.2	Framework for Melt Curve Identification and Clas- sification	80
	5.3.3	Classification Algorithm	82
	5.3.4	Uncertainty measure and outlier detection	83
	5.4	Materials and Methods	84
	5.4.1	Data Generation and Signal Processing	84
	5.5	Discussion	86
	5.6	Acknowledgements	87
Chapter 6		Conclusion	88
References		89

LIST OF FIGURES

Figure 1.1: Global causes for neonatal mortality.	1
Figure 2.1: Iterative design methodology	14
Figure 2.2: Interpretation of ideal behavior of a birthing center provider based on CPQCC toolkit	15
Figure 2.3: Data entry and recommendation Screen	16
Figure 2.4: Additional features	16
Figure 2.5: Neurologic assessment Tool	17
Figure 2.6: Flow chart for decision support	18
Figure 2.7: Survey results	19
Figure 2.8: Perception of impact on liability for birth center providers . . .	19
Figure 2.9: Familiarity and use of CPQCC toolkit	20
Figure 3.1: Sepsis detection technologies time-to-results compared to blood culture	27
Figure 3.2: Summary sensitivity, specificity of emerging PCR based methods	37
Figure 3.3: U-dHRM process schematic	40
Figure 3.4: Comparison of the processes of the pathogen-targeted PCR- based technologies	43
Figure 4.1: Schematic of U-dHRM platform	56
Figure 4.2: Controller performance	57
Figure 4.3: Surrogate chip behavior	58
Figure 4.4: Derivative melt-curves	59
Figure 4.5: Controller performance using three temperature calibrators with known melting temperatures.	60
Figure 4.6: Intra-run variability	62
Figure 4.7: Controller performance for different ramp rates	64
Figure 4.8: Surrogate chip behavior	65
Figure 4.9: Rate dependent melt curves	66
Figure 4.10: Rate dependence of melt curves in bacteria with one melt tran- sition	67
Figure 4.11: Line fitting to estimate chip temperature	71
Figure 5.1: Difference in classification accuracy	79
Figure 5.2: Differences in melt curves at different temperature ramp rates. .	79
Figure 5.3: Framework for phenotyping using melting curves.	80
Figure 5.4: Estimated Cumulative density function for Dynamic Time warp- ing measure for all classes	81
Figure 5.5: Confusion matrix for classifying melt curves	83
Figure 5.6: Shannon Entropy measure for melt curves	84

LIST OF TABLES

Table 2.1:	Practice information of respondents	20
Table 3.1:	Emerging technologies for rapid diagnosis of infections from whole blood	28
Table 3.2:	Characteristics of studies reviewed for IRIDICA	31
Table 3.3:	Characteristics of studies reviewed for SeptiFast	33
Table 3.4:	Characteristics of studies reviewed for Sepsitest	37
Table 5.1:	Cut-offs calculated from statistical model for dynamic time warp- ing to assign outlier	82
Table 5.2:	Data set	82

ACKNOWLEDGEMENTS

Very Special Thanks to..

Todd, Shelly, Tom and Stephanie, my mentors, who were willing to bet on me. To the Coleman lab camaraderie for making this roller coaster fun and memorable and to my husband for being there every step of the way.

Co-Authors and Publishers

Chapter 1, in part has been submitted for publication as it may appear in Clinical Microbiology Review 2017. Sinha, Mridu; Jupe, Julietta; Mack, Hannah; Coleman, Todd; Lawrence, Shelly; Stephanie, Fraley. The dissertation author was the primary investigator and author of this paper.

Chapter 2, in part is currently being prepared for submission for publication of the material. Sinha, Mridu; Glass, Hannah; Shelly, Lawrence; Verma, Prachi; Bohn, Roger; Lee, Henry; Wusthoff, Courtney; Shimotake, Tom. The dissertation author was the primary investigator and author of this material.

Chapter 3, in part, is in submission for for publication as it may appear in Clinical Microbiology Review 2017. Sinha, Mridu; Jupe, Julietta; Mack, Hannah; Coleman, Todd; Lawrence, Shelly; Stephanie, Fraley. The dissertation author was the primary investigator and author of this material.

Chapter 4, in full, is in submission for publication as it may appear in Society for Laboratory Automation and Screening, 2017, Sinha, Mridu; Mack, Hannah; Coleman, Todd; Stephanie, Fraley. The dissertation author was the primary investigator and author of this material.

Chapter 5, in part is currently being prepared for submission for publication of the material. Sinha Mridu, Mack Hannah, Lawrence Shelly, Coleman Todd, Stephanie Fraley. The dissertation author was the primary investigator and author of this material.

VITA

- 2010 B. S. in Electrical Engineering, Manipal University, India
- 2012 M. S. in Electrical Engineering, University of Wisconsin-Madison
- 2017 Ph. D. in Bioengineering, University of California, San Diego

ABSTRACT OF THE DISSERTATION

**Improving Clinical Practices in the Neonatal Intensive Care Unit: A
Bioengineering Approach**

by

Mridu Bhashini Sinha

Doctor of Philosophy in Bioengineering

University of California, San Diego, 2017

Professor Todd P. Coleman, Chair

The greatest risk of childhood deaths occurs in the first few weeks of life. Two of the major concerns, birth asphyxia, and sepsis are responsible for the loss of over 2.5 million infants in this vulnerable period. Worse, the survivors are at a high risk for long-term morbidity. This doctoral research work focuses on developing screening tools to influence timely clinical decision-making for targeted treatment for such high risk-infants. First, we developed a web-based decision support tool to encourage timely initiation of therapeutic hypothermia, the only available therapy for infants at risk for brain injury due to birth asphyxia. This tool provides access to widely accepted clinical guidelines and strategies in a simplified way which can be easy to follow and access in clinical settings. Such a clinical decision support tool

can obviate some of the time and effort needed for rigorous training and refresher sessions for providers at low acuity, low volume birthing centers. Second, we developed a platform for rapid, reliable and automated identification of bloodborne pathogens responsible for neonatal sepsis using DNA melting analysis directly after digital PCR amplification. Specifically, we designed a high resolution digital melt platform with precise thermal control to accomplish reliable, high-throughput heat ramping of microfluidic chip digital PCR reactions. We characterized the sources of variability to minimize run to run variations with the system using synthetic DNA oligos. We also demonstrate the use of novel rate-dependent melt signatures for enhancing automated melt genotyping. Further, we developed software for analysis to classify melt curves and identify novel pathogens. Our hope is that in future, this platform can translate into a near-point of care, cost-effective technology for screening for sepsis.

Chapter 1

Introduction

1.1 Neonatal Mortality: Overview

Majority of under-five deaths occur in the neonatal period (0-27 day of life). In 2015, this amounted to 2.6 million deaths [1]. Globally, intrapartum complications at birth (birth asphyxia) and infection are responsible for the vast majority of these deaths [2] as shown in Figure 1.1.

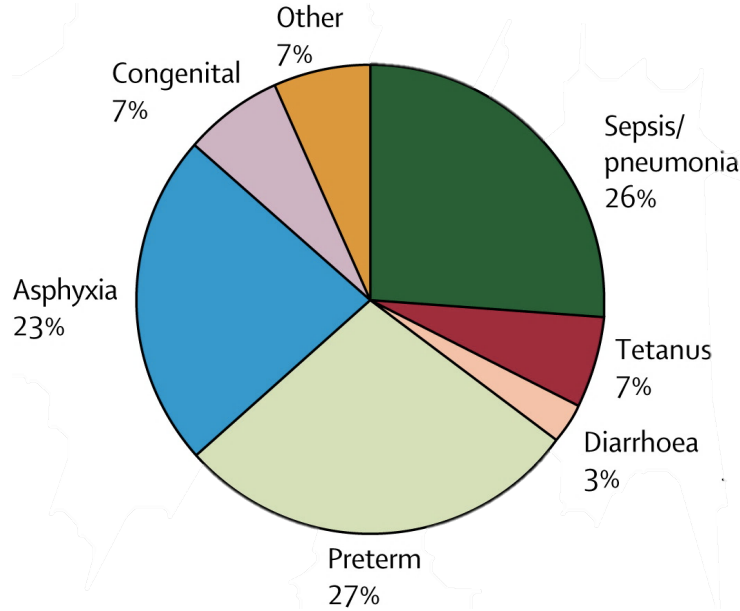


Figure 1.1: Global causes for neonatal mortality.

For both these conditions, timely identification is crucial to inform clinical decision-making. For birth asphyxia, in the event of a hypoxic-ischemic injury to the brain, therapeutic hypothermia must be provided in the first few hours of life for neuronal rescue [3]. Similarly, in the case of neonatal sepsis, targeted antimicrobial therapies must be started within few hours of contracting infection either during birth or later from the environment [4]. Failure to receive appropriate therapy leads to significant risk of morbidity and mortality. Therefore, to facilitate timely delivery of these therapies, it is crucial to have diagnostics and screening technologies that help in the early identification of at-risk infants. Further, these technologies must have the potential to scale up in low-resource settings in the low and middle-income countries where the burden of neonatal mortality is most severe. Any developmental delays and any physical and cognitive impairments among the survivors may have a higher impact on the quality of life and survival in developing countries than in the developed world, leading to significant societal and economic burden.

1.2 Understanding Hypoxic-Ischemic Encephalopathy(HIE)

Birth asphyxia or intrapartum hypoxia may interrupt the blood flow and oxygen supply to the fetal brain. This acute or intermittent insult can damage the brain tissue making the neonatal brain most important concern while managing infants with birth asphyxia [5]. Hypoxic-Ischemic Encephalopathy or HIE is used to describe such subset of cases of neonatal encephalopathy following such an intrapartum, hypoxic-ischemic event. The diagnosis of HIE relies on clinical markers such as Apgar score, labs to assess the acid-base status and clinical history of sentinel events along with the use of the Sarnat exam to assess altered consciousness, muscle tone, reflexes and seizure [6, 7]. Hypoxic Ischemic Encephalopathy(HIE) occurs in 1-3 per 1000 live births in the US [2, 8] and is one of the leading causes of neonatal mortality across the globe. HIE results in the death of 10-60% of affected infants, while 1 in 4 survivors will suffer debilitating neuro-developmental

impairment [9, 10]. These numbers are even more staggering in low and middle-income countries. The management of HIE due to perinatal asphyxia is far from satisfactory and is the single most important cause of neonatal mortality among hospital delivered infants in regions such as India and Africa. With significant associated morbidity, it adds to the socio-economic burden of proving for a disabled child which is much heavier in the developing world. The only available treatment for infants with moderate to severe HIE besides supportive care is Therapeutic Hypothermia (cooling) [11]. Meta-analysis of cooling trials indicates a reduction in adverse outcome including death or major neuro-developmental disability with a relative risk of 0.75 (95% CI 0.68-0.83) with a number needed to treat of 6-8 infants [12]. However, it is yet to be adopted in routine care most low-resource settings and remains to be a challenge even in the US, despite evidence-based medicine supporting this treatment as the standard of care for neonatal HIE. A recent study reported that 22% candidates that met treatment criteria in California were not cooled [13]. Remarkably, the risk for birth asphyxia was significantly higher and associated with around the clock, in-house pediatric or neonatology coverage, suggesting under-recognition of symptoms [14]. Therefore, timely and appropriate administration of cooling remains a challenge for skilled first responders to neonatal emergencies [15].

1.2.1 Challenges in proving Therapeutic Hypothermia for HIE

First, a majority of the birthing hospital do not provide cooling and the infants require screening and transfer to a regional cooling center within the first few hours of life. The current consensus advocates a short six-hour window of opportunity after birth for initiation of cooling. This is crucial, as the degree of energy failure in the second phase of brain injury post the hypoxic-ischemic insult, is predictive of neurodevelopmental outcome [16]. Therefore, to be beneficial, cooling must be administered after resuscitation before the beginning of second phase of brain injury [17]. Unfortunately, this six-hour window for therapy does not fit the community staffing model which lacks 24-hour extensive ob-gyn and

pediatric coverage for swift assessment and transfer. Moreover, the recognition of HIE can be challenging for birthing hospitals amidst the time pressures in the clinic as the signs and symptoms of HIE are often subtle and are somewhat similar to other likely conditions at birth, such as sepsis. Moreover, due to low incidence rates, birthing hospitals are not accustomed to performing detailed screening and a neurologic exam to identify infants who may benefit from cooling. The difficulty in acquiring new skills and going through refresher training to cater to this relatively small population at the birthing hospitals adds to the challenges. Unfortunately, infants born outside of regional cooling center account for the majority of HIE case presentations and are often associated with higher time to therapy and worse outcomes [15,18].

1.3 Understating Sepsis

Sepsis is a serious and life-threatening clinical condition that generally results from a primary bacterial infection, or less frequently from, a fungal and/or viral infection. Septic patients usually present with malaise, fever, chills, and leukocytosis, which often prompts care providers to evaluate for the presence of bacteria in the bloodstream (bacteremia) using blood culture analysis. Considered a medical emergency, bacteremia can rapidly progress to organ dysfunction and death despite immediate and aggressive medical therapies [19]. Because of the high mortality rate associated with bacteremia, the dangers of undertreating some infections, or concerns about using inappropriate antibiotics, physicians tend to order blood cultures liberally [19]. However, bacteria are isolated in only 4-12% of processed blood culture tests, and this occurs days to weeks after the patient has been treated [19–22] Alarmingly, the incidence of bloodstream infections (BSI) is increasing, with a rise of 17% in documented cases between 2000 to 2010 [23], while sepsis-related deaths have surged 31% between 1999 and 2014 [24]. In the United States, the incidence of adult bacteremia is approximately 10 per 1000 hospital admissions [25–27]. Mortality rates are associated with approximately 30,000 deaths annually with particularly high rates in critically ill patients admitted to intensive

care units (ICU) [19,23,28]. Septicemia, a severe form of bacteremia, affects nearly 1 out of every 23 hospitalized patients and is the sixth most common reason for hospitalization [23, 29]. At present, septicemia is the most expensive condition treated in U.S. hospitals with an aggregate cost of \$15.4 billion in 2009, whereas non-specific diagnoses of sepsis account for another \$23.7 billion each year [30,31]. Almost two-thirds of patients will contract their primary infection outside the hospital and the majority will have one or more pre-existing comorbidities [19]. Additionally, survivors of sepsis may experience substantial long-term complications including prolonged length of stay, discharge to a long-term care setting, or death [30]. Neonates, or infants within 28 days of life, comprise an additional at-risk group for infection due to the relative deficiency of their adaptive immune responses from lack of antigen exposure in utero as well as immaturity of innate immune responses, impairments which are directly related to their gestational age at birth. Worldwide, infectious disease is the second leading cause of neonatal mortality and results in the loss of one million newborns annually (half in the first week of life) [32, 33]. In the United States, sepsis is the fifth leading cause of neonatal mortality, surpassed only by complications related to prematurity and pregnancy [34]. Low birth weight premature infants have a 10-fold increased risk of serious infection or sepsis compared to their full-term counterparts, with a 30% mortality rate [34–36]. Devastatingly, 25% of all neonates in the U.S. admitted to the Neonatal Intensive Care Unit (NICU) will be diagnosed with sepsis and 18-35% (21,000/year) will die from their infection [32,37,38]. Pathogen detection by blood culture methods is, unfortunately, worse in this vulnerable patient population when compared to older children and adults. Although more than 60% of sepsis evaluations occur in the first three days of life, less than 1% of blood culture tests detect an organism. Even in symptomatic neonates, blood culture methodologies can detect the offending microorganism in only 10-15% after contaminants are excluded [39, 40]. This burden is worse in underserved communities. For example, in the U.S., black preterm neonates have the highest incidence of and case fatality from neonatal sepsis [41]. Around the world, neonates born in low and middle-income countries suffer the greatest rates of sepsis [42]. Critically, in low

and middle-income countries, resistant bacterial strains are implicated in the majority of the cases, highlighting the need for rapid susceptibility testing. Survivors of neonatal sepsis are at an increased risk for poor neurodevelopmental outcomes, including cerebral palsy, deafness, blindness, and cognitive delays [32,43]. A recent meta-analysis involving 977 infants reported decreased cognition, general developmental delay, and/or learning difficulties in 74% of newborns diagnosed with sepsis. Survivors of sepsis were at risk of developing cerebral palsy (36%), hearing impairments (10%), and vision impairments including blindness (32%) [44].

1.3.1 Sepsis: Challenges in the Clinics

Under-recognition of illness in addition to the emergence of resistant pathogens, delay in diagnosis, and the inability to access or afford specialized medical care contribute to the high mortality and morbidity associated with sepsis [45]. For each hour that a patient goes undiagnosed and/or is inadequately treated for sepsis, the likelihood of survival dramatically decreases [46]. For example, a 5-fold reduction in survival has been reported as a consequence of inappropriate antimicrobial therapy in the first 6 hours of recognition of septic shock [47]. Unfortunately, findings from standard diagnostic tests are not available within the critical time frame to allow focused, effective, and potentially life-saving medical interventions. Routine blood cultures can take up to one to two days to identify the offending organism but up to five days to finalize results and report antibiotic sensitivities. Other faster adjunct standard hematological analyses used in routine clinical practice have low sensitivity and specificity, particularly in neonatal patients [48]. Recently, biomarkers such as C-reactive protein, procalcitonin, and the neutrophil marker CD64 have made their way into sepsis evaluations, with limited success. Clinically, sepsis presents as a complex multifactorial syndrome, yet most diagnostic approaches that are currently employed rely on individual biomarkers, with binary yes or no answers. A diagnostic strategy that incorporates multiple biomarkers capable of signifying the host response to a pathogen, as well as pathogen and resistance identification, is greatly needed to distinguish patients who are truly septic and will benefit from antibiotic therapy. The absence of robust diagnostic tests fosters the use of broad-

spectrum antibiotics based on a clinician's best judgment and historic use instead of evidence-based medicine. In the neonatal population, clinical signs related to sepsis are similar to other non-infectious life-threatening conditions, such as perinatal asphyxia, respiratory distress syndrome, and symptoms associated with severe prematurity. Hence, the accurate diagnosis of infectious disease is imperative to limit antibiotic exposure. The reflexive utilization of broad spectrum and highly potent antibiotic treatment in patients suspected of having sepsis has contributed to the emergence of drug-resistant organisms and atypical pathogens. The correct initial choice of antibiotic therapy alone has been shown to save more lives than any other medical intervention [4, 49–51]. For these reasons, the Surviving Sepsis Campaign advocates for diagnostic identification of the pathogen within one hour of the patient's presentation to the care facility and prior to the administration of antibiotics. Additionally, integrating diagnostics that can profile antimicrobial resistance markers into the clinical workflow can assist with the appropriate use of antibiotics and hence, antibiotic stewardship. To be useful in a wide variety of clinical settings, sepsis diagnostics should also be easy to use and require low technical expertise to process samples and interpret results.

1.3.2 Limitation of Gold Standard Diagnostic Blood Culture Methodologies

Robert Koch first described the use of agar culture plates for the purification and identification of disease-causing bacteria in the early 1880s, forming the foundation of modern blood culture technology [52]. Today, the use of standard culture techniques for the detection and isolation of pathogenic organisms from a sterile body fluid is still considered the Gold Standard for the diagnosis of infection and sepsis. However, this technology can take up to five days to finalize results and is plagued by many complicating factors. First, the quantity of microbes present in circulation during a bloodstream infection is usually low, ranging only from 1 to 1×10^4 CFU/mL [43, 53–55]. In older children and adults, routine blood culture tests are drawn in timed sequences of up to four separate replicates comprising of approximately 20 to 30 mL of blood volume each. This repeat blood

sampling improves pathogen detection to capture the causative organism in 73 to 95% of cases [55–59]. Small sample volumes can, therefore, lead to false-negative results with conventional practices [60–62]. Unfortunately in neonates, especially in very low birth weight premature infants (VLBW, birth weight \leq 1500 grams), blood collection is restricted to a single sample with minimal volume (1 mL), which can further hinder pathogen capture, particularly when bacteremia is low [63–65]. False-negative results can also occur due to infectious etiologies not readily recovered by routine blood culture techniques after initiation of antibiotic therapy, which affects 28–63% of adults with suspected sepsis [55, 62, 66, 67]. Exposure to antimicrobials prior to blood culture testing is magnified in neonatal patients, as an estimated 30–35% of laboring women receive empiric intrapartum antibiotics for the prevention of neonatal Group B Streptococcus (GBS) disease [36]. Subsequently, compliance with the Centers for Disease Control and Prevention (CDC) GBS guidelines exposes an estimated 65% of VLWB infants to antibiotics prior to birth [68–70]. Prolonged delays in pathogen identification and antibiotic sensitivity testing, which can take up to 4–5 days, also cause neonates to be unnecessarily exposed to broad-spectrum antibiotics, leading to bacterial antibiotic resistance in non-infected neonates while preventing targeted antimicrobial therapy in septic neonates. Additionally, prolonged broad-spectrum antibiotics exposure in neonates can lead to invasive fungal (*Candida*) infection, necrotizing enterocolitis, and/or death [37, 38, 71]. Failure to adhere to standard antiseptic procedures during sample collection can also lead to contaminated, or false-positive, blood culture results. In 2005, The College of American Pathologists reported an overall mean blood culture contamination rate of 2.89% in 356 institutions, with 2.08% noted in neonatal and 2.92% for non-neonatal patients [72]. Contamination rates for individual institutions in this study ranged from 2.15% to 3.67% and contributed to an additional estimated cost of \$5506 per patient [72]. Thus, contaminated samples can have enormous financial and clinical ramifications in adult populations in the U.S. including 1,372 to 2,200 extra hospital days and an extra \$1.8 to \$1.9 million in medical costs each year [73, 74]. In pediatric patients, these tainted samples are associated with readmission rates of 14 - 26% [62, 75, 76] and increased length of

stay from 1 to 5.4 days [62,74,77]. In low and middle-income countries, where there is a dearth of trained medical staff and quality health care services, blood culture contamination is not uncommon and can have grave consequences. Notably, almost half of patients with false-positive blood cultures are treated with antimicrobials as compared to those with true positive test results [26,62,78,79]. Additionally, 40 - 50% of adult patients with bacteremia (and 70% with fungemia) received incorrect antimicrobial therapy during their empiric treatment period before microbiology culture results were available [23,25,80]. This misuse of antimicrobial agents and delays in pathogen identification cause prolonged exposure to broad-spectrum antibiotics, which can also result in an increased number of *Clostridium difficile* infections, antibiotic allergic reactions and drug toxicity, antimicrobial-resistant bacterial strains, prolonged length of stay, and medical costs [23,62,81–83]. In summary, routinely used blood culture methods are not an ideal Gold Standard, as the results often come too late, are incomplete or not sensitive enough, and can be misleading and relatively labor-intensive. There is a crucial unmet need to shorten as well as improve current laboratory procedures for the detection and identification of microorganisms.

1.4 Thesis

This doctoral work focuses on addressing the gaps in timely identification of at-risk newborn. In chapter 2, we discuss the development of a web-based decision support tool to encourage timely identification of neonates who may benefit from cooling. In subsequent chapters we discuss emerging technologies for screening for neonatal sepsis followed by development of one such promising technology, the universal digital high melt platform(U-dHRM). Specifically, in chapter 3, we motivate our work for developing the U-dHRM platform by including discussions on emerging technologies in light of the characteristics for an ideal sepsis diagnostic. This is followed by design and characterization of the hardware platform for our technology using synthetic DNA in Chapter 4. In the last chapter we discuss the development of software platform for identification of pathogens samples.

1.5 Acknowledgements

Disclaimer: all figures in Chapter 1 consist of at least one image, which were found through Google image search of relevant term, and were modified slightly for the purposes of this dissertation. They are not property of the dissertation author or his co-authors. Chapter 1, in part has been submitted for publication as it may appear in *Clinical Microbiology Review* 2017. Sinha, Mridu; Jupe, Julietta; Mack, Hannah; Coleman, Todd; Lawrence, Shelly; Stephanie, Fraley. The dissertation author was the primary investigator and author of this paper.

Chapter 2

Web-Based Decision Support Tool for Identification of potential candidates for Neonatal Hypothermia

2.1 Introduction

Hypoxic Ischemic Encephalopathy(HIE) occurs in 1-3 per 1000 live births in the US [2,8] and is one of the leading causes of neonatal mortality across the globe. HIE results in the death of 10-60% of affected infants, while 1 in 4 survivors will suffer debilitating neuro-developmental impairment [9,10]. The only available treatment for infants with HIE, besides supportive care, is therapeutic hypothermia (cooling therapy) [11]. Despite evidence-based medicine supporting this treatment as the standard of care for neonatal HIE, a recent study reported that 22% of neonates in California who qualified for therapeutic hypothermia did not receive it [13]. Another study paradoxically found a higher risk for birth asphyxia associated with around the clock, in-house pediatric or neonatology coverage, suggesting under-recognition of symptoms in the absence of specialty care [14]. Therefore, timely and appropriate administration of cooling remains a challenge for skilled

first responders to neonatal emergencies [15]. Many challenges may explain delays. First, cooling therapy must be initiated within 6-hour window after birth with best neurologic outcomes occurring in those with short intervals to therapy. Second, most of the birthing hospitals do not provide cooling. Hence, ill newborns must be transferred to regional cooling center if established [84]. Timely identification of neonates at risk for HIE can be challenging for the birthing hospital, since it can present with subtle signs and symptoms similar to other likely conditions at birth, such as sepsis. Moreover, due to low incidence rates, birthing hospitals are not accustomed to performing detailed screening and neurologic exam to identify infants who may benefit from cooling. The difficulty in acquiring new skills and going through refresher training to cater to this relatively small population at the birthing hospitals adds to perceived challenges. The California Perinatal Quality Care Collaborative(CPQCC) recently published the Early Screening and Identification of Candidates for Neonatal Therapeutic Hypothermia Toolkit to advocate accurate neurologic assessments and timely consultations with regional cooling centers [85]. This toolkit provides a strategic approach and reliable tools to assist birth hospitals in the timely identification of newborns that are potential candidates for therapeutic hypothermia. However, routinization of these strategies at low volume and non-tertiary birthing centers requires familiarity of current recommendations, which can be inconvenient to remember or access. Hence, we created a web-based clinical decision support tool (CoolTool) to complement the CPQCC toolkit and provide tools to assist birthing hospitals to routinize these strategies for timely and appropriate initiation of cooling. This can facilitate early screening, consultation, and initiation of cooling by providing: (1) recommendations to consult cooling center, (2) access to a database with cooling centers, (3) management guidelines, and (4) instructions for targeted neuro exam and tools for appropriate documentation. Such a clinical decision support tool can obviate some of the time and effort needed for rigorous training and refresher sessions. Moreover, CoolTool supports the goal of the CPQCC toolkit in influencing the standardization of care by promoting the use of evidence-based guidelines to facilitate timely consultation and initiation of cooling in a consistent fashion.

2.2 Methodology

We adopted a user-centered approach to developing the tool in partnership with the community [86]. Health care providers providing for newborns in community and academic birthing centers were approached for voluntary participation in the development of the tool. This included physicians and nurses in family medicine, pediatrics, neonatology, and ob-gyn across the state of California. We interviewed and observed the clinical workflow to identify the ideal target behavior and barriers to cooling. In parallel, providers were engaged through interviews and focus groups to understand the barriers to these ideal behaviors. To do so, we explored this ideal target behavior in relation to capability, opportunity and motivational components under the premise of the behavioral change wheel to develop our tool [87].

2.2.1 Prototype Development

- Paper prototype: The initial prototype was developed on paper for internal purposes and were discussed as a class project.
- Web prototype: Multiple web prototypes were developed to explore various input-output configurations and layout of the design. These were discussed at a focus group with fellows (n=12) and interviews with attendings at cooling centers (n=4). We also conducted focus groups with researchers in biomedical engineering (n=10) to get feedback on the layout.
- Neurologic assessment module was incorporated into the tool based on feedback from user interviews.
- The prototype was then iteratively modified to include protocols and guidelines with feedback from physician interviews (n=15) across five cooling centers in California. In addition, we reached out to four community centers to further iterate through the design features. Changes were made to the design based on learning from observing new users (n=15) in an iterative manner (Figure 2.1).

- Intermittently, the work was presented at local collaboratives and conferences including the Bay Area Cooling Summit Conferences, The California Association of Neonatologists Annual Cool Topics in Neonatology Meeting, and the Pediatric Academic Society (PAS) Annual Meeting [88]. At the PAS conference, the poster session allowed us to collect feedback from users from outside California (n=15) who were willing to try the tool poster-side and provide feedback.

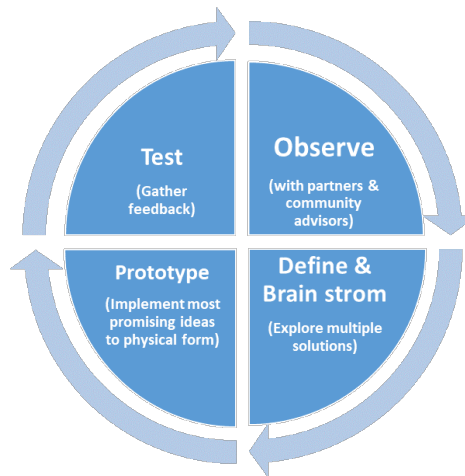


Figure 2.1: Iterative design methodology

2.2.2 Design Consideration

Ease of use with minimal training was prioritized as design criteria. Scripting for data validation and tooltips were included along with features to encourage implicit learning of initial screening criteria. Through the development process, users were observed to understand if users could navigate the tool without any prompts and recognize the design features. These guided the iterative design of the tool (Figure 2.1).

2.2.3 Surveying Intent for Adoption

To understand sentiments for adoption, we sampled cross-section of providers that were new to the Cool Tool. Users were invited by sending out a link to tool

via email.

2.3 Results

2.3.1 Interface Design

The tool breaks down the workflow into a series of checklist-like steps to standardize behavior by promoting the use of scientific knowledge correctly and consistently [89] (Figure 2.2).

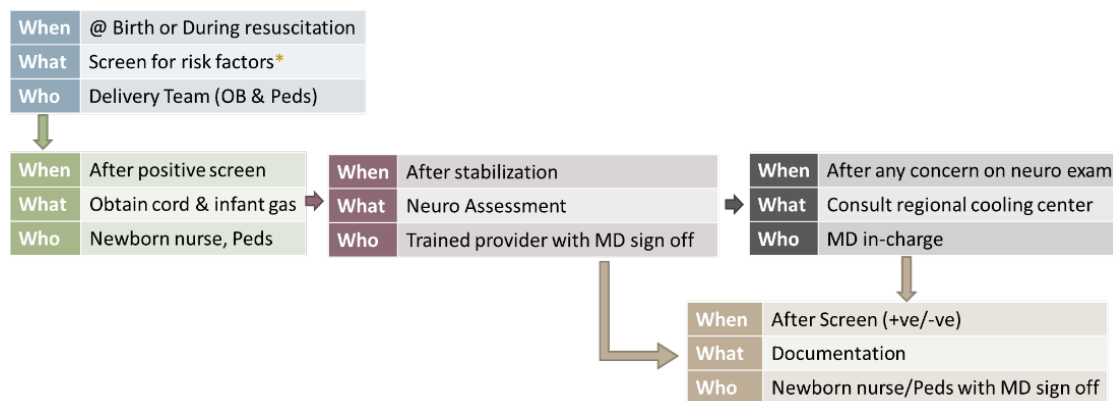


Figure 2.2: Interpretation of ideal behavior of a birthing center provider based on CPQCC toolkit

CoolTool requires users to input: (1) gestational age, (2) time of life (in hours), (3) blood gas values, and (4) history of sentinel event and resuscitation, which are routinely recorded and accessible to healthcare providers. The results are displayed in a single response screen to indicate whether the infant is at risk for HIE, is a potential cooling candidate, and suggests next steps for the patients management (Figure 2.3). If the infant is at risk, the tool highlights input variables with significant values and suggests additional lab test and neurologic assessment, as appropriate. This module guides users through the neurologic examination via an interactive tool with short example videos for assessment of consciousness, spontaneous activity, posture, tone and reflexes (gag, suck, and moro) (Figure 2.4). CoolTool also provides specific management guidelines, protocols, list of cooling center and options to include any center specific guidelines along. The interface

has tool-tips to explain the variables along with links to provide the rationale for recommendations provided by the tool (Figure 2.5). As appropriate, it presents the option to generate printable reports that can be faxed to or sent with the infant to the regional cooling center or, alternatively, for inclusion into the birth hospital chart to document initial care. Additional tabs to host resources for parents and providers were created. The tool is hosted on a domain name that is easy to remember (cooltool.info) and will be maintained by CPQCC with support from the Bay Area Cooling Summit.

Enter details below

Gestational Age >= 35wks * ? Yes No unknown

Age in Hours * ? 5

Sentinel Events ?
 Fetal Exsanguination
 Amniotic Embolus
 Maternal Cardiovascular Cr
 None of the above

Apgar @10min ? 5

Worst Cord Blood Gas ? 6.9 | 9

Infant Blood Gas within 1hr of life ?
 pH BaseDef

CPR/Epinephrine ? None

Continued need for assisted ventilation at 10 mins of life. ?
 Yes No unknown

[Change Input](#) [Determine Recommendations >>](#)

Recommendations

AT RISK; Perform further screening steps.

Suggested Actions:
1. Obtain infant gas immediately
2. Perform neurologic assessment after resuscitation.

Use [NeuroTool](#) or print form

Refer the table below for suggested action after the neurologic assessment.

Neurologic Assessment Result	Clinical Suggestions
Normal	Screens negative at this time. Symptoms may change. Continue to monitor as per CPQCC guidelines .
Mild	Call cooling center to discuss case. Provide care as per the management guidelines for potential candidates
Moderate to Severe	Call cooling center to discuss the need for transfer and cooling. Provide care as per the management guidelines for potential candidates
Incomplete Exam	Call cooling center to discuss case immediately.

[Find Regional Cooling Center](#)

If directed to cool, see [management of Cooling Candidate](#), [tip sheet](#), [passive cooling protocols](#), [flow sheet](#)

[Print Report](#)

Figure 2.3: Data entry and recommendation Screen

Cooling Centers in California

- Kaiser, Oakland
- Children's Hospital & Research...
- UC Irvine
- Lucille Packard Children Hos...
- UC Davis
- UC San Diego
- Rady Children HOSPital; San ...
- Sharp Mary Birch Hosp for W...
- Calif Pacific Med Ctr, SF
- UC San Francisco
- Santa Clara Valley MC, San J...

Refer the table below for suggested action after the neurologic assessment.

Neurologic Assessment Result	Clinical Suggestions
Normal	Screens negative at this time. Symptoms may change. Continue to monitor as per CPQCC guidelines .
Mild	Call cooling center to discuss case. Provide care as per the management guidelines for potential candidates
Moderate to Severe	Call cooling center to discuss the need for transfer and cooling. Provide care as per the management guidelines for potential candidates
Incomplete Exam	Call cooling center to discuss case immediately.

Figure 2.4: Additional features (A) Map with list of all cooling centers. (B) Protocols and management guidelines.

Neonatal Neuro Tool [Back](#)

Time of life at neuro exam: Hr Min

Seizures: No known episode EEG Confirmed Suspected/Clinical

Click to select characteristics for each row Switch to detailed view

Level of Consciousness	Normal See example	Irritable/Hyperalert	Lethargic/Obtunded See example	Stupor/Unresponsive	Cannot Assess
Spontaneous Activity	Normal	Jittery/Increased See example	Decreased	No Activity See example	Cannot Assess
Posture	Normal See example	Slight flexion/extension See example	Distal Flexion/Complete Extension See example	Decerebrate	Cannot Assess
Tone	Normal See example	Normal/Increased See example	Hypotonic See example	Flaccid See example	Cannot Assess
Suck	Normal See example	Uncoordinated	Weak See example	Absent See example	Cannot Assess
Moro	Normal See example	Exaggerated	Incomplete	Absent	Cannot Assess
Gag	Normal		Absent		Cannot Assess

Likely severity: **Moderate** Evaluate Print

Consciousness Activity Posture Tone Reflexes

Question 1 of 5 - Assess Level of Consciousness

- Normal** - opens eyes and moves with repeated tactile stimulation; appropriately wakes and falls back to sleep. [See example](#)
- Mild** - Irritable, hyperalert and/or agitated, maintains awake state, may have high pitched cry
- Moderate** - Reduced eye opening and movements to tactile stimulation. [See example](#)
- Severe** - Baby is unresponsive on only responds to painful stimuli, responses are stereotyped
- Cannot Assess**

Likely severity: **Unable to Assess** Evaluate Print

Figure 2.5: Neurologic assessment Tool. (A) Short Version (B) Long version

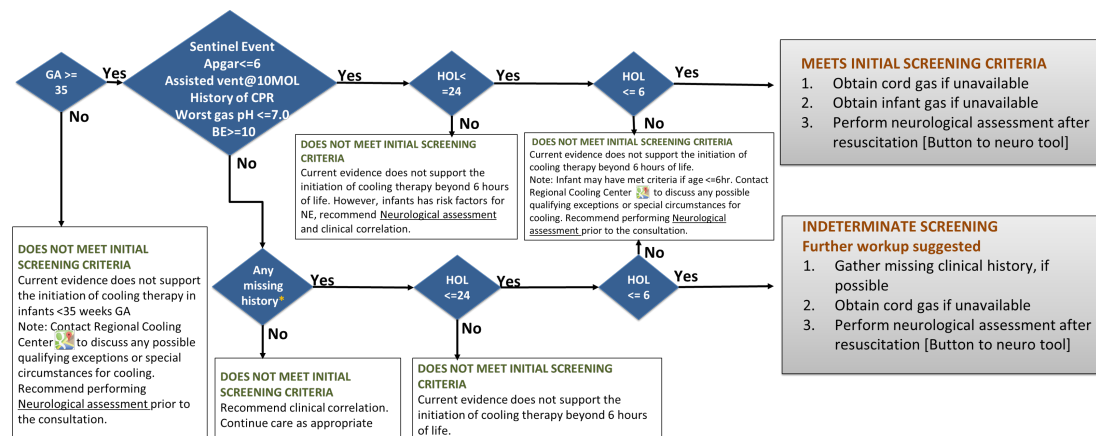


Figure 2.6: Flow chart for decision support

2.3.2 Early Adoption Survey Results

We collected survey results from 21 users from southern California across 2 cooling centers and their referring centers and 2 birthing centers in northern California (Table 2.1). The surveys collected characteristic and practice information of respondents along with ease of use of the tool and relevance and perceived impact on liability with the tool (Figure 2.7-2.9). As shown in figure 7, most users found the tool very easy (13/21) or fairly easy (6/21) to use and rated the tool good (7/21) or Very good (14/21) for utility and relevance for the tool. Interestingly most providers supported our hypothesis that Cool Tool may decrease liability for birthing center providers (13/21), however few believed that it would increase the risk/liability for birthing centers (4/21) (Figure 2.8). 71% recorded the neuro assessment tool as a useful feature.

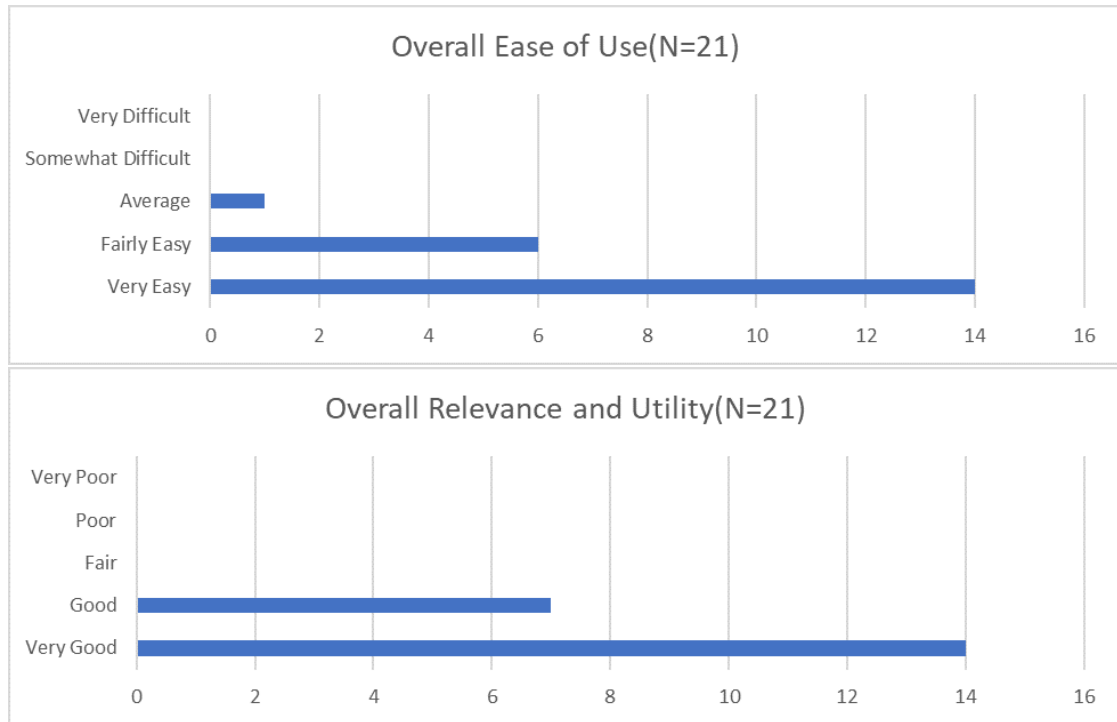


Figure 2.7: Survey results. (A) Ease of Use and (B) Overall relevance of Cool Tool

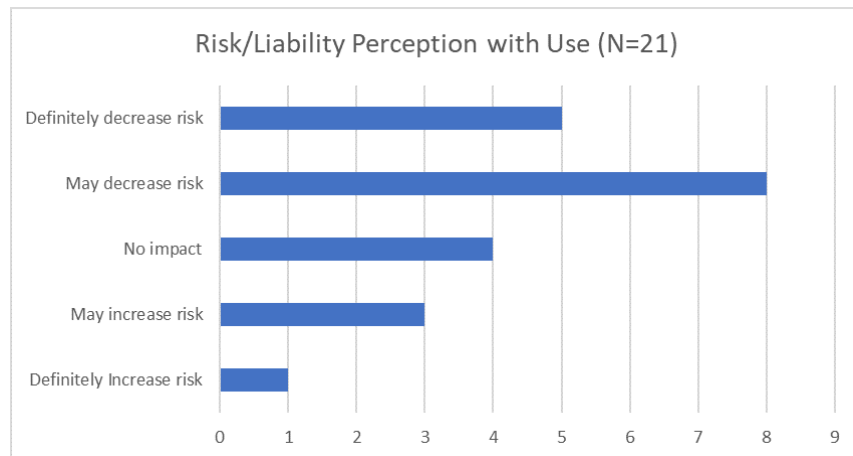


Figure 2.8: Perception of impact on liability for birth center providers

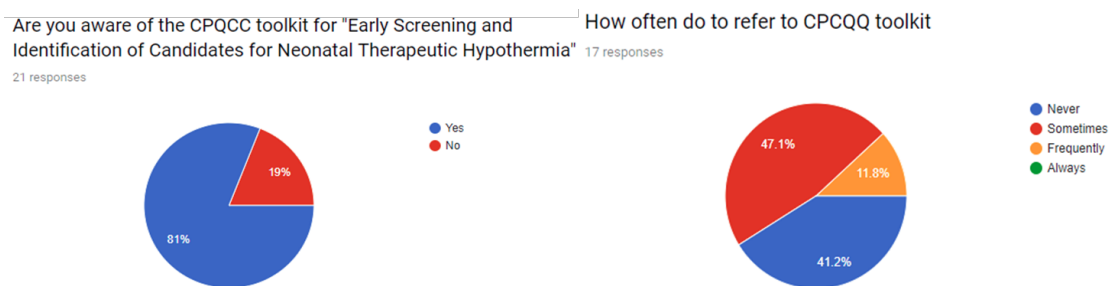


Figure 2.9: Familiarity and use of CPQCC toolkit

Table 2.1: Practice information of respondents

Variable		Users (N=21)
Medical service area	Rural	2
	Urban	19
	Frontier	0
Specialty Role	Obstetrics-gynecology	0
	Neonatology	17
	Pediatrics	3
	Family Medicine	0
	Neurology	1
Nursery Level	Level IIIB/IV	12
	Level IIIA	3
	Level II	4
	Level I	0
	Outpatient	1
Provider Role	MD/DO	20
	NP	0
	RN	1
	CNM	0
Level of training	Attending Physician	15
	Fellow	4
	Resident	1
Number of newborns seen	<10	2
	11-15	2
	16-20	5
	>20	12
Age	<30	3
	30-45	14
	>45	4

2.4 Discussion

The algorithm was largely derived from the existing CPQCC toolkit (Fig 6). However, few changes were made based on feedback from target users. Changes were made to the definitions of sentinel events for HIE based on [reference]. A neurologic assessment tool was added with options to go through a more extensive questionnaire or a simpler one screen layout based on Sarnat staging to cater to different levels of expertise/comfort with neonatal neuro exam [6]. Additionally, management guidelines were created for providers to use while waiting to establish communication with the cooling center and after establishing candidacy for cooling with the cooling center. In addition, considering the recent late hypothermia trials, we also incorporated delayed cooling in the recommendations. If any infant meeting criteria by history but is older than 6 hours, the tool advises to perform neuro exam and contact a cooling center that provides late cooling. In comparison to paper guidelines, computerized guidelines have been shown to improve adherence. In neonatology, web tools such as BlliTool [90] and Kaiser sepsis calculator [91] have shown increased adherence to the clinical guidelines and improved outcomes. Likewise, the web-based tool we developed can aid the uptake of widely accepted clinical guidelines disseminated by the CPQCC Toolkit. Here, we demonstrate that CoolTool presents the clinical guidelines in a simplified way which can be easy to follow and access in clinical settings. Since the historic randomized controlled trials that established therapeutic hypothermia as the standard of care in the mid-2000s, the clinical practice for administering cooling has changed. The inclusion criteria for therapy has broadened and often relies on clinical judgement [92]. Therefore, it is critical to balance the standardization of care and freedom to exercise clinical judgment. The CPQCC toolkit does so by providing lower acuity birthing centers with a broader criterion to screen potential cooling candidates while entrusting the final decision in the hands of the regional cooling centers. The screening criteria is based on lab values and clinical history that are routinely available, followed by a physical exam for neurologic assessment. CoolTool supports this strategy by providing a calculator for lab values, perinatal history, and neurologic assessment module to help the birthing center perform accurate neurologic examinations for

documentation and discussion with cooling centers.

The current consensus is to cool within 6 hours, however, considering the late hypothermia trials, some centers have decided to cool infants beyond six hours of age [93]. We are also now cooling more infants with mild HIE. Liberalizing lab values and cooling criterion over recent years has led to a higher emphasis on the performance of an accurate neurological exam to adequately diagnose hypoxic ischemic encephalopathy after birth. Concerns for medical-legal implication with HIE also often prevents providers from collecting cord blood gas values in at-risk infants, increasing the importance of thorough neurological exam in identifying newborns at a risk for brain injury. The module for neurologic assessment presented here can also be a valuable standalone tool for the neurologic exam of any newborn for educational purposes. Interestingly, the neuro assessment module was perceived as the most useful feature of the cool tool. Access to specific procedures and videos may improve efficacy and confidence associated with the neurologic examination. We must continue to develop these procedural instructions and help videos and evaluate their ability to improve provider skill and confidence.

CoolTool provides a general protocol for passive cooling that can be initiated at the birth hospital while awaiting transport to a higher level of care. It also provides the option to include center-specific passive cooling protocols for referral centers. Research indicates that access to specific management and transfer protocols improve infant safety and long-term outcomes [94]. Moreover, options to generate printable reports allow a more comprehensive medical chart to be compiled and transferred with the patient to a regional cooling center. The consistent use of scientific knowledge and proper documentation may also decrease liability for the birthing center. The survey suggest that the use of the tool may reduce the liability. These features of the CoolTool need to be investigated further after its dissemination, though, to determine if it performs similarly. An unintended use of this tool is for teaching the novice physician. Fellows and residents may benefit the most from the tool by referring to the standardized procedures. It has been shown that while checklist help streamline the workflow, they also help in skill building of novice users.

Lastly, dissemination of the CoolTool through the CPQCC website allows for the evaluation and validation of this tool with continual improvement based on advancement in the scientific literature. With CPQCC, we can leverage existing partnership with community centers to track outcomes. The platform can be expanded to add teaching tools and resources for sharing protocols and data among centers. It is important to highlight the need for continued development of this procedural workflow and education for familiarity with HIE. Awareness about current gaps in cooling, benchmarking to track outcomes, educational program and clinical vignettes for training and skill improvement are warranted.

2.5 Future work

The tool is currently in review by the CPQCC to align the paper toolkit and web-based CoolTool. Recommendations beyond those published in the early screening toolkit will be approved by the quality improvement committee before being published online for clinical use. Additionally, a web link may be enabled to pop up in the EMR system - suggesting the health care provider to screen for HIE based on variables routinely entered in the EMR. However, the utility of linking to the EMR remains to be evaluated. Currently, most of the birthing centers may not have access to EMR and even when present, the providers may populate the notes in EMR after a considerable amount of time. None the less, by linking to the EMR, a standard template for documentation can be provided which will help with data abstraction in future. Long-term follow-up to study changes in rates of referral is warranted. We will develop clinical vignettes for continued education and skill building along with tool dissemination. Resources for parents will be further developed to include what to expect and what to watch for to empower parents to take charge of their child's treatment and development.

2.6 Acknowledgements

Chapter 2, in part is currently being prepared for submission for publication of the material. Sinha, Mridu; Glass, Hannah; Shelly, Lawrence; Verma, Prachi; Bohn, Roger; Lee, Henry; Wusthoff, Courtney; Shimotake, Tom. The dissertation author was the primary investigator and author of this material. Authors would like to extend thanks to the Bay Area Cooling Summit, Dr. Yao Sun, Dr. Priya Jegatheesan, Dr. James McGuire, Dr. Katey Hoffman, Dr. Dawn Gano, UCSF Bridge Team, Dr. Jeff Gold, and UCSD residents for discussions and inputs on the tool design. Additional thanks to Prof. Todd Coleman, Dr. Mary J Harbert and Dr. Sheila Rosenberg. This work was supported by the Science Policy Fellows Program by the school of Global Policy and Strategy, UCSD.

Chapter 3

Emerging Technologies for Sepsis Diagnostics

3.1 Abstract

Rapid and accurate profiling of infection-causing pathogens remains a significant challenge in modern health care. Despite advances in molecular diagnostic techniques, blood culture analysis remains the gold standard for diagnosing sepsis. Yet, this method is too slow and cumbersome to significantly influence the initial management of patients. Swift initiation of precise and targeted antibiotic therapies depends on the ability of a sepsis diagnostic to capture clinically relevant organisms along with antimicrobial resistance within 1-3 hours. The administration of appropriate, narrow spectrum antibiotics demands that such a test be extremely sensitive with high negative predictive value. In addition, it should utilize small sample volumes and detect polymicrobial infections and contaminants. All of this must be accomplished in a platform that is easily integrated into the clinical workflow. In this review, we outline the limitations of routine blood culture testing and discuss how emerging sepsis technologies are converging on the characteristics of the ideal sepsis diagnostic. We include seven molecular technologies that have been validated in clinical blood specimens or mock samples using human blood. In addition, we discuss advances in machine learning technologies that use electronic

medical record data to provide contextual evaluation support for clinical decision making.

3.2 Ideal Sepsis Diagnostics

Considering the current clinical challenges and the need to impact clinical management by informing targeted treatment, the ideal technology should include the following characteristics [95, 96]:

- (a) Rapid detection, the pathogen needs to be identified in less than 3 hours [4, 46].
- (b) Broad-based detection, including bacteria, viruses, and fungi.
- (c) Minimally invasive, utilizing clinical samples with low specimen volumes. Pediatric patients including neonates: under 1mL blood [63–65].
- (d) High sensitivity and specificity for the initiation of targeted antibiotic use in the presence of signs and symptoms of systemic inflammation. The diagnostics should not compromise on sensitivity with low pathogen levels in the specimen.
- (e) Polymicrobial detection of pathogens in the presence of contaminants across a wide range of pathogen loads (1-100,000 CFU/ml blood).
- (f) Detection of drug resistance.
- (g) Integration into the clinical workflow. The process should be easy and require minimal technical expertise to process samples and interpret test results. For greatest impact, the technology must be usable in non-centralized low-resource settings.
- (h) Ability to detect unknown and emerging pathogens. Detection capabilities must be able to easily expand without compromising robustness of detection and required specimen volume.
- (i) Ability to distinguish inflammatory response as host or pathogen driven [97, 98].

3.3 Detection from whole blood

In the United States today, nearly all sepsis molecular diagnostics are post-culture technologies, meaning that a blood sample must be cultured to allow mi-

crobes to increase in number before the diagnostic test can be conducted. This initial growth-based amplification ensures sensitive detection, but extends the diagnostic timeline such that test results do not effectively impact patient management. It also restricts the breadth of organisms detected by relying on a single culture medium formulation, which cannot support the growth of all organisms. While molecular diagnostic tests are completed within 20 minutes to 2 hours, the initial step of blood culture takes days to weeks and may not be successful. Likewise, determining the antibiotic sensitivity of the pathogen also depends first on additional culture methods. Current technologies do not benefit antibiotic stewardship programs aimed at de-escalating empiric antibiotic therapy and encouraging timely targeted treatment. Recent reviews by Opota et al. [55, 99], Kothari et al. [100], Afshari et al. [101] and Ecker et al. [102], describe the state of the art for such BSI diagnostics in more detail. In this review, we will focus on emerging technologies that are not dependent upon initial microbial growth. All technologies described in the following paragraphs are summarized in Table 3.1 and their time to result in Figure 3.1.

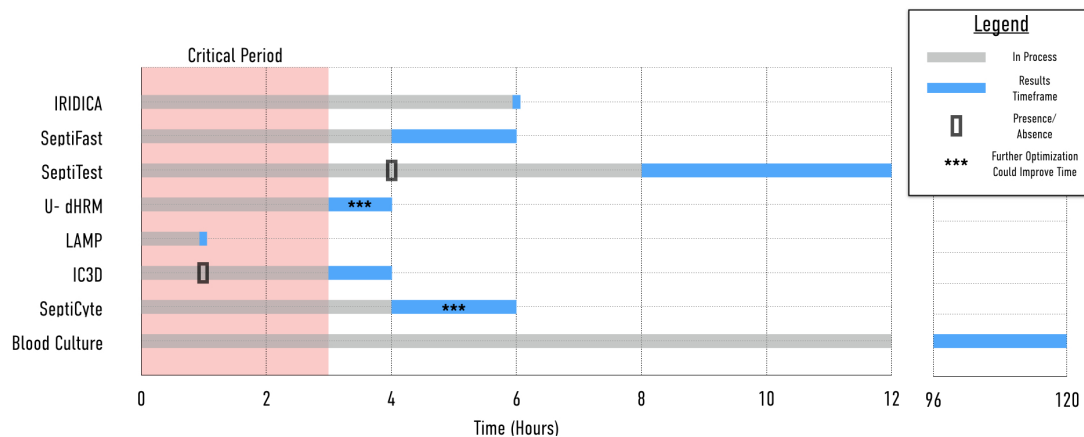


Figure 3.1: Sepsis detection technologies time-to-results compared to blood culture

Table 3.1: Emerging technologies for rapid diagnosis of infections from whole blood

Assay	Technique	Sample Volume	Sensitivity	Specificity/ Accuracy	Breadth of Detection	Polymicrobial Detection	Antibiotic resistance information	Limitations
Iridica, Plex-ID platform Abbott Molecular	Multiplex broad-range PCR/ESI-MS	5 mL	83%	94%	Currently 780 bacteria and Candida Highly expandable	Yes with semi- quantification of load, limited clinical validation	four antimicrobial resistance markers (mecA, vanA/B, and blaKPC)	Use in young children/infants due to 5 ml blood required; Detection of four antibiotic resistance markers to date
LightCycler SeptiFast Test MGRADE Roche Diagnostics	Multiplex broad range or specific primer/probe PCR/insitu Hybridization/Melt Analysis	1.5 mL	43%-80%	86%-98%	25 pathogens Low expandability	Yes, limited clinical validation	mecA antibiotic resistance gene after testing positive for Staphylococcus aureus	Detection of one antibiotic resistance marker
SepsiTest™-UMD Molzyme	Universal PCR/sequencing	1 mL (capability of processing up to 10 mL)	85%-88%	83%-86%	>345 bacteria Highly expandable	Yes, limited clinical validation	no antibiotic resistance marker	No antibiotic resistance markers
Digital high resolution melt (U-dHRM)	dPCR amplification U-dHRM Machine learning	1 mL	Single-cell	99.90%	Currently 37 bacteria Can include more bacteria, viruses and fungi Highly expandable	Resolve all organisms with absolute load quantification, need clinical validation	Can be added in the future	Automation of unexpected pathogen discovery
Oxford Nanopore MiniON Oxford Nanopore Technologies	Nanopore Sequencing	10 ng high molecular weight DNA (bacteria identification is not validated in whole blood)	About 100 copies per mL	97-100%	No integrated platform for broadbased detection Highly expandable	Potentially yes with load quantification	Potential to include	Routine implementation into clinical setting; Bioinformatic pipeline is needed for analysis; Improvement of sequence quality
LAMP technology	Loop-mediated isothermal amplification	Varies on specific LAMP technique used (~30 uL to a few mL)	Single-cell	100%	No integrated platform for broadbased detection Highly expandable	Limited	Could detect 1 antibiotic resistance gene at a time in a separate sample	Limited choice of only Bst-polymerase; Optimization of loop- primers for target detection
Integrated Comprehensive Droplet Digital Detection technology (IC 3D) Velox Biosystems	DNAzyme-based sensors droplet microencapsulation 3D particle counter system	Microliters to milliliters of diluted blood	Single-cell	n/a yet	No integrated platform for broadbased detection Highly expandable	Limited	Can be added in the future; limited by number of fluorescent channels available	Detection of only one type of bacteria per analysis
SeptiCyte Lab Immunexpress	RTq-PCR to quantify the host response of 4 RNA biomarkers Machine learning	2.5 mL	n/a (able to discriminate SIRS from sepsis with AUC ~ 0.9)	95%	All pathogens	n/a	No	Results need to be evaluated in conjunction with other clinical signs/symptoms or follow-up diagnostic devices

3.3.1 Modern Nucleic Acid Amplification Technologies

For several years, Nucleic Acid Amplification technologies (NAATs) have promised to circumvent the need for bacterial growth. These technologies function by rapidly creating copies of DNA or RNA originating from pathogen or host cells through biochemical reactions, amplifying the nucleic acid sequences to a detectable level. The sequences are then used to identify the infecting agent or the status of the immune response. However, the promise of NAATs for revolutioniz-

ing sepsis diagnosis has yet to be realized. This can be attributed to challenges in reliably capturing and amplifying pathogen nucleic acids from complex samples like blood, where the infecting agents are present at low levels or as polymicrobial mixtures within a high background of human DNA. In this sample context, traditional NAATs cannot simultaneously satisfy the need for sensitive, specific, and broad-based detection. The emerging technologies discussed herein represent novel integrations of NAATs with other cutting edge techniques that together are capable of overcoming many current diagnostic limitations. We also discuss the exciting promise that further synergistic integration holds for producing the ideal sepsis diagnostic.

IRIDICA PLEX ID (Abbott Molecular)

The IRIDICA platform boasts the most broad-based detection of any direct-from-blood emerging technology, identifying an impressive 780 bacteria and *Candida* species, as well as four antimicrobial resistance markers (*mecA*, *vanA/B*, and *blaKPC*) with a turnaround time of six hours [55, 103, 104]. IRIDICA accomplishes this by integrating multiplexed PCR amplification of pathogen DNA with electrospray ionization mass spectrometry (ESI-MS) for sequence identification. The process starts with automated DNA extraction from a 5ml whole blood sample. The extracted DNA is distributed across several PCR reactions containing different primers targeting conserved regions of pathogen genomes, including the 16S and 23S rRNA genes for bacteria and *Candida*, respectively. These primers and reaction components have been optimized to limit interference due to human DNA, which can otherwise lead to non-specific amplification or poor amplification efficiency. Amplified copies from each reaction are selectively enriched by removing over 98% of human DNA. Then, they are assessed by ESI-MS, which generates nucleotide base composition data. Finally, the data from each amplicon is compared to a library of all expected base compositions and used to triangulate the pathogen species [Figure 3.4]. [54, 105] While this approach achieves a wide breadth of detection, clinical studies show that IRIDICA's sensitivity, specificity and negative predictive value (NPV) vary widely from 45%- 83%, 69%-94%,

and 80%-97% respectively against conventional culture methods [Table 3.2, Figure 3.2]. After exclusion of possible contaminant bacteria and estimating true positives rates based on PCR test replicates or clinical chart and culture results for patient-matched specimens, sensitivity and specificity values can be improved from 77% to 91% and 87% to 99% respectively [54, 104]. Improvement with multiple test replicates suggests that sample heterogeneity and sampling error remain problematic. For the case of a low level pathogen, sampling error occurs first at the point of the blood draw, is combined with any inefficiency in nucleic acid extraction, and then occurs again when the sample is split across multiple distinct amplification reactions targeting different genes on the IRIDICA platform. Improving sensitivity and reliability of detection will require circumventing these sources of error. For the same reasons plus amplification competition, polymicrobial samples may present another challenge for this approach. Some evidence suggests that IRIDICA can detect mixed pathogen populations, but its utility in clinical samples is currently inconclusive. We found only one study that investigated polymicrobial specimens. Here, IRIDICA identified only one causative organism in four out of nine cases of blood culture positive polymicrobial infection [106]. IRIDICA has been evaluated in a limited number of clinical studies across patients with suspected sepsis, systematic inflammatory respiratory syndrome (SIRS) and febrile neutropenia [54, 104–107]. Interestingly, significant differences have been reported in sensitivity across ICU and ER patients ($p=0.005$) with higher sensitivity seen in ICU patients [104]. This may derive from higher pathogen loads in this patient population, which would have the effect of reduce sampling error. Limits of detection on the IRIDICA platform range from 0.25-128 CFU/mL for bacteria, depending on the target species, and 4 CFU/mL for *Candida* species [54, 105]. This broad-based semi-quantitative technology shows promise for use on whole blood samples (sterile or non-sterile) to detect a wide variety of pathogens. The use of 5 mL blood is promising for adult patients but limits feasibility for use in pediatric patients [108]. It can detect four antibiotic resistance markers, to date, and benefits from the ability to expand this in the future. IRIDICA is an end-to-end diagnostic solution with a structured and easy to use workflow. Individual steps

are automated, thus reducing labor and increasing efficiency. Time to detection ranges between six and eight hours with only 30 minutes of hands-on time for a batch of 6 samples [105, 106]. However, this technology fails to meet the ideal turnaround time of 1-3 hours. This technology is not yet approved by the U.S. Food and Drug Association (FDA) but is Conformit Europeenne (CE) marked, meaning that it complies with the European In-Vitro Diagnostic Devices Directive and is commercially available in Europe [?, 55, 102, 103]. However, it may fall short in non-centralized clinical settings due to dependence on multiple bulky devices and high upfront costs of about US\$200,000 [101].

Table 3.2: Characteristics of studies reviewed for IRIDICA

Study	Patient Setting	Paired Tests	Blood volume	Inclusion criteria	Against Blood Culture		
					Sensitivity	Specificity	NPV
Bacconi 2014	ICU	331	5 mL	Suspected bloodstream infection	83	93.6	98.9
Vincent 2015	ICU	616	5 mL	Suspected or proven sepsis or severe infection	81	69	97
Jordana-Lluch 2015	ICU, ER	408	5 mL	Suspected sepsis	74.8	78.6	74.1
	ICU	220	5 mL		78.4	70.8	95
Metzgar 2016	ER	285	5 mL	≥ 2 SIRS criteria for sepsis	83	72	94
Desmet 2016	Hematology	105	5 mL	Febrile neutropenia	45	93	80

ICU=Intensive Care Unit, ER=Emergency Room, SIRS=Systemic Inflammatory Response Syndrome, NPV=Negative Predictive Value

SeptiFast (Roche Diagnostics)

SeptiFast is a commercially available (in the EU), broad-based microbe identification test for whole blood [109]. It can identify over 16 bacteria, five *Candida* species, and *Aspergillus fumigatus* fungi using a 1.5 mL whole blood sample within six hours. In addition, it can detect the *mecA* antibiotic resistance gene after a sample tests positive for *Staphylococcus aureus*. The technology is CE-marked but not yet FDA approved. The SeptiFast test integrates multiplexed real-time PCR with probe hybridization and DNA melting analysis. The test begins with nucleic acid extraction from whole blood under a contamination-controlled workflow. This is followed by real-time PCR amplification using a combination of universal

and specific primers in three parallel reactions for Gram-positive bacteria, Gram-negative bacteria, and fungi [110]. The primers target the internal transcribed spacer (ITS) regions between the 16S and 23S genes for bacteria and between the 18S and 5.8S genes for fungi. PCR products are detected using species-specific probes that fluoresce in one of the four detection channels. Species identified in the same detection channel are subsequently differentiated using melting temperature analysis [Figure 3.4] [110,111]. SeptiFast has a reported sensitivity between 3 and 100 CFU per mL, depending on the microorganism [110]. A meta-analysis of 41 studies reported a summary sensitivity and specificity of 68% (95 % CI 63%73%) and 86% (95 % CI 84%89%) on a total of 10,493 SeptiFast tests compared against blood culture [112]. Another meta-analysis that included only journal publications reported slightly better overall sensitivity and specificity of 75% (95 % CI 65%83%) and 92% (95 % CI 90%95%) based on 8438 tests [113]. Recent studies show similar heterogeneous results [Table 3.3, Figure 3.2] [41,111,114–151]. These numbers improved when studies incorporated clinical markers along with blood culture results [135,136,148,152]. However, as much as 35% of the SeptiFast positive episodes were not supported by any microbiological or clinical data [120,131]. On the other hand, low sensitivity prevented SeptiFast from identifying culture-positive organisms in 20-30% of the cases [153]. SeptiFast has been reported to resolve polymicrobial infections with higher detection rates ($2 = 4.50$, $P = 0.0339$) than blood culture [143,144,154–156]. However, detection of mixed pathogens may be hindered by competing amplification due to the use of multiple specific primers and needs further investigation [148]. In summary, SeptiFast may be considered broad-based, with coverage of the 25 most relevant pathogens for sepsis, and incorporates the ability to detect mixed pathogen populations. However, it is missing pathogens that are highly relevant in neonatal sepsis. The technology considerably lowers the blood volume needed for testing compared to conventional technologies, which could be beneficial for pediatric patients [111]. However, 1.5 mL of blood is excessive for neonates, for whom samples are limited to 1mL. SeptiFast, when used with MagNA Pure (Roche) automated DNA extraction, shortens the complete workflow to 3.57 hours for eight parallel loads [126]. The diagnostic

may be of added value in the management of patients with suspected sepsis who are SeptiFast positive but blood culture negative [117,132,140,157,158]. However, low sensitivity deems negative results non-actionable. Other limitations include incomplete antibiotic resistance information and the inability to expand due to a limited number of detection channels.

Table 3.3: Characteristics of studies reviewed for SeptiFast. PCR test was compared to blood culture by identified organisms. Comparison was made by samples if data by identified organism was unavailable

Study	Patient Setting	Paired Tests	Blood volume	Inclusion criteria	Against Blood Culture		
					Sensitivity	Specificity	NPV
Louie 2008	ICU, ER, Other hospital admits	200	3 mL	Suspected BSI with ≥ 2 SIRS criteria	65.1	89.2	90.3
Mancini 2008	Hematology	103	1.5 mL	Febrile oncohaematological patients	95.2	83	98.6
Vince 2008	ICU, Hematology, Other hospital admits	36	NA	Suspected sepsis with empiric antibiotic treatment	50	71	84.6
Dierkers 2009	ICU, Surgery, Other hospital admit	101	3 mL	Suspected sepsis	60.1	82.9	87.5
Lilienfeld-Toal 2009	Hematology /Oncology	134	1 mL	Febrile neutropenia after chemotherapy	25.6	80.2	65.5
Paolucci 2009	Neonatal ICU	34	1.5 mL	Suspected late onset sepsis	75	86.7	96.3
Varani 2009	Hematology	154	1.5 or 3 mL (weight \leq or $>$ 45 kg)	Fever in immunocompromised patients	57.9	89.1	83.7
Westh 2009	NA	558	5 mL	NA	67.6	75.5	94.1
Avolio 2010	ER	144	1.5 mL	suspected BSI and \geq two SIRS criteria	69.7	90.1	87.5
Bloos 2010	ICU	236	3 mL	Suspected sepsis	79.5	74.1	94.8
Lehman 2010	ICU	453	1 mL	Clinical suspicion of severe sepsis	68.9	81.2	94.6
Maubon 2010	Hematology /Oncology	110	1.5 mL	Suspected sepsis	53.1	85.6	81.7
Obara 2011	ER, ICU	78	3 mL	Suspected BSI and \geq two SIRS criteria	91.7	84.8	98.2

ICU=Intensive Care Unit, ER=Emergency Room, SIRS=Systemic Inflammatory Response Syndrome, NPV=Negative Predictive Value

Table 3.3: Characteristics of studies reviewed for SeptiFast, Continued

Study	Patient Setting	Paired Tests	Blood volume	Inclusion criteria	Against Blood Culture		
					Sensitivity	Specificity	NPV
Tsalik 2010	ER	306	1.5 mL	Suspected infection or \geq two signs of SIRS	60.6	94.6	89.7
Wallet 2010	ICU	100	1.5 mL	Fever or Hypothermia	40	88	93.1
Yanagihara 2010	ER, ICU, Hematology, others	400	1.5 mL	Suspected of SIRS	68.7	93.7	97.2
Bravo 2011	ICU	86	1.5 mL	febrile neutropenia	48.4	78	66.7
Josefson 2011	Hospital admit	1141	1.5 mL	Suspected Sepsis	36.8	93.3	91.2
Lucignano 2011	ER, ICU Hematology	1553	>1.5 mL	Suspected sepsis in neonates and children	85	93.5	98.1
Grif 2012	ICU, Hematology /Oncology, Other hospital admit	71	1.5 mL	Suspected Sepsis	62.5	80.9	94.4
Guido 2012	Hematology	166	1.5 mL	Febrile neutropenia	91.3	88.1	98.4
Hettwer 2012	ER	119	1.5 mL	Suspected sepsis	76.4	91.9	82.6
Lodes 2012	ICU	148	1 mL	SIRS	83.3	71.1	94.4
Mauro 2012	Hematology /Oncology	79	1.5 mL	suspected of sepsis in immunocompromised patients	84.4	89.4	89.3
Pasquilani 2012	Hospital admit	391	1.5 mL	Suspected sepsis	56.1	91.6	92.4
Rath 2012	ICU	225	3 mL	Suspected sepsis after liver transplant	71.2	75.9	82.7
Tschiedel 2012	ICU	110	1.5 mL	Suspected Sepsis	63.2	84.6	91.7
Herne 2013	ICU, Other hospital admit	160	1.5 -3 mL	Suspected sepsis or septic shock	71.4	70.7	89.2

ICU=Intensive Care Unit, ER=Emergency Room, SIRS=Systemic Inflammatory Response Syndrome, NPV=Negative Predictive Value

Table 3.3: Characteristics of studies reviewed for SeptiFast, Continued

Study	Patient Setting	Paired Tests	Blood volume	Inclusion criteria	Against Blood Culture		
					Sensitivity	Specificity	NPV
Avolio 2014	ER, ICU	525	1.5 mL	suspected BSI and \geq two SIRS criteria	59.7	89.9	86.4
Burdino 2014	ICU, ER, Other hospital admit	1186	1.5 mL	SIRS	69.2	90.6	94.1
Ibarra 2015	Hospital admit	86	1 mL	clinical sepsis suspicion and those presenting a score of > 8 points on the NOSEP-1 scale in neonates	69.2	65.7	92.3
Mongelli 2015	ICU	138	1.5 mL	Bacteremia with empiric antibiotic	83.3	81.5	94.6
Tafelski 2015	ICU	78	1.5 mL	Suspected pulmonary or abdominal sepsis	58.3	74.2	90.7
Dinc 2016	ICU	78	3 mL	Suspected or diagnosed Sepsis or septic shock	70.4	50	80.4
Ratzinger 2016	Surgery, Other hospital admit	220	1.5 mL	\geq two SIRS criteria	69.4	89.7	91.2
Suberviola 2016	ICU	119	1.5 mL	Severe sepsis or septic shock	90.6	68.7	94.8
Troger 2016	Hospital admit	214	100 μ L	Late onset sepsis in VLBW neonates	58.1	59.1	80.3
Korber 2017	ICU, ER, outpatient	470	NA	Sepsis, endocarditis, fever, pneumonia and immunosuppression	73.3	88	95.3

ICU=Intensive Care Unit, ER=Emergency Room, SIRS=Systemic Inflammatory Response Syndrome, NPV=Negative Predictive Value

SepsiTest (Molzyme)

SepsiTest is a commercially available (in the EU) broad-based microbial identification test with whole blood. It can identify over 345 bacteria and 13 fungi in eight to ten hours from a 1 mL whole blood sample [159]. The technology is CE-marked and commercially available in Europe, but not yet FDA approved. SepsiTest integrates universal PCR with Sanger sequencing after a unique sample preparation step, whereby selective lysis and human DNA degradation is used to improve sensitivity [160]. After DNA is isolated, PCR is performed with a universal primer targeting the 16S and 18S rRNA genes for bacteria and fungi, respectively. Bacteremia or fungemia is reported in under four hours. Further purification followed by Sanger sequencing accomplishes species detection, which

takes an additional 4-6 hours [Figure 3.4]. SepsiT_{est} can detect as low as 10-80 CFU/mL with some organism bias [161, 162]. It has a reported sensitivity ranging from 11% to 87% and higher specificity from 85% to 96% when compared to blood culture in adult and pediatric patients with SIRS, sepsis, febrile neutropenia and infectious endocarditis [Table 3.4, Figure 3.2]. Multiple studies report promising NPV close to 97% against blood culture with detection of multiple fastidious organisms [141, 163, 164]. Similar sensitivities ranging from 37.5% to 78.6% and specificity from 86.8% to 94.4% were observed in studies adjusting for clinical context by excluding contaminants [141, 165]. Additionally, as many as 45% of PCR positive tests were reported as contaminants [165]. Pathogens detected in the mixed populations were often identified as contaminants [163, 166]. In one reported study, only one organism was identified in three of four blood culture positive polymicrobial specimens [163].

SepsiT_{est} is a broad-based test that requires a small amount of blood, appropriate for both adult and pediatric patients. It can, in principle, detect polymicrobial infections; however, its ability to inform clinical decision making needs further study. SepsiT_{est} provides the option to automate DNA extraction (SelectNA plus, Molzyme) and process up to 12 samples in one run, making it easy to integrate into the clinical workflow. However, it does not provide any information on antibiotic sensitivity. In addition, it still requires multiple steps that are not integrated into one platform, increasing the risk of contamination and turnaround time. This limits its utility for informing clinical decisions regarding targeted antimicrobial therapy. The use of Sanger sequencing is the time-limiting step for SepsiT_{est}. In the future, massively parallelized next generation sequencing technologies may enhance this approach and provide antibiotic resistance information. In the next paragraph, we provide a short summary of such an emerging sequencing technology.

Table 3.4: Characteristics of studies reviewed for SepsiT_{est}

Study	Patient Setting	Paired Tests	Blood volume	Inclusion criteria	Against BC		
					Sensitivity	Specificity	NPV
Wellington 2009	ICU, Hematology/Oncology	342	1 mL	SIRS or sepsis; hematology/oncology with febrile neutropenia; or immunodeficiency and fever	87	85.2	97.2
Kühn 2011	Surgery IE	30	1 mL	Infectious Endocarditis	85	NA	NA
Leitner 2013	Critical care	75	NA	NA	28.6	85.3	92
Loonen 2014	ER	125	1 mL	≥ 2 SIRS criteria for sepsis	11	96	80
Orszag 2014	ICU	160	1 mL	High risk patients on ECMO	78.6	88.4	97.7
Nieman 2016	ICU	236	1 mL	SIRS or suspected sepsis	33	82.9	84.7

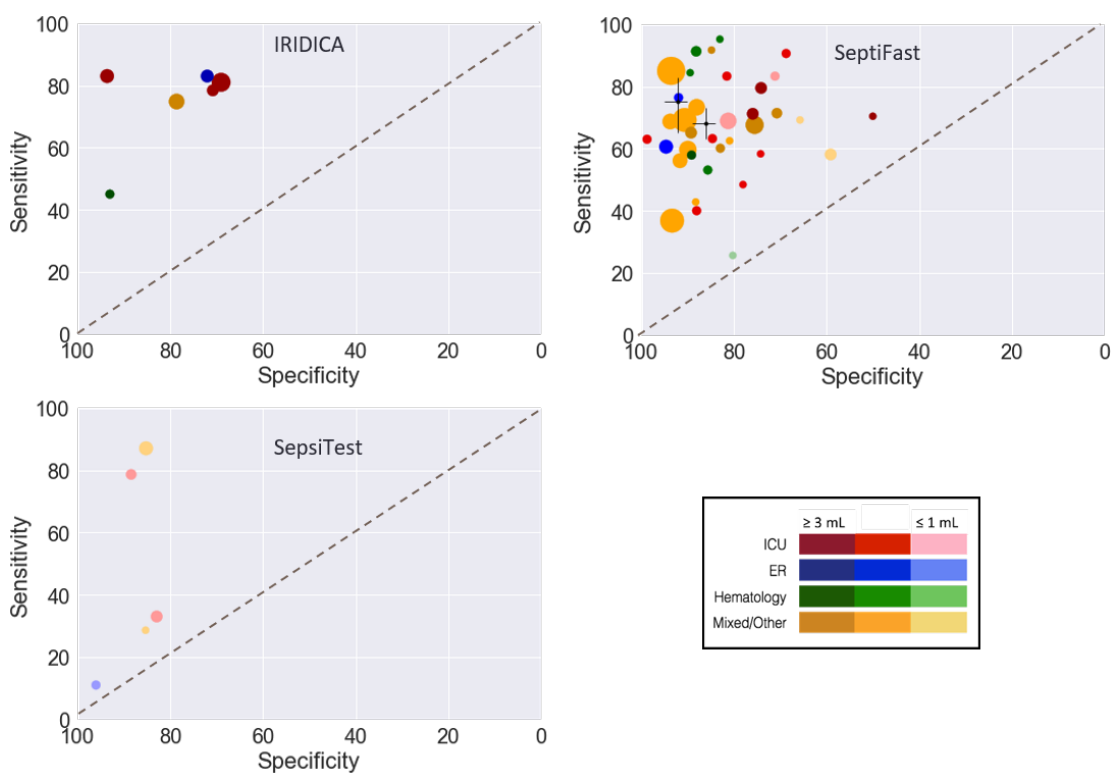


Figure 3.2: Summary sensitivity, specificity of emerging PCR based methods. Figure shows sensitivity plotted against specificity of test results compared against gold standard blood culture for IRIDICA, SeptiFast and SepsiT_{est}. Marker/symbol area is proportional to number of paired blood tests in the study. Darker shades of color signify larger blood volume used for the test. Clinical context is color coded as per the legend on bottom right. **(A)** For IRIDICA we included 6 publications found using literature search PubMed. **(B)** For SeptiFast we included paper publications from 2 meta-analysis (summary statistics from analysis shown in black, along with the confidence interval) in addition to 8 new relevant studies. **(C)** For SepsiT_{est} we included 5 publications found using literature search PubMed.

Nanopore Sequencing, MinION

The MinION by Oxford Nanopore Technologies (UK) is a portable, real-time, USB powered DNA/RNA sequencer with a 10 to 50 min library preparation step. The main advantages of the MinION platform over other Next-Generation sequencing technologies are (i) rapid turnaround; (ii) low capital cost; and (iii) small size. This technology was released to researchers for alpha testing as part of an early access program in 2014 [167,168]. It is a generic sequencing system, that has shown the potential for rapid identification of pathogens (under four hours [169]) directly from blood when combined with a PCR amplification step using the 16S Rapid Amplicon Sequencing kit [167]. Because it sequences at the single-molecule level, it offers new possibilities to study microbial diversity in clinical samples and also allows for multiplexing of samples. The technology has been validated for viral pathogen identification from 140uL whole blood in under 40 mins with 100% sensitivity and specificity [170,171]. For bacteria, it has only been validated in clinical urine and feces samples [169,171]. Polymicrobial pathogen identification has been demonstrated using genomic DNA mixtures of 20 bacterial strains in equal amounts (100,000 copies per organism per L) [172–174]. By using specific primers that amplify a wide range of bacterial 16S rRNA gene, 90% of the full-length 16S rRNA could be reconstructed with the MinION Nanopore technology. However, pathogen assignment could be completed for only 8 of the pathogens from the DNA mixture due to low sequencing coverage. This was attributed to non-optimized 16S PCR amplification, despite the use of universal primers [172]. This points to the need for optimization and validation of this technology as a complete system in whole blood. Other improvements are needed to transition MinION into the clinic. These include automation and standardized external and internal spike-in controls that run in parallel to prevent carryover contamination [175], as well as optimization of the bioinformatic pipeline used to identify organisms, resistance genes, and/or mutations [169,176,177].

Universal digital High Resolution Melt (U-dHRM)

The Universal-digital High Resolution Melt (U-dHRM) platform is a broad-based microbial identification technology used with whole blood samples. It can currently detect 37 bacterial pathogens with single organism and single genome sensitivity, as well as resolve polymicrobial infections in under four hours using less than 1 mL whole blood [178,179]. This technology is in the validation phase and is not yet commercially available. U-dHRM integrates universal digital PCR (dPCR) with high resolution melt (HRM) on a microfluidic chip to enable probe-free differentiation and quantification of bacteria within a sample [179]. The test procedure begins with DNA extraction followed by sample digitization, which separates all pathogen genomes into their own PCR reaction by spreading the sample across a microfluidic chip containing 20,000 picoliter-sized reactions. In each reaction, universal dPCR amplification takes place targeting the 16S rRNA gene. Subsequently, precise heating and simultaneous imaging are performed on all reactions to generate HRM melt curve fingerprints for each pathogen's 16S gene sequence [Figure 3.2]. HRM generates sequence specific melt curves by unwinding DNA amplicons in the presence of a fluorescent double-stranded intercalating dye [180–183]. Each distinct DNA sequence melts uniquely, generating a loss of fluorescence signature as a function of temperature that is then used for species identification [Figure 3.4]. A supervised machine learning algorithm automatically identifies the microbial species by its melt curve. U-dHRM has reported a classification accuracy of 99.9% for the 37 pathogens tested, with load quantification for individual pathogens [178]. The technology was validated in mock blood samples, demonstrating its ability to identify pathogens in the presence of excessive human DNA [179].

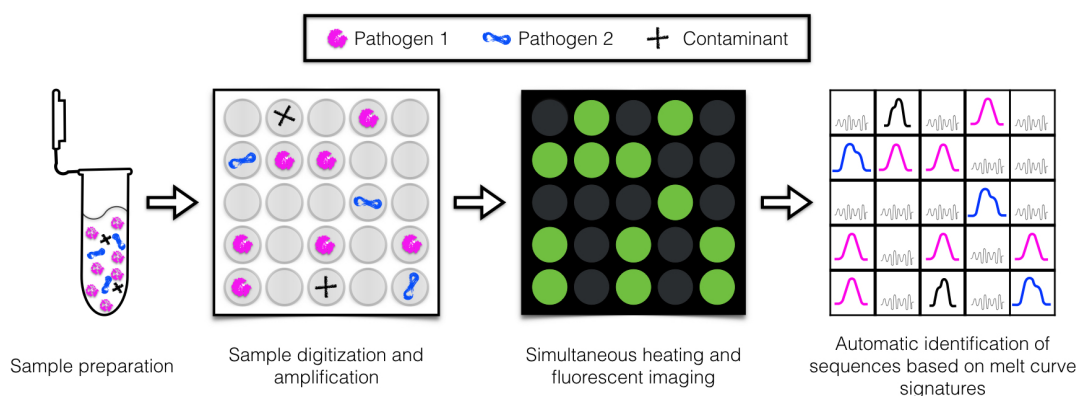


Figure 3.3: U-dHRM process schematic

U-dHRM is rapid, broad-based test to detect multiple organisms in a blood sample of less than 1mL, which is suited for pediatric patients and neonates. While it is currently limited to 37 bacteria relevant to neonatal sepsis, it has the potential to expand to include additional bacteria, fungi, and viruses in the future. Since this technology is probe-free and digitized, it has the potential to detect all sepsis-causing organisms contained in a single sample, including polymicrobial infections. Early studies show promising single genome sensitivity and 99.9% specificity, but further evaluation with clinical blood samples is needed. In addition, automation is required to accomplish a sample-to-answer time under 3 hours. The system is easy to use and can incorporate detection of antibiotic resistance determinants. Its machine learning framework provides the potential identification of new and unknown pathogens and allows for an expanding library. The speed and simplicity of U-dHRM along with its integrated technology platform suggest a promising first-pass screening method for neonatal sepsis. The technology also shows the potential to deliver at or near the point-of-care diagnosis. The possibility to move U-dHRM towards a portable, inexpensive system can be of immense value to non-centralized systems in low resource settings.

Summary of Modern Nucliec Acid Amplification Technologies

In summary, the results of clinical studies using PCR-based technologies are heterogeneous. For the most part, these results are reported in comparison with the gold standard blood culture, which is far from ideal and may contribute significantly to this heterogeneity. Blood may be drawn with varied timing, at different bodily locations, and in varying amounts for blood culture. This contributes to the challenge of validating emerging technologies against blood culture. Hence, it is important to interpret diagnostic results in conjunction with clinical context.

(i) Interpreting false positives against blood culture.

One of the major advantages of a PCR-based technology is its ability to detect non-viable, fastidious and unculturable organisms that would otherwise be missed by blood culture. A PCR-positive, blood culture negative specimen may reflect a real pathogen, yet leads to a biased lower sensitivity and specificity value of the PCR test. It should be noted that false positives could also be due to cell-free pathogen DNA circulating in the blood originating from an old or controlled infection or contamination [184]. Both IRIDICA and SepsiTesT have reported higher rates of contamination than blood culture [107, 165]. This is to be expected, since PCR tests that accomplish broad range detection capability by using universal primers are able to amplify non-viable organisms. In addition, SepsiTesT and IRIDICA involve more sample transfers steps in comparison to SeptiFast and U-dHRM [Figure 3.4]. This further increases the risk of contamination [165]. Both SeptiFast and IRIDICA use semi-quantitative methods to detect contaminants and limit false positives. SeptiFast uses a cut-off value that represents the number of PCR cycles at which DNA is adequately amplified to identify contaminants [185, 186]. IRIDICA also uses similar thresholds based on the number of genomes per well to limit contaminant and reduce false positives. However, these techniques may need further optimization as they can conversely lead to false negatives [104, 186]. Absolute load quantification in conjugation with clinical characteristics may improve diagnostic accuracy as well [185]. An emerging theme is a need for integrating quantitative results with clinical context, potentially provided by a

machine learning framework. For example, a diagnostic algorithm has been proposed that uses a patients CD64 index to determine whether to perform SepsiT_{est}. This approach showed improved detection of pathogens in patients with suspected BSI [187]. A similar approach has been suggested in conjunction with neutrophil-lymphocyte count ratio and levels of presepsin and procalcitonin [188, 189]. U-dHRM manages contamination through the use of small reaction volumes, which keeps contaminants from overwhelming low level pathogen DNA in the amplification step. This also enables absolute quantification, since each organisms genome is amplified individually, without affecting detection sensitivity [190]. It also integrates the amplification (dPCR) and detection (HRM) steps into a single closed system, which eliminates contamination due to sample transfer and reduces hands-on time [178]. Importantly, the ease of use, speed, and quantitative power of this technology could enable repeated testing to track the appearance and removal of bacterial DNA in the blood during antibiotic treatment. In combination with host inflammatory markers, such repeated testing could lend deeper insights into the progression of sepsis. Having the ability to conduct repeated testing over time could reveal novel disease dynamics that may contribute further understanding of pathogen detection inconsistencies that often arise in technology comparison studies. U-dHRM also holds promise to address the need for point of care diagnostics, whereas other commercially available PCR tests typically need bulky and expensive equipment that are not feasible for use in non-centralized systems. Advertised turnaround times for such commercially available technologies are optimistic for non-centralized and low resources settings, where sample to result time can be as high as 15.9 hours [146].

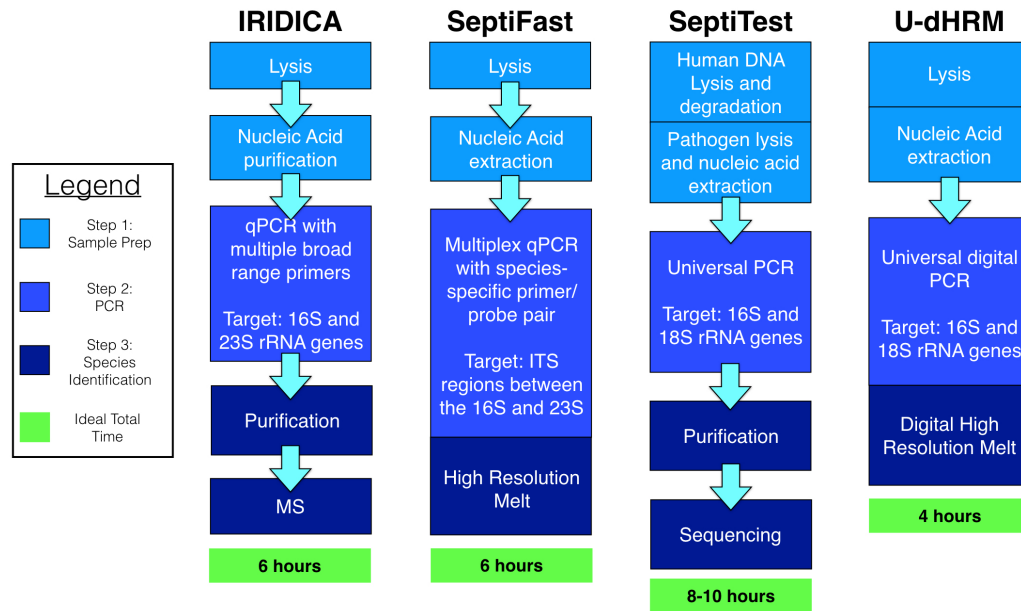


Figure 3.4: Comparison of the processes of the pathogen-targeted PCR-based technologies

(ii) Interpreting false negatives against blood culture.

While false positives may result in the inaccurate overuse of antibiotics and contribute to the generation of resistant organisms, false negatives and the inaccurate withholding of antibiotic treatment are more immediately threatening to patient welfare [191]. Accurately withholding empiric antibiotic use will require an improved sensitivity of PCR technologies (>98% negative predictive value). PCR tests can be limited in their ability to detect pathogens for a variety of reasons [191], including the need for effective lysis across a broad range of microbes, the interference of human DNA or other inhibitory substances carried over from blood into the assays, the effect of off-target interactions, and amplification bias [192,193]. It is interesting to note that even though all the above technologies rely on an initial PCR amplification step for microbe detection followed by a secondary step for species identification, they differ in their diagnostic sensitivities. The two major contributors to these differences are 1) the approach used for reducing interference from human DNA, and 2) the amplification strategy using either a single universal primer (SeptiTest, U-dHRM) or multiple broad range or species specific

primers (IRIDICA, SeptiFast), which may suffer from amplification competition [Figure 3.4]. All commercially available PCR tests have optimized their workflow to improve pathogen DNA amplification, yet none show promise to replace blood culture due to limited sensitivity in clinical specimens [Figure 3.2]. The IRIDICA platform has recently increased sample volume five-fold, from 1 mL to 5 mL, under the assumption that poor sensitivity arises from inefficient capture of pathogen in low volume blood samples. The enhanced sensitivity of U-dHRM is attributed to the diluting effect of the digital reaction format on inhibitory substances and the optimized dPCR reaction conditions ensuring amplification of single copies of bacterial DNA. U-dHRM has been shown to significantly reduce false negative error rates compared to traditional dPCR, indicating that amplification errors can be reliably identified and accounted for [178]. In addition, U-dHRM is the only test that provides absolute load quantification, to enable resolution of polymicrobial infections and contamination. Further investigation in clinical samples will determine how this approach compares with commercially available technologies.

3.3.2 Host-targeted technologies

SeptiCyte LAB (Immunexpress Inc, Seattle, Washington).

SeptiCyte LAB is the first RNA-based technology that targets specific human inflammatory markers using 2.5 mL whole blood for sepsis determination in 4-6 hours [194]. It has 510(k) clearance from U.S. Food and Drug Administration (FDA) for use as an aid in differentiating infection-positive (sepsis) from infection-negative (SIRS) systemic inflammation in critically ill patients on their first day of ICU admission. SeptiCyte LAB is a host response, reverse transcription quantitative polymerase chain reaction (RT-qPCR) based test that quantifies the relative expression levels of four RNA biomarkers (CEACAM4, LAMP1, PLA2G7, and PLAC8) known to be involved in innate immunity and host response to infection. In the discovery phase, microarray analysis was used to identify RNA biomarkers that could differentiate patients with sepsis from patients with post-surgical infection-negative systemic inflammation [195]. These biomarkers were then converted to a RT-qPCR format and used to develop the Septicyte LAB test for sep-

sis(108). SeptiCyte Lab is rapid, robust and accurate for classifying patients with infection-related sepsis across gender, race, age and date of ICU admission [195]. It is suggested to be an indicator of the probability and not the severity of sepsis [196, 197]. In a pilot study using 2.5 mL of blood, SeptiCyte LAB effectively discriminated between two groups of critically ill pediatric patients (40 children with clinical severe sepsis syndrome versus 30 children with congenital heart disease). Area-under-curve (AUC) in receiver operating characteristic (ROC) curve analysis, which describes the probability that a test will rank a positive incident higher than a negative one when chosen at random, was used to discriminate between the two cohorts. Even for different RNA analysis techniques an AUC value ≥ 0.9 was obtained (0.99 vs 0.95), indicating high accuracy. In another prospective observational study with 129 adult ICU patients, AUC of 0.88 was obtained to discriminate SIRS from sepsis. SeptiCyte Lab scores have shown the ability to classify sepsis better than individual or a combination of other clinical, demographic, and laboratory markers [198]. SeptiCyte is a promising, novel, broad-based diagnostic for sepsis. The current 4-6 hours of turnaround time can potentially be reduced to a targeted 1.5 hours by optimizing the RT-qPCR platform on which the test is implemented. One drawback is the requirement of 2.5 mL of blood, which is not feasible for use in pediatric and neonatal populations. Additionally, this test does not provide any information about the pathogen or its antibiotic resistance. More clinical studies across different patient populations are needed to confirm SeptiCyte's ability to improve outcomes in the clinic. Nonetheless, it has the potential to play a role in reducing inappropriate empirical antibiotic use, which could be of tremendous value in light of recent antibiotic resistance epidemic. Combining SeptiCyte with pathogen and resistance targeted tests that work within the same critical timeframe could generate significant synergy with the potential to enhance the overall negative predictive value of these diagnostics and their impact on antibiotic use. Further, such combined approaches may deepen our understanding of the progression of infection related sepsis.

3.3.3 Amplification-Free Technology

Droplet digital detection technology.

An emerging technology termed Integrated Comprehensive Droplet Digital Detection (IC 3D) claims to selectively detect individual bacterial species directly from small quantities of whole blood within 1-4 hours [199]. In a one-step, culture- and amplification-free process, the IC 3D method provides quantitative bacterial detection with single-cell sensitivity. IC 3D combines DNAzyme-based sensors with real-time droplet microencapsulation and a particle counter. First, blood samples are directly partitioned into billions of micrometer-sized droplets containing bacteria and a solution containing a fluorescent DNA sensor. The sensor is a DNA probe conjugated to a fluorescent reporter. Upon hybridizing to the target sequence, the probe is cleaved and generates a fluorescent signal. Thus, droplets containing bacterial genetic material can be identified by fluorescence. A three-dimensional particle counter is then used to rapidly, robustly, and accurately quantify the fluorescent droplets containing bacteria(113,114). Distribution of the blood sample into many small droplets minimizes the interference from components of blood, making it possible to directly detect target bacteria without sample preparation and purification [200]. In a proof-of-concept study, where blood was infused with *E. coli*, the IC 3D confirmed the presence or absence of this target bacteria within an hour. Quantitative measurement of the amount of *E. coli* was accomplished in about 3.5 hours. In samples containing 1 cell per mL, the assay detected bacteria about 77% of the time [199]. This technology accomplishes rapid pathogen detection with a small blood volume at single-cell sensitivity in a relatively easy to use format. Additional probes could be added to detect antibiotic resistance markers. However, the current system design is limited by its ability to detect only one bacteria species (e.g. *E. coli*) per analysis. There is potential to expand the sensor set and develop a multiple-wavelength detection system for multiple bacteria or pathogen detection [199]. However, the extent of this expansion would be limited by a small number of fluorescent channels and would not be able to incorporate detection of emerging pathogens. Further, the specificity of this technology has not yet been determined and this technique has not yet been validated using clinical

samples.

3.3.4 Machine Learning Applied to Molecular Detection Patterns and Clinical Data for Diagnosis

The predictive power of machine learning techniques applied to the clinical data gathered for patients can be a valuable tool to improve diagnosis and management of sepsis. Even though it is difficult to discuss purely electronic medical record (EMR) based machine learning algorithms in the light of the characteristics for ideal sepsis diagnostics, we think it is worth summarizing some of the promising machine learning approaches that have been evaluated in a clinical cohort. The combination of molecular diagnostics with EMR machine learning approaches could provide valuable synergy to impact the clinical management of sepsis.

HeRO score (MPSC)

Recently, heart rate characteristics (HRC) have been used in clinics to provide an early warning of patient distress. Available commercially as the HeRO score algorithm [201], the technology uses signal processing and machine learning to identify subtle irregularities in heart rate variability. The HRC index used by HeRO was shown to reduce mortality from 10% to 8% in an industry sponsored randomized controlled clinical trial of 3,003 VLBW infants [202]. However, the mechanisms for mortality reduction remain unclear. An independent, academic study of HRC monitoring in VLBW infants reported a higher utilization of antibiotics and more sepsis evaluations in a cohort with HRC monitoring as compared to controls without monitoring. This study also determined that no differences existed in the rates of blood culture positive sepsis or clinically suspected sepsis as a function of HeRO index [203]. An additional single-center retrospective study reported that elevated HRC scores had limited ability to detect bloodstream infection among neonates in the NICU, emphasizing that HRC alone may not be adequate [204]. Thus, HeRO may represent another technology that could provide synergy in an integrated format with other diagnostic measures.

Other machine learning approaches for sepsis diagnostics. Unlike the HeRO score, which uses a single modality, heart rate variability, a machine learning framework also allows the incorporation of multiple diagnostic markers from large clinical datasets. One study reported the use of canonical correlation analysis (CCA) and sparse support vector machine (SSVM) classifiers to select the best subset biomarkers, such as band neutrophils, platelets, neutrophil CD64, white blood cells, and segmented neutrophils in a dataset of 1,383 sepsis evaluations from 749 neonates with suspected sepsis in the NICU [205]. Another research group developed predictive models for late-onset neonatal sepsis using EMR data from 1,826 NICU infants with 299 sepsis evaluations [206]. This group developed a variety of machine learning algorithms and their models matched the treatment sensitivity and specificity of clinicians in blood culture positive cases. These algorithms need to be validated in a prospective study, but present a promising opportunity for improving early diagnosis and antibiotic management practices in the NICU. The recently developed targeted real-time early warning score, which incorporates continuous sampling of variety of physiological inputs including platelets, ratio of blood urea nitrogen (BUN) to creatinine, arterial pH, temperature, bicarbonate, respiratory rate (RR), white blood cell count, systolic blood pressure (SBP), heart rate, and heart rate/SBP (shock index), was able to predict the development of septic shock in adult ICU patients 28 hours before the clinical onset [207]. This machine learning technique allows for the use of heterogeneous datasets to inform clinical decisions. The future may see the use of Bayesian statistical methods to enable incorporation of EMR data with broad-based molecular detection technologies, thus providing significant potential to increase the reliability of these technologies. In this era of large-scale data integration, combining broad-based techniques with the EMR presents tremendous opportunities for timely and accurate diagnosis and management of sepsis.

3.4 Conclusion

An exciting new era of molecular diagnostics for bloodstream infections is emerging through innovations in sample preparation, single-molecule detection methods, sequencing, and applications of machine learning. Yet each emerging technology harbors unique benefits and drawbacks. For example, U-dHRM addresses the challenge of detecting in low blood volume with high sensitivity while resolving polymicrobial infections, all in a potentially portable format and clinically actionable timeframe. However, sample preparation and handling are still required which increases the time and may lead to some loss of sensitivity. Likewise, SeptiCyte provides a robust way to detect whether a pathogen is present based on host response and provides this information in a similar timeframe as U-dHRM, but requires a higher volume of blood and initial sample preparation. The IC3D technology is limited in the number of targets it can detect in a single sample but is capable of skipping sample preparation entirely to accomplish the simplest and most direct testing from blood samples. This may be of significant value for rapidly tracking the spread of individual organisms in the context of outbreaks and hospital acquired infections. Further, in the era of big data, advances in the field of machine learning can add patient-specific contextual information to each diagnostic test to potentially increase their sensitivity. The integration of host and pathogen targeted diagnostic technologies and their combination with EMR datasets using machine learning constitutes a promising new frontier. Combining diagnostic technologies that build on distinct approaches could be a rapid way to improve positive and negative predictive power and truly impact antibiotic usage in the clinic. Together, these emerging technologies have the potential to identify microorganisms and provide relevant subspecies and antibiotic resistance information in a clinically relevant timeframe that is much shorter than that currently required for blood culture. Such an integrated approach may overcome the limitations of each technology individually to facilitate targeted and precise antibiotic use.

In the next chapters, we focus on optimizing the U-dHRM platform, discussed above as an emerging technology. As explained previously, the U-dHRM

has several advantages that make it one of the more promising technologies for neonatal sepsis (Figure 3.4). For successful implementation in the clinic, we set out to design a system for generation of reliable melt curves with minimal run to run variation and develop algorithms to identify pathogens using these melt curves.

3.5 Acknowledgements

Chapter 3, in part, is in submission for publication as it may appear in *Clinical Microbiology Review* 2017. Sinha, Mridu; Jupe, Julietta; Mack, Hannah; Coleman, Todd; Lawrence, Shelly; Stephanie, Fraley. The dissertation author was the primary investigator and author of this material.

This research was supported by a UCSD Clinical and Translational Research Institute Pilot Grant and an Accelerating Innovations to Market Award. SF is supported by a Burroughs Wellcome Fund Career Award at the Scientific Interface; other lab members are supported by the UCSD Frontiers of Innovation Scholars Program.

Chapter 4

Development of Universal Digital High-Resolution Melt Device

4.1 Abstract

DNA melting analysis provides a rapid method for genotyping a target amplicon directly after PCR amplification. To transform melt genotyping into a broad-based profiling approach for heterogeneous samples, we previously proposed the integration of universal PCR and melt analysis with digital PCR. Here, we advanced this concept by developing a high resolution digital melt platform with precise thermal control to accomplish reliable, high-throughput heat ramping of microfluidic chip digital PCR reactions. Using synthetic DNA oligos with defined melting temperatures, we characterized sources of melting variability and minimized run-to-run variations. Within-run comparisons across a 20,000 reaction chip revealed that high melting temperature sequences were significantly less prone to melt variation. Further optimization using bacterial 16S amplicons revealed a strong dependence of the number of melting transitions on heat ramping speed during curve generation. These studies show that reliable high resolution melt curve genotyping can be achieved in digital, picoliter-scale reactions and demonstrate that rate-dependent melt signatures may be useful for enhancing automated melt genotyping.

4.2 Introduction

A technology that accomplishes fast, easy, inexpensive, and sensitive DNA screening is an attractive way to profile samples prior to or in lieu of deeper sequencing investigations. The increased availability of deep sequencing facilities to identify low-level genotypes in complex samples has made deep sequencing an increasingly common research tool. However, the cost, time, computation, and expertise required to carry out deep sequencing still represent significant hurdles for use in many applications [208–210]. High resolution DNA melting analysis, wherein double stranded DNA is heat denatured into its single stranded form in the presence of fluorescent intercalating dyes is capable of rapidly genotyping sequences. This closed-tube method is performed directly after PCR amplification of specific targets and has traditionally been used for 1) mutation or single nucleotide variation (SNV) detection based on melting temperature (T_m) shifts or 2) heterozygote detection based on a curve shape change when aligned to the homozygous sequence melt curve [211, 212]. In combination with machine learning algorithms and universal primers or adapters, we and others have proposed that high resolution melt analysis could be extended to accomplish broad-based sequence identification tasks such as microbial or microRNA profiling [178, 213–221]. However, in its traditional PCR well-plate format, melt analysis of heterogeneous samples precludes detection of low level genotypes and generates complex melt curves that are difficult to interpret [218, 222, 223].

We conceived digital melt analysis to overcome these limitations. It involves partitioning a heterogeneous sample into many small volume PCR reactions, such that each contains zero or one target molecule, and subsequently conducting universal PCR and melt analysis on all reactions. Since each reaction amplifies from a single target molecule, each digital melt curve is a sequence fingerprint of only one sequence within the heterogeneous sample. Subsequently, machine learning algorithms are used to automatically identify melting curve signatures and quantify the number of reactions containing each signature. This form of melt analysis distinguishes itself from previous forms by relying not only on T_m or aligning melt curve shapes, but on all the temperature points encompassed by the curve. Like-

wise, digital melt analysis distinguishes itself from digital PCR (dPCR) by virtue of its goal to amplify an entire class of sequences through universal priming for subsequent identification, as opposed to the amplification of a specific sequence by targeted priming for quantification purposes only.

Commercially available digital PCR systems accomplish sample partitioning that can effectively isolate sequences from a mixture into homogeneous digital reactions. However, these systems cannot be extended to accomplish high resolution digital melt analysis, as nearly all have heating and imaging components that are physically separated into individual pieces of equipment [190,224]. Microfluidic droplet-based digital PCR devices (Bio-Rad) perform endpoint PCR detection in a continuous flow format without temperature control, one droplet at a time, preventing in-situ, real-time monitoring of fluorescence in droplets needed for digital melting. A microvalve-based digital PCR devices by Fluidigm is the only system with integrated heating and imaging; however the capabilities of this system for performing high resolution melt is unclear and the cost per sample associated with the system limits our ability to test [190]. Therefore, we developed a dedicated digital melt analysis platform [224]. Demonstrating proof-of-principle of digital melt analysis required integration of a dPCR chip to partition the sample, with sensitive optics to capture dim intercalating dye fluorescence from picoliter scale reactions, and a chip-heating device. Further, to achieve fully digital partitioning, a dPCR chip with 20,000 partitions was desired [178,222]. Although our integrated device showed the capability of capturing digital melt curves, a significant limitation remained due to the poor reproducibility of the temperature ramp, which altered the shape and melting temperature (T_m) of the amplicons from run-to-run. This limitation hampers the ability of melt curve database matching through machine learning to reliably recognize sequence melt fingerprints and also severely restricts the scalability of the database, limiting the breadth of detection available for profiling. Well-to-well variations in loading, heating, and evaporation could also negatively impact the ability of dPCR to quantify and digital melt analysis to profile, but these have not been characterized.

Commercial melt curve analysis instruments, designed for traditional large

volume reactions, suffer from similar melt curve reliability issues depending on sample format and heat transfer methods. A recent study found that nine melt instruments vary significantly in melt precision, offer limited ability to achieve user-defined heating and imaging rates, and struggle to accurately collect fluorescence data from multiple wells [225]. An earlier study also found that instruments that accommodated high-throughput 96-well sample formats produced T_m differences as large as 1.24°C across the plate, forcing comparison of melting curve shapes to often require shifting and alignment of curves at the users discretion [226]. Further complicating matters is the fact that different instruments use different ways of specifying the melting and imaging rates that require complex conversions and empirical measurements to estimate the melt rate [227]. Melt curve resolution relies on matching an imaging rate to a heating rate, both of which are presumed to be constant. Imaging rates are more easily controlled than heating rates, and the presumption of a constant heating rate (linear with constant slope) cannot be taken lightly. Manufacturers typically focus optimization on a single melting rate for the highest quality of data, which limits the flexibility of their system [179]. There remains a significant need for improved uniformity and linearity of thermal control during melting analysis in general, and especially if melt analysis is to achieve the goal of broad-based melt genotyping in a higher-throughput format.

The aim of the current study was to design and characterize a robust high resolution digital melt heating device to minimize melt curve variation across 20,000 reactions and across runs for reliable automated identification. Heating rate linearity and reproducibility were controlled and characterized using continuous two-point physical temperature measurements. Further characterization and optimization of well-to-well and run-to-run variations was carried out using DNA oligos as T_m calibrators and amplicons from the bacterial 16S gene. The devices ability to precisely control various user-defined heating rates revealed a novel dependence of melt curve dynamics on melting rate that was independent of imaging rate (fluorescence measurement/ $^\circ\text{C}$), or melt curve resolution. Within-run comparisons across the 20,000 picoliter scale reactions also revealed that high T_m sequences were significantly less prone to melt variability.

4.3 Results

System Design. To optimize the heat ramp control of the microfluidic chip for identification of sequence-specific melt curve signatures, we redesigned the thermal control system of our previously described digital high resolution melt platform. Previously, the chip was housed in a copper block, which was heated or cooled by a thermoelectric (TEC) device. To precisely control the TEC, we added a proportional-integral-derivative (PID) controller with temperature feedback from the copper block. The feedback was provided by a highly accurate resistance temperature detector (RTD) sensor that was embedded in the middle of the copper block. As described previously, a thin layer of thermal grease was added between the chip, copper block, and the TEC device to ensure efficient heat transfer. Heating dissipation from the reverse side of TEC was enhanced by attaching a fan to the aluminum heat sink. The speed of the fan was also controlled by the PID controller, commensurate with the sink temperature, using a negative temperature coefficient thermistor (NTC). The addition of the fan improved our ability to precisely heat to higher temperatures and allowed us to rapidly cool the chip back to room temperature, decreasing the wait-time between two consecutive runs. The use of an off-the-shelf digital PCR chip did not allow us to place a temperature probe inside the chip in use. Therefore, to ensure that the thermal control achieved for the copper block efficiently transferred to the chip, we placed a surrogate chip with a temperature sensing thermocouple embedded at its center next to our test chip on the copper block. The entire chip-heating device assembly was held in place inside a custom designed 3D printed stage adaptor to securely mount the device on a microscope for imaging (Figure 4.1). While the copper block was independently controlled by standalone software, the proxy temperature measurement from the surrogate chip was synchronized with fluorescent imaging by the microscope control software (NIS-Elements). However, synchronizing imaging with temperature measurement required the use of an NIS-Elements compatible temperature acquisition system (Tokai Hit Co., Japan) using a K-type thermocouple probe. This integrated imaging and temperature acquisition system limited the resolution of temperature measurement to 0.1°C with a temperature sampling rate

of 0.2Hz irrespective of the imaging rate. Therefore, our strategy was to precisely control the copper block temperature, establish a repeatable relationship between the copper block-embedded RTD and the surrogate chip-embedded thermocouple, and then use the integrated thermocouple temperature data and fluorescence imaging data to plot melting curves.

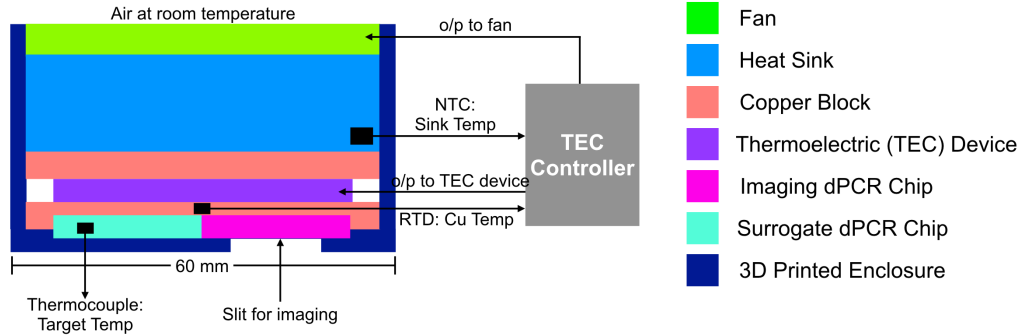


Figure 4.1: Schematic of U-dHRM platform

Thermal Profile Characterization. The PID controller provided temperature control of the copper block as per the desired ramp rate of $0.1^{\circ}\text{C}/\text{s}$. The maximum difference in the expected block temperature and observed temperature recorded using the RTD embedded within the block was measured as 0.004°C (Figure 4.2A). Across all runs, the expected ramp rate of $0.1^{\circ}\text{C}/\text{s}$ was observed with maximum root mean squared error (RMSE) of 0.001°C (Figure 4.2B). This confirmed that precise temperature control of the copper block was achieved by our new heating system.

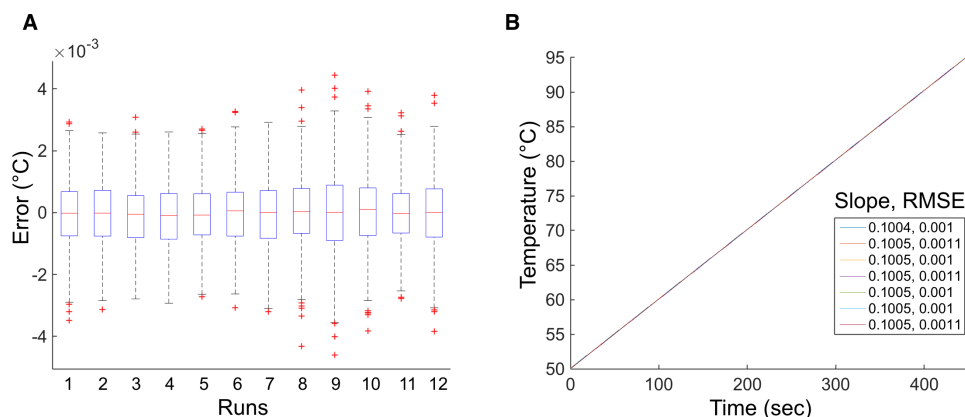


Figure 4.2: Controller performance. (A) Box plot of error (observed - expected temperature) for the copper block across all runs with temperature calibrator at a ramp rate of $0.1^\circ\text{C}/\text{s}$. Red crosses denote outliers that are larger than the 75th percentile plus 1.5 the interquartile range or smaller than the 25th percentile minus 1.5 the interquartile range. This corresponds to approximately $\pm 2.7\sigma$ and 99.3% coverage assuming normal distribution of the data. At least 2000 wells were chip were used per run. (B) Table with slope and root mean square error for each run shows the highly reproducible ramp rate of $0.1^\circ\text{C}/\text{s}$ across runs with average root mean squared error of 0.001°C .

Next, we investigated the relationship between the block temperature and surrogate digital chip temperature. Figure 4.3 shows temperature ramp measurements taken using the surrogate chip-embedded thermocouple for the same runs as depicted in Figure 4.2A for the copper block-embedded RTD. Across all runs, the thermocouple measured a ramp rate of approximately $0.98^\circ\text{C}/\text{s}$ on the chip, as compared to $0.1^\circ\text{C}/\text{s}$ measured with the RTD in the block. The relationship between the thermocouple and RTD was highly repeatable across seven runs (Figure 4.2B and Figure 4.3A). To test the linearity of the slope, we analyzed different temperature ranges of the thermocouple readings and found the slope to be consistent. This justified the use of a straight-line fit for the thermocouple data, revealing a maximum RMSE of 0.05°C across runs (Figure 4.3A). Instantaneous heating rates on the chip were also analyzed and showed no significant deviation ($R^2 = 1$) from linearity due to heat transfer losses from block to chip (Figure 4.3B) to achieve precise and linear heating control on the digital PCR chip.

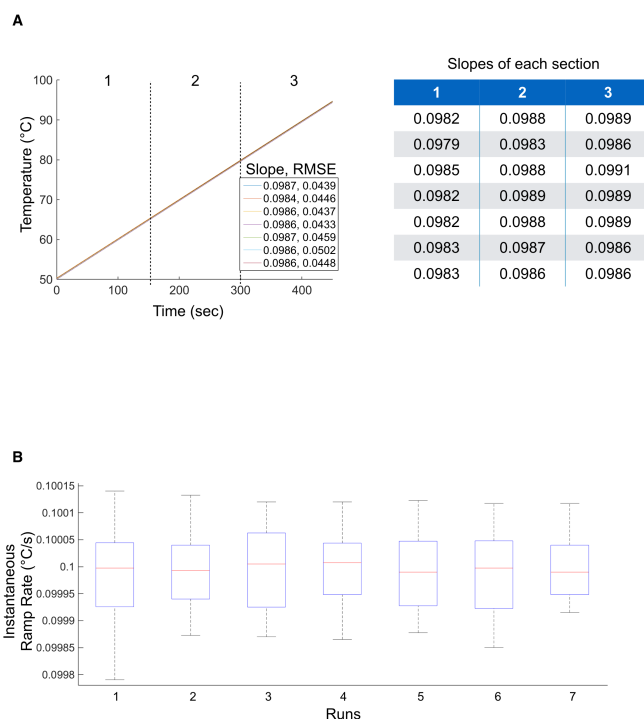


Figure 4.3: Surrogate chip behavior. **(A)** Slope and RMSE of fitted thermocouple temperature for each run. The slope of entire run is close to the slope for data in three sections, justifying the use of straight-line fit. Root mean squared error was calculated by comparing the polynomial fit with degree 1 and observed data. **(B)** Instantaneous ramp rate of acquired thermocouple measurements.

Melt Characterization with Temperature Calibrator sequences.

In theory, if heat ramping is linear and heat transfer is efficient, any inaccuracies in the absolute temperatures measured during the melting process could be reliably removed using temperature calibrator sequences. Such control DNA oligos of known T_m can be included in all reactions and designed so that they melt outside of the amplicons melting temperature range [228]. As long as the heat ramping rate is linear and of a constant slope, the distance between the calibrator T_m and the amplicon T_m is reliably maintained. Therefore, temperature offset errors occurring from run-to-run or well-to-well because of imperfections in temperature control or uniformity can be removed by simply shifting each melt curve to align the calibrator T_m peaks to their correct melting temperature. Therefore, to further characterize the reliability of melting behavior on the chip, we used three syn-

thetic oligo sequences with predicted T_m ranging from 57-93°C to generate melt curve data for run-to-run and well-to-well variability analysis. These temperature calibrator sequences varied in GC content and length to achieve a high(92.9°C), mid(62.8°C) and low(57.3°C) melting temperatures. For this analysis, melt curves were generated on-chip at a heating rate of 0.1°C/s across seven replicate runs over several days. Figure 4.4A shows plots of derivative melt curves across the runs.

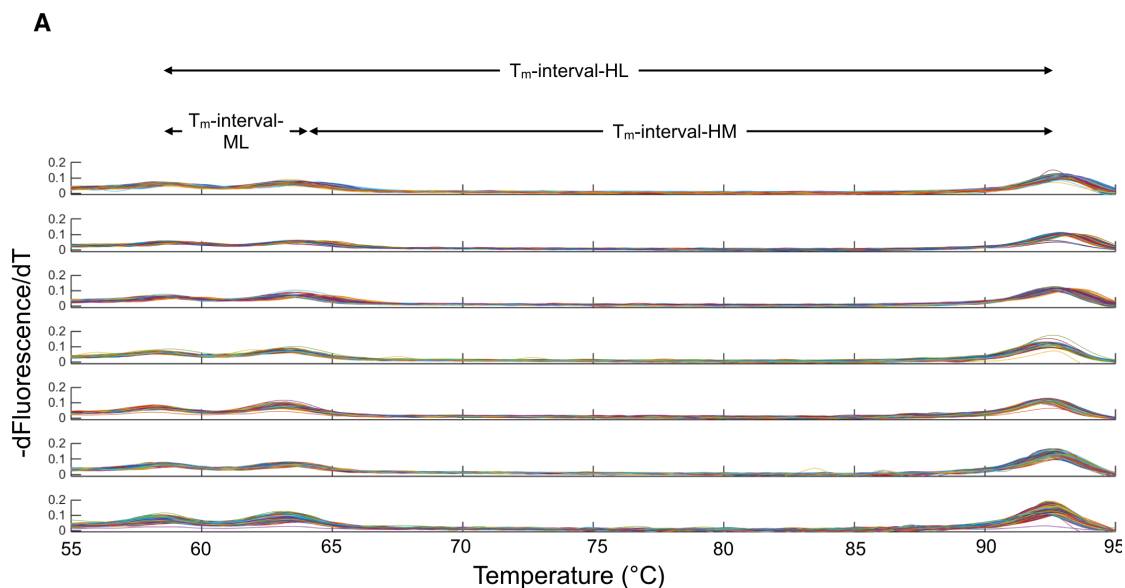


Figure 4.4: Derivative melt-curves. Negative derivative of melt (EvaGreen normalized by ROX) with respect to temperature for temperature calibrator sequence. The figure shows difference between T_m -interval and their denotation.

Run-to-run variation. First, we applied a peak detection algorithm to the derivative melt curves (Figure 4.4) to find the T_m melting peaks in a $\pm 3^\circ\text{C}$ region around the predicted T_m for each calibrator sequences (uMelt(26): T_m -low 57.3°C, T_m -mid 62.8°C, and T_m -high 92.9°C). Then, we calculated the difference between the T_m of each calibrator to characterize run-to-run variations in linearity. Linearity differences among runs would be expected to produce stretching or compression of the melting curves along the temperature axis that would change the interval between T_m peaks. However, if linearity is consistent, calibrator T_m peaks can be shifted to match their predicted values to overcome offset errors. Thus, the high, mid, and low T_m -intervals were calculated as the difference between

T_m-high and T_m-low (T_m-interval-HL), T_m-high and T_m-mid (T_m-interval-HM), and lastly T_m-mid and T_m-low (T_m-interval-ML). The mean of these T_m-intervals within runs is shown in Figure 4.5A. To compare across runs, we calculated the standard deviation of these mean T_m-intervals. The T_m-intervals varied across runs with a standard deviation less than 0.1°C for all the three intervals, showing run-to-run-repeatability within the accuracy and precision limits of the combined temperature acquisition system (see System Design) and imaging system. Next, to quantify the spread of the data across runs, we calculated the median absolute deviation (MAD) for the difference of the T_m-intervals of each well to the mean T_m-interval that is representative of the chip. Figure 4.5B shows similar magnitudes of spread in well-to-well variation across runs. These run-to-run variability results are within the expected error limits of the system. However, the spread was slightly higher in magnitude for the T_m-interval-ML data.

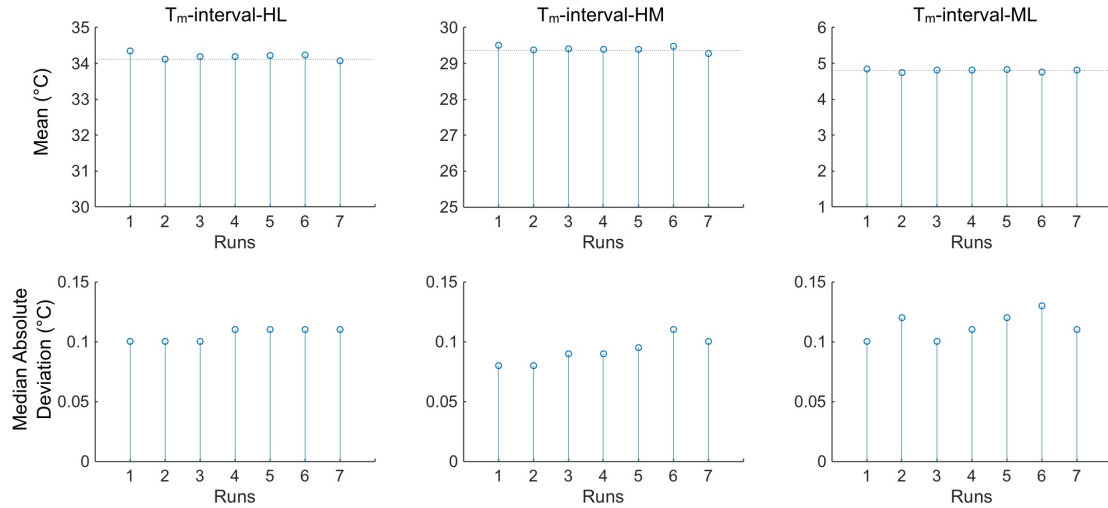


Figure 4.5: Controller performance using three temperature calibrators with known melting temperatures (A) Mean of difference in T_m-intervals are shown. (left) Difference between T_m-High and T_m-Low (T_m-interval-HL) (middle) T_m-High and T_m-Mid (T_m-interval-HM), (right) T_m-Mid and T_m-Low (T_m-interval-ML). (B) Intra-run variability associated with each run. Median absolute deviation (MAD) for (left) T_m-interval-HL (middle) T_m-interval-HM, (right) T_m-interval-ML. The MAD varied from 0.1 to 0.11, 0.09 to 0.12 and from 0.11 to 0.14 for T_m-interval-HL, T_m-interval-HM, and T_m-interval-ML, respectively.

Well-to Well variation. Once we established that the repeatability of T_m-intervals between runs were within expected error limits of the system, we sought to characterize the intra-run variability. This variability does not depend on the heat ramp, but rather the thermal gradient, loading differences, and evaporation anomalies across the chip. Interestingly, when we then investigated variability in T_m peak values across the chip by plotting the difference of the T_m peaks of each well to the corresponding mean T_m for the chip, we found a lower intra-run variability in T_m-High as compared to T_m-Mid and T_m-Low (Figure 4.6A). The largest median absolute deviation for T_m-High was 0.1°C, in comparison to the higher values of 0.13°C, and 0.14°C observed for T_m-Mid and T_m-Low, respectively. Scatter plots for the difference in T_m-High and T_m-Mid from their representative mean-T_m values for each chip revealed higher variability in the T_m-Mid (Figure 4.6B). Further, T_m-Low behaved similar to T_m-Mid. To investigate the location of wells with higher variability, we plotted the difference of T_m of each well from the mean value (Figure 4.6C). This showed higher variability in T_m-Low and T_m-Mid as compared to T_m-High throughout the chip reactions, with the majority of outliers (± 2.7 SD) located around the edges and corners of the digital chip. Analysis of the ROX reference dye intensity across the chip also revealed wells with significantly lower intensity located at the edges and corners; however, this pattern was not highly correlated with the T_m variability (Figure 4.6C). These results suggest that the high calibrator sequence is inherently less susceptible to variability in melting than the low and the mid calibrator sequences, and further that there is a spatial dependence of variability coinciding with the well location on the chip.

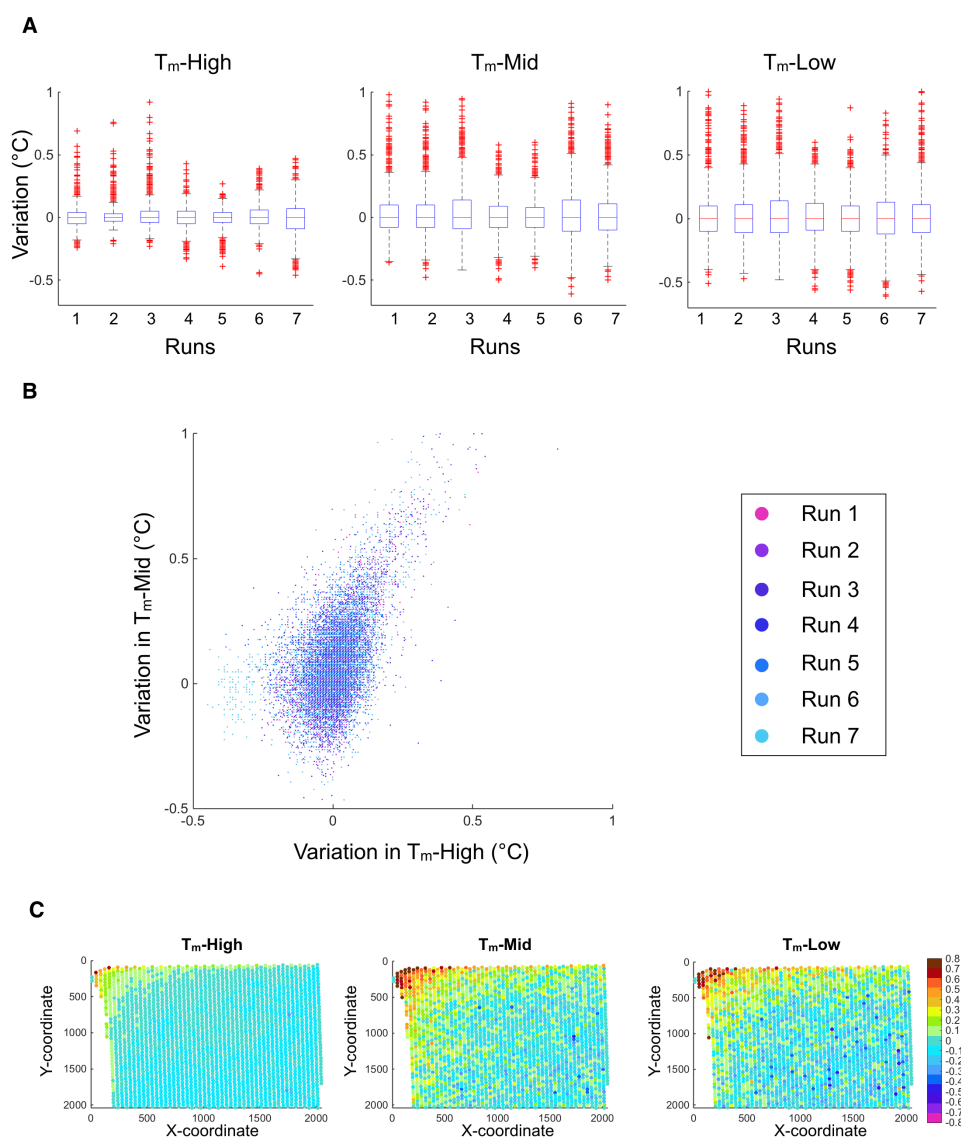


Figure 4.6: Intra-run variability. (A) Variation in (left) T_m-High (middle) T_m-Mid (right) T_m-Low. Variation was calculated as difference in T_m for each well about the mean T_m of the chip. Red crosses denote outliers that are larger than the 75th percentile plus 1.5 the interquartile range or smaller than the 25th percentile minus 1.5 the interquartile range. This corresponds to approximately $\pm 2.7\sigma$ and 99.3% coverage assuming normal distribution of the data. At least 2000 wells were used per run. (B) Variation in T_m-Mid plotted against variation in T_m-High. Figure shows a greater variation in T_m-Mid as compared to T_m-High (C) Variability in (left) T_m-High, (middle) T_m-Mid and (right) T_m-Low with respect to spatial location of wells on the chip for a characteristic run. Absolute temperature difference about the mean T_m of the chip is shown in false color as indicated in the key to the right.

Ramp Rate Dependence of Melt Curves. Having fully characterized the reliability of our melting device hardware and validated its performance biochemically, we next sought to investigate the dependence of the melt curve characteristics on ramp rate. Since our goal is to use melt curves to profile heterogeneous samples for multiple genotypes, we wanted to understand whether ramp rates could be optimized to enhance the effect of sequence differences on melt curve features. As a model genotyping task, we performed these experiments with bacterial DNA amplified from the 16S rRNA gene that included the hypervariable regions 1-6 (1 kb in length). We chose *Acinetobacter*, *Moraxella*, and *Salmonella* genomic DNA as our templates because we have previously observed that their 16S sequences melt uniquely with either one or two transitions at ramp rate of $0.1^{\circ}\text{C}/\text{s}$ in bulk qPCR reactions [215, 216].

First, we generated 16S amplicons on 3 independent chips for each bacterium. These chips were then used to generate melt curves at ramp rates of $0.01^{\circ}\text{C}/\text{s}$, $0.05^{\circ}\text{C}/\text{s}$, $0.1^{\circ}\text{C}/\text{s}$ and $0.2^{\circ}\text{C}/\text{s}$. We adjusted our imaging settings to maintain 0.1°C resolution in fluorescence measurement by matching the imaging rate to heating rate. To ensure that our thermal control was accurate for varying ramp rates, we observed the temperature profile in the proxy chip and in the copper block. These profiles were similar to what was seen for a ramp rate of $0.1^{\circ}\text{C}/\text{s}$, reported above. The slopes of the block temperature and fitted chip temperature were repeatable across all ramp rates, and there were negligible deviations in instantaneous rates throughout the runs (copper block and surrogate chip behavior for all ramp rates are shown in Figure 4.7 and Figure 4.8).

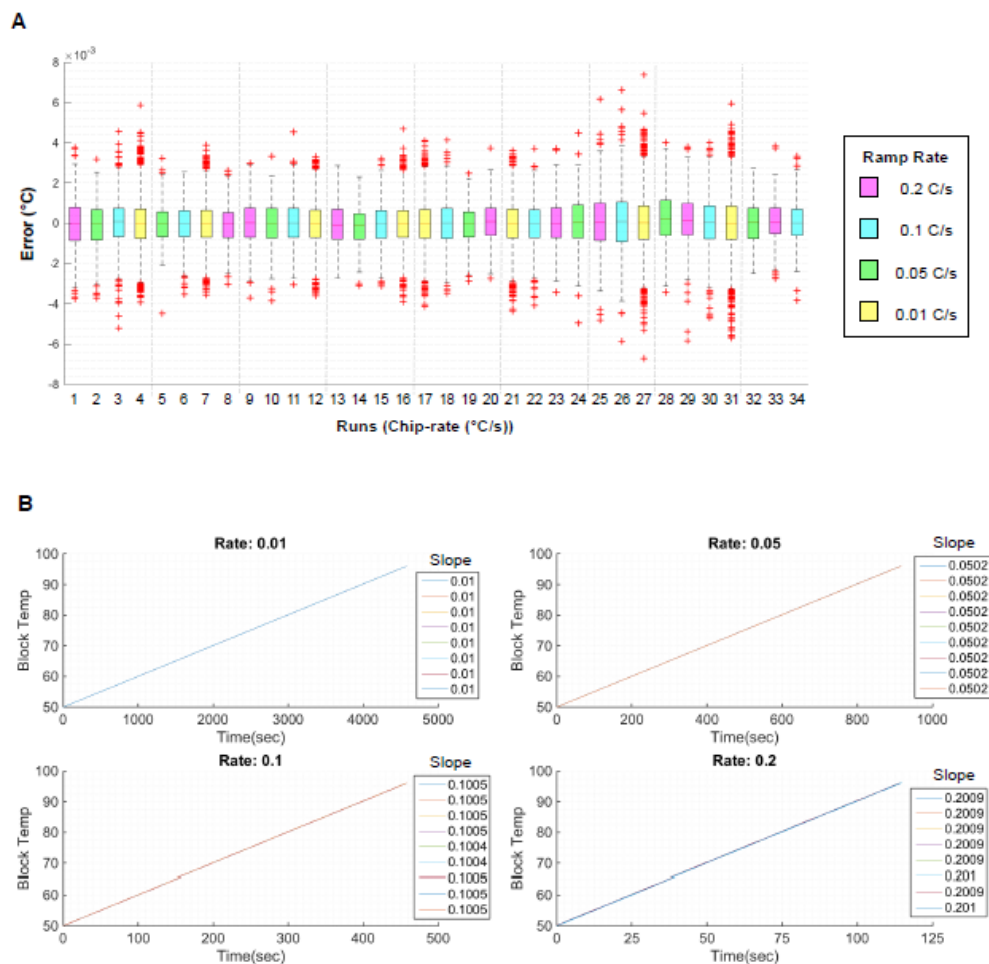


Figure 4.7: Controller performance for different ramp rates (A) Box plot of error (observed - expected temperature) for the copper block across all runs with temperature calibrator at a ramp rate of 0.01°C/s , 0.05°C/s , 0.1°C/s , 0.2°C/s . (B) Slope of straight line fit for RTD temperature for each run.

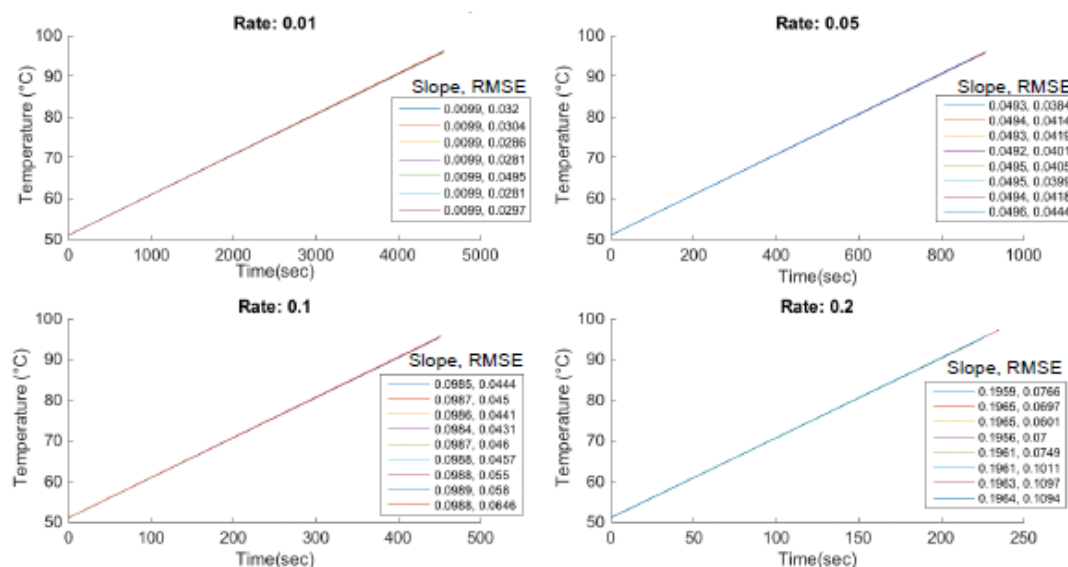


Figure 4.8: Surrogate chip behavior. Slope and RMSE of fitted thermocouple temperature for each run at different heating rates.

The 16S amplicons for *Acinetobacter baumannii* revealed multiple melt domains for higher ramp rates of $0.1^{\circ}\text{C}/\text{s}$ and $0.2^{\circ}\text{C}/\text{s}$. However, a single melting domain was observed for $0.01^{\circ}\text{C}/\text{sec}$ as seen in Figure 4.9A. The second derivatives of the melt curves further highlight the difference in curve shape at different rates (Figure 4.9B). Similar rate dependent melting (RDM) behavior was seen with *Moraxella catarrhalis* (Figure 4.9 C and D.) However, *Salmonella enterica* serovar Heidelberg amplicons showed no significant RDM (Figure 4.9 E and F), and neither did *Salmonella enterica* serovars Enteritidis and Typhimurium for 2 chips (Figure 4.10). Statistically significant differences in curve shape (skewness) were observed for *A. baumannii* ($p=0.005$) between the melt rates of $0.01^{\circ}\text{C}/\text{s}$ and $0.2^{\circ}\text{C}/\text{s}$ but not for *S. enterica* Heidelberg ($p=0.6$). Interestingly, our previously published machine learning algorithm for automated melt curve genotyping was able to differentiate between melt curves generated at $0.01^{\circ}\text{C}/\text{s}$ and $0.2^{\circ}\text{C}/\text{s}$ for *A. baumannii* with 97% accuracy, but failed to do so for *S. enterica* Heidelberg (60% accuracy). The sequence specificity of the RDM phenomenon could be an additional feature used for melt-based sequence identification.

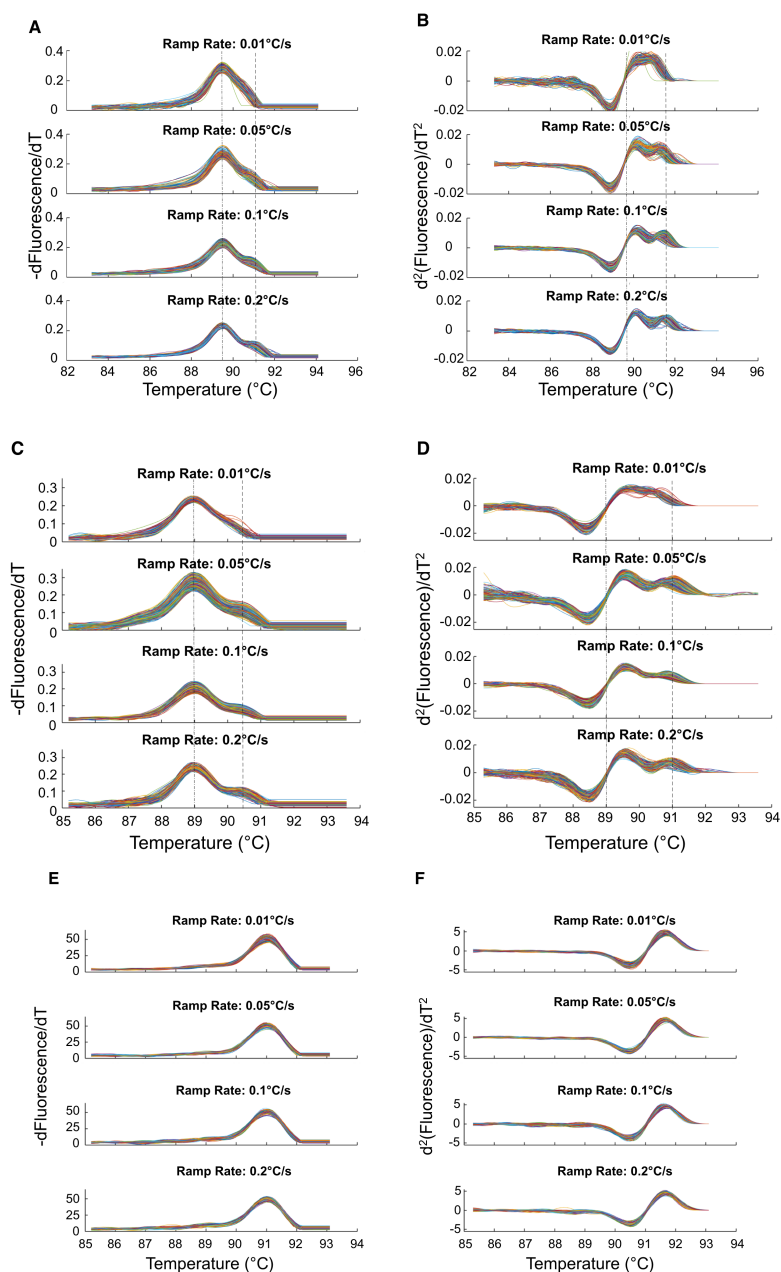


Figure 4.9: Rate dependent melt curves (A) Negative first order derivative of melt with respect to temperature for *Acinetobacter baumannii*. (B) Second order derivative of melt with respect to temperature. (C) Negative first order derivative of melt with respect to temperature for *Moraxella catarrhalis*. (D) Second order derivative of melt with respect to temperature. (E) Negative first order derivative of melt with respect to temperature for *Salmonella enterica serovar Heidelberg*. (F) Second order derivative of melt with respect to temperature

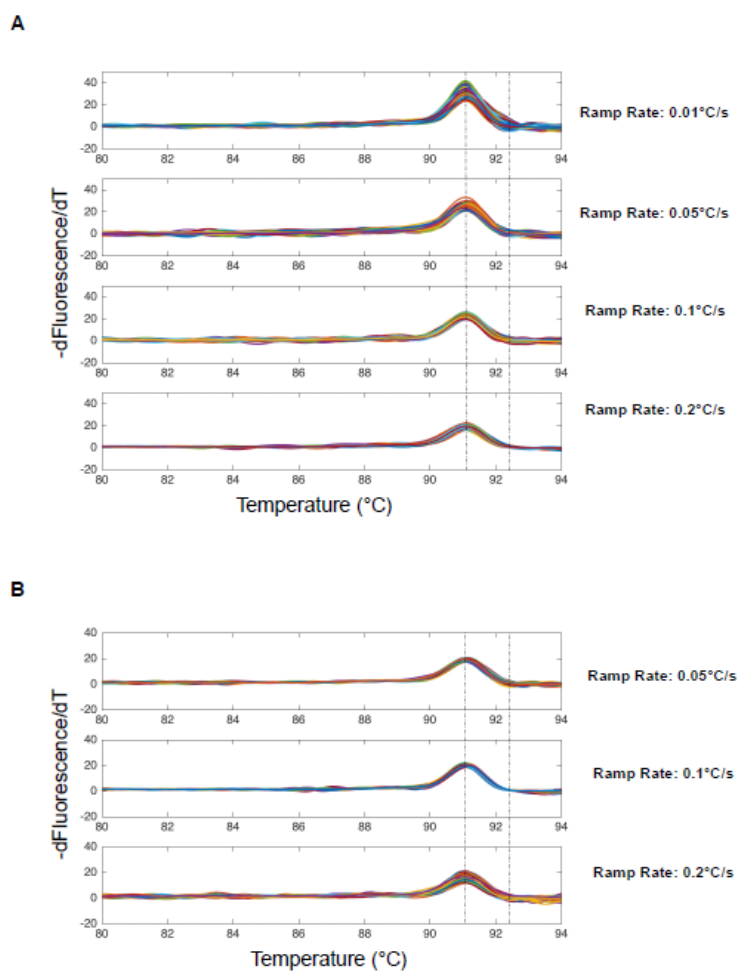


Figure 4.10: Rate dependence of melt curves in bacteria with one melt transition. Negative derivative of melt with respect to temperature for *Salmonella enterica* serovars (A) Enteritidis (B) Typhimurium

4.4 Materials and Methods

Sample Preparation for Temperature Calibrator Sequences. Three temperature calibrator sequences with varying GC content and known melting temperatures were used to optimize the heating of our system: 0% GC (TTAAATTATAAAATATTTATAATATTAATTATATATATAAATATAATA-C3), 12% GC (TTAATTATAAAGGTATTTATAATATTGAATTATACATATCTAATATAATC-C3), and

76% GC (GCGCGGCCGGCACCCGAGACTCTGAGCGGCTGCTGGAGGTG CGGAAGCGGAGGGGCGGG-C3) (Integrated DNA Technologies, Coralville, IA). The master mix containing the three temperature calibrators was created as follows: 1X Phusion HF Buffer containing 1.5 mM MgCl₂ (Thermo Fisher Scientific, Waltham, MA), 4 M of equal mixtures of the three temperature calibrator sequences, 1X ROX (Bio-Rad Laboratories, Hercules, CA), 2X EvaGreen (Biotium, Fremont, CA) and Ultra Pure PCR water (Quality Biological Inc., Gaithersburg, MD) to bring the total volume to 15 L. A volume of 14.5 L of the 15 L master mix was then loaded onto a commercially available dPCR chip containing 20,000 picoliter-sized reaction wells, the QuantStudio 3D Digital PCR 20K Chip V2 (Applied Biosystems, Foster City, CA), as described in Ortiz et al. The chips were filled with a PCR-grade oil, QuantStudio 3D Digital PCR Immersion Fluid (Applied Biosystems, Foster City, CA), to prevent sample evaporation during thermocycling and sealed with an adhesive lid which contained an optical window for imaging (included in 3D Digital PCR 20K Chip V2 Kit, Applied Biosystems, Foster City, CA).

Sample Preparation for Bacterial Samples. Bacterial gDNA was isolated from an overnight culture of bacteria using the Wizard Genomic DNA Purification Kit (Promega Corporation, Madison, WI). The stock DNA concentration was determined by the biospectrometer absorbance readings. Next, the desired DNA concentration was achieved through serial dilutions and added to the master mix which contained the following concentrations: 1X Phusion HF Buffer containing 1.5 mM MgCl₂ (Thermo Fisher Scientific, Waltham, MA), 0.15 M forward primer 5-GyGGCGNACGGGTGAGTAA-3 (Integrated DNA Technologies, Coralville, IA), 0.15 M reverse primer 5-AGCTGACGACANCCATGCA-3 (Integrated DNA Technologies, Coralville, IA), 0.2 mM dNTPs (Invitrogen, Carlsbad, CA), 2.5X EvaGreen (Biotium, Fremont, CA), 2X ROX (Thermo Fisher Scientific, Waltham, MA), 2X ROX (Bio-Rad Laboratories, Hercules, CA), 0.02 U/L Phusion HotStart Polymerase (Thermo Fisher Scientific, Waltham, MA), 0.3 M temperature calibrator sequence with 0% GC-content (see above) and Ultra Pure PCR water (Quality Biological Inc., Gaithersburg, MD) to bring the total volume to 15 L. A reaction

volume of 14.5 L was spread onto the dPCR chip (see above). A flatbed thermocycler was used to amplify the hypervariable regions, V1 to V6, of the 16S rRNA gene using the following PCR cycle: 1 cycle of 98C for 60 s; 70 cycles of 95C for 15s, 58C for 30s, 72C for 60s.

Cell Culture. Clinically isolated *Moraxella*, *Acinetobacter*, and *Salmonella* Enterica were grown separately overnight in Luria-Bertani (LB) broth. Sterile conditions were used to ensure uncontaminated growth of each bacteria.

Chip Heating Device. The thermoelectric heating/cooling (TEC) device was purchased from TE Technology, Inc. (Traverse City, MI). The Proportional-Integral-Derivative (PID) controller was purchased from Meerstetter Engineering GmbH (Rubigen, Switzerland). RTD (Class 1/3B) and thermocouple (K type) sensors were purchased from Heraeus (Hanau, Germany) and OMEGA Engineering (Stamford, CT), respectively. Medium to high amount to thermal paste gave the most repeatable results (data not shown).

Fluorescent Imaging. Nikon Eclipse Ti (Nikon, Tokyo, Japan) platform is customized to accomplish imaging for the dHRM system, as described in our earlier work. Fluorescent images are captured with a melt curve intercalating dye, EvaGreen, and a control dye, ROX, at 488/561 nm and 405/488 nm excitation/emission filters, respectively, with an exposure time of 100 ms at a LED intensity of 40%. The microscope is interfaced with Hamamatsu digital camera, C11440 ORCA-Flash4.0 for image acquisition at a rate commensurate with the heat ramp. The imaging rate is adjusted based on the heat ramping to maintain a resolution of 0.1C between images. NIS-Elements software is programmed to automatically image the chip as the heating device ramps by running a time lapse to image for every specified time point. For every image, the microscope automatically records the temperature of the surrogate chip registered by the thermocouple temperature probe within the metadata of the image. For this experiment, we used Nikon Plan/Fluor 4X objective with a numerical aperture of 0.13 and a working distance of 16.5X, to image a corner of the chip. Hence, every section of the chip was imaged as a part of separate run with simultaneous heating of the entire chip. This allowed us to maximize the number of runs/data per chip to characterize our

heating system. For an ideal use case, as described in our previous publication, we can sweep imaging location to image the entire chip for all runs.

Image analysis. Melt curve data generation. First the acquired fluorescence images are aligned using a template matching plugin in ImageJ. Then, melt curves are then generated using an automated image processing algorithm implemented in MATLAB. The algorithm applies median filter to remove salt and pepper noise in the images. It then generates a binary mask for each well on the chip and tracks them on all images. Pixels within 80% of the detected well radius are recorded and averaged to generate the fluorescence value in both ROX and EvaGreen channels for the specified well. The fluorescence values are tracked for each well across all images to generate curves for both EvaGreen and ROX channels. Filter (EvaGreen) curves generated are normalized against filter (ROX) values to account for any localized errors/noise due to bubbles in the chip or any abrupt change in ambient light as described in our previous publication(20).

Temperature Measure. Imaging software records the temperature corresponding to each image from the surrogate chip. However, the temperature acquisition rate is limited to an approximate 0.20Hz. Line fitting is performed using the unique temperature, time pair acquisitions to estimate temperature for each acquired image for faster imaging rates (Figure 4.11). A melt curve for each well is plotted against this estimated temperature. The negative derivative is taken with respect to temperature. Normalization and smoothing is performed as described in previous publications. To studying rate dependence of melt curves, bacterial melt curves generated were aligned the curves to their T_m . accuracy, but failed to do so for *S. enterica* Heidelberg (60% accuracy). The sequence specificity of the RDM phenomenon could be an additional feature used for melt-based sequence identification.

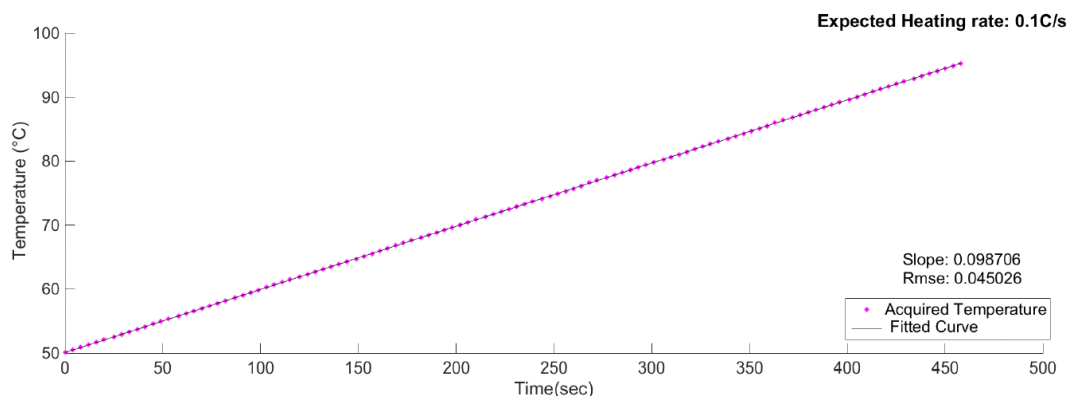


Figure 4.11: Line fitting to estimate chip temperature. Asterisk shows unique temperature-time pairs acquired by the NIS-Elements software. Solid line shows estimated temperature using line fitting for a characteristic run

4.5 Discussion

We have successfully designed and characterized a high resolution digital melt platform. Our design achieves highly repeatable temperature profiles for a range of melt rates and commensurate imaging frequencies. The run-to-run errors we observed were similar to the expected theoretical error limits of our system, approximately 0.14°C . Precision in temperature control is an important factor in being able to resolve melt curves. However, imaging systems can contribute to melt errors as well. The resolution of our imaging system is one image per 0.1°C . Thus, the minimum total RMSE error due to imaging (± 0.05) and heating (± 0.05) for our system is expected to be $\pm 0.07^{\circ}\text{C}$. These error limits can be improved with the development of a custom optical system with integrated and tunable image and temperature acquisition capabilities. Such design improvements would allow us to integrate a chip temperature probe with better accuracy and resolution into the imaging system. This, in addition to increasing our sampling rate for fluorescent data acquisition, would enhance the devices ability to resolve smaller T_m differences. Beyond hardware limitations, other potential sources of variation

could arise due to interactions in AT-GC content and the length of amplicons [211,229] slight differences in salt environments [229,230] or DNA concentrations [183,231,232], concentration and stability of DNA saturating dye [233] and reference ROX dye [234], pipetting errors, differential evaporation across reactions, and data processing methods [225].

The reliability and performance of our heating and hardware system enabled us to identify and characterize other sources of melt variation. Understanding well-to-well variation across the chip is crucial for absolute load quantification and sequence profiling at single genome sensitivity. We observed that wells producing outlier T_m peaks are typically present at the corners and along the edges of the chip, as shown in Figure 4.6C. These outliers could represent reactions where evaporation has altered the chemistry of the reaction, specifically the concentration of ions, which can shift T_m [229,230]. Analysis of the ROX reference dye intensity across the chip revealed a somewhat similar pattern of outliers with significantly lower intensity located at the edges and corners. It is known that thermal cycling and heating causes the ROX dye to become insoluble in water and precipitate out of solution, which leads to a slight drop in fluorescence at high temperatures. But this cannot account for the spatial pattern we observed, which was present even before heating. During melting, we did note a drop in ROX fluorescence and variations from well-to-well. This could introduce errors during the processing of the image data, since we normalize EvaGreen dye intensity to ROX as a loading control and to account for localized errors due to air bubbles released at high temperatures. In the future, we may benefit from either using other more thermally stable referencing dye, or including mathematical methods for error correction.

As compared to conventional PCR, the smaller reaction volumes of digital PCR could be expected to lead to larger variations in T_m due to evaporation. On the other hand, the small form factor of the digital chip is expected to maintain a more uniform thermal gradient across the chip, leading to smaller variations in T_m . A previously published study reported T_m differences ranging from 0.35°C to 1.24°C across 32-96 well plate melt instruments with standard deviations of 0.018°C to 0.274°C [226]. In comparison, after excluding the outliers due to evap-

oration at the corners and edges of our chips, differences in the high temperature calibrator T_m on our digital melt platform were observed to vary from 0.22°C to 0.6°C . This represents a significant improvement in heating uniformity compared to the standard well-plate format. Even with evaporation outliers included, median absolute deviation ranging from 0.05°C to 0.1°C and standard deviation of 0.06°C to 0.13°C were observed across the chip, which is less than that of the well-plate format. Optimizing for loading errors and evaporation would be expected to further improve performance. For example, the application of oil onto the loaded reaction wells could be sensitive to timing and amount deposited, and automation would ensure that the corner wells are covered as quickly as the central wells to minimize evaporation.

Our observation that the T_m -Low and T_m -Mid for the temperature calibrator sequences were more variable than the T_m -High calibrator is somewhat expected. Unfortunately, our high-throughput platform revealed that the T_m variations of these low and mid calibrators were large enough to prevent their utility for melt curve normalization across runs. It is important to note that their variability was not correlated within individual wells or regions, indicating that it is not a function of location on the chip or differences in reaction conditions from well-to-well. Kinetic binding rates of DNA are known to vary based on GC content, as association rates of GC-rich oligomers are higher than rates of AT-rich equivalents [235]. Here, the low and mid calibrators have lower GC content (0% and 12% respectively) and are also shorter in length compared to the high calibrator (76% GC) [235, 236]. DNA dissociation rates are also known to increase exponentially with temperature. Further, physical models of DNA melting behavior predict that AT duplexes go through several cycles of hydrogen bond breakage and reformation, often involving an overall shift by one or more bases along the helix, before fully and finally disassociating. In contrast, the corresponding GC duplexes usually come apart only once [237]. Taken together, this suggests that it may be possible to design more reliable low and mid temperature calibrators by using very short GC-rich sequences.

It is generally thought that heating rate changes only result in shifts in

melt curve T_m , whereas the dynamic melting characteristics of a PCR product are thought to be primarily determined by GC content, sequence length, and nucleotide order [238, 239]. However, our study revealed that some long amplicons are highly sensitive to melting ramp rate, which not only shifts their T_m , but also changes the number and size of distinct melting transitions present. Our ability to identify a heating rate dependence of melt curve shape is in large part due to the tunability, uniformity, and throughput of the digital melt platform. For the long amplicon sequences, we studied, slower heating rates resulted generally in a single melt transition, whereas faster rates generated multiple melting domains. Interestingly, though, this response to heating rate was highly sequence dependent. Some long amplicon sequences maintained the same melt curve shape for multiple heating rates, while others do not. Thus, the response of a long amplicon to heating rate changes provides additional sequence-specific information that could enhance the specificity of melt curve-based sequence profiling. That is, where one ramp rate cannot discriminate two sequences by their melt curve, a combination of multiple ramp rates may reveal distinct melt responses. The mechanism underlying these differences may involve kinetic sampling of transition states. For example, slower rates would be expected to enable amplicons to sample a wider range of transition states, where shifting, re-organized binding, or secondary structure formation could effectively average out the fluorescence decay across the bulk population of amplicons. Faster rates may induce more uniform transition behavior involving abrupt local DNA bubbles that melt separately at a different temperature than the remainder of the sequence. Indeed, faster rates of melting have previously been associated with higher T_m accuracy in homozygous melt analysis [183]. Alternatively, since heteroduplex melting has been found to be more apparent at faster heating rates, the multiple melt domains we observe at faster ramp rates may be the result of distinct heteroduplex binding transition states induced in homoduplex molecules [183].

In conclusion, our novel digital melt analysis platform with well-controlled and well-characterized heating across 20,000 reactions advances the concept of digital melt curve-based sequence profiling and could also support fundamental

studies of DNA dissociation kinetics.

4.6 Acknowledgements

Chapter 4, in full, is in submission for publication as it may appear in Society for Laboratory Automation and Screening, 2017, Sinha, Mridu; Mack, Hannah; Coleman, Todd; Stephanie, Fraley. The dissertation author was the primary investigator and author of this material.

This research was supported by a Burroughs Wellcome Fund Career Award at the Scientific Interface 1012027, NSF CAREER Award 1651855, and UCSD CTRI, FISP, and AIM pilot grants.

Chapter 5

5 Software Platform for Classification and Anomaly Detection

5.1 Abstract

U-dHRM platform presents a promising molecular approach for a first pass screening technology for sepsis. Our previous work focused on developing a platform for reliable melt curve generation with minimal run-to-run and well-to-well variation. We have shown that the ability to control ramp rates for digital melt curve generation revealed rate dependent melt curves. Here, we propose a framework for melt curve analysis for pathogen profiling. Previous work has used support vector machines to classify bacteria from a pre-defined library of melt curve signatures. However, classification with respect to a pre-defined library may not be enough for clinical decision support. Statistical information is more relevant to clinical decision makers over a hard yes-no decision. There is also a need to identify new organisms that are not a part of our library. To address these challenges, we developed a framework to enable identification of novel melt profiles that are not included in the training set, followed by a classification methodology that also generates a measure for uncertainty using Shannon entropy.

5.2 Introduction

The U-dHRM platform relies on high resolution melt analysis post digital amplification of nucleic acid sequences. In high resolution melt (HRM), a double stranded binding dye is introduced into the sample and heated. As the temperature increases, the double-stranded DNA denatures into single strands, releasing the intercalating dye. This loss in fluorescence with heating is recorded as a function of temperature. This generates a characteristic loss-in-fluorescence curve that is unique to the DNA sequence in question and is then used to fingerprint the sequence. HRM is a quick, cheap and powerful characterization technique that can be used for profiling pathogen [211,212]. However, not much effort has been put into fully automated phenotyping using melt curves [213,224]. Typically, either the melting point (T_m) or difference curve created with respect to a standard template is used for discrimination. However, both approaches have their limitations. A single melt point T_m does not provide sufficient information to discriminate more than a few species. The difference curve, on the other hand, typically relies on temperature shifting and visual inspection at users discretion to account for run-to-run or well-to-well variations. While this may suffice in some experimental and lab settings, it falls short in pathogen identification for clinical settings. Moreover, application of HRM with digital PCR for our platform generates a large number of melt curves. Thus, our platform requires the characterization of over 20,000 curves per sample as individual melt curves are generated for every genome to achieve single genome sensitivity which enables absolute load quantification of DNA in the sample [178,224]. This requires an objective and automated approach to parse individual curve generated by the U-dHRM platform, as subjective methods get too time-consuming and are no longer feasible.

In the previous chapter, we demonstrated optimization of U-dHRM platform to minimize run-to-run and melt-to-melt variation for reliable and repeatable melt curve generation. We demonstrated linearity in heating rate, eliminating any warping in the melt curve along temperature axis. Any offset or shift in the melt curves can now either be corrected using a calibrator sequence or an off the shelf accurate temperature measurement system integrated with our platform. The ability

to precisely control temperature also showed the presence of rate-dependent melt curves. These improvements and novel findings can allow us to develop robust classification algorithm for identification of pathogens using the U-dHRM platform. Here, we present preliminary results to show that classification for bacteria with melt curves similar in shape at a particular ramp rate, can be enhanced by including curves from a different ramp rate.

In addition, previous work has demonstrated the use of SVM to classify melt curves either in small or large reaction format. However, a probabilistic model is needed to identify pathogens that are not present in the library. We explored the use of Gaussian Nave Bayes(NB), multinomial Logistic regression(LR) and Multi-layer Perceptron (MLP). We also explored dynamic time warping as a distance measure for outlier detection. In addition, we investigated Shannon entropy as a measure of uncertainty in the posterior probability. We propose a framework to identify new curves and perform classification along with generating an uncertainty score.

5.3 Results

5.3.1 Ramp rate dependent melt curves for enhanced classification

We generated melt curves from 4 different homogeneous DNA samples at two heat ramp rates of $0.01^{\circ}\text{C}/\text{s}$ and $0.2^{\circ}\text{C}/\text{s}$. Out of the 4 pathogens, two belonged to different subspecies for the same species(Salmonella) an other two were from Acinetobacter and Moraxella.

Classification with supervised learning suggests differential discriminatory power at different melting rates of our long amplicon sequences. The class accuracy for Moraxella was 92% for classification of melt curves generated at $0.01^{\circ}\text{C}/\text{s}$ and 8% of Moraxella curves were misclassified as Acinetobacter (Figure 5.1). This compared to a class accuracy for 98% for Moraxella with melt curves generated at $0.2^{\circ}\text{C}/\text{s}$. For other classes of pathogen, the accuracy was similar at both ramp rates.

The T_m of *Moraxella* and *Acinetobacter* are less than 0.5°C apart. Therefore, the presence of double peaks in the melting curves of these organisms at ramp rate of 0.02C/s provides additional features in comparison to relying on the only the T_m for classification of melt curves generated at 0.01C/s (Figure 5.2).

		Ramp Rate = 0.01C/s				Ramp Rate = 0.2C/s			
True Label	<i>Acinetobacter</i>	98	2			99%	1%		
	<i>Moraxella</i>	8	92			2%	98%		
	<i>Salmonella</i>			100				0	
	Calib				100				0
		<i>Acinetobacter</i>	<i>Moraxella</i>	<i>Salmonella</i>	Calib	<i>Acinetobacter</i>	<i>Moraxella</i>	<i>Salmonella</i>	Calib

Figure 5.1: Difference in classification accuracy. Confusion matrix for classifying melt curves from *Salmonella*, *Acinetobacter* and *Moraxella* and Calibrator sequences generated at (A) ramp rate of 0.01°C/s and (B) 0.2°C/s

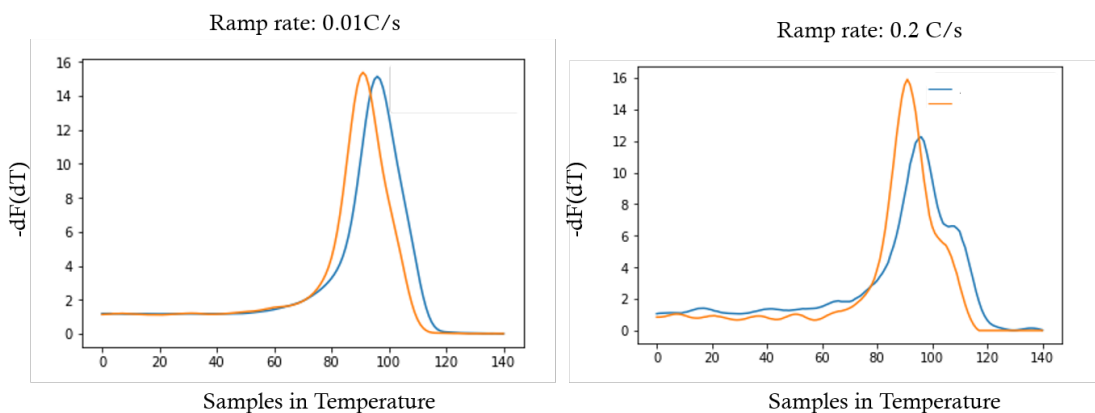


Figure 5.2: Differences in melt curves at different temperature ramp rates. Characteristics curve for *Acinetobacter* and *Moraxella* generated at (A) ramp rate of 0.01°C/s and (B) 0.2°C/s

5.3.2 Framework for Melt Curve Identification and Classification

Here, we propose a framework for anomaly detection using Dynamic Time Warping measure along with a supervised learning model for classification. In addition, Shannon entropy is used as a confidence measure on the prediction.

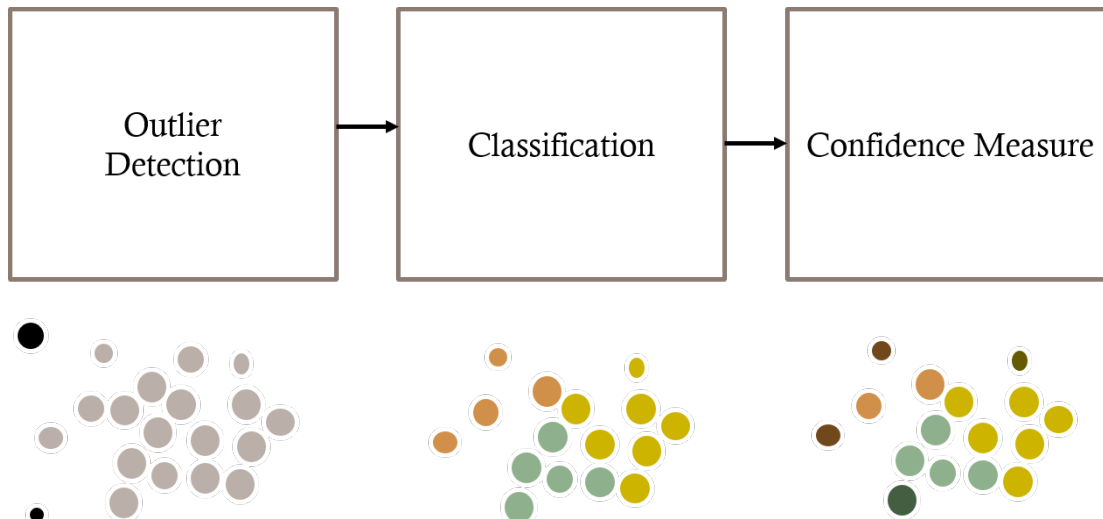


Figure 5.3: Framework for phenotyping using melting curves.

Dynamic Time Warping for Anomaly Detection

Dynamic temperature warping (DTW) as a method to calculate a distance-from-class measure for outlier detection. DTW is typically a measure for estimating the similarity between two temporal sequences. For our system, temperature sequences replace temporal sequences. By sweeping one melt curve over the other, DTW calculates the optimal match between the sequences, by trying to explain any fluctuations in the y-axis of melt curve by warping the temperature axis. We developed a model for the distribution of DTW measure for each class of pathogen on the training set. For each new test data, we calculate the likelihood for belonging to every class. As explained in the methods, if the likelihood probability is near zero across all classes, we label the curves as an outlier. Figure 5.4 shows the empirical CDF calculated for each class along with the estimated cut offs for

DTW ($\mu_c + \tau_c$) that were used for labeling curves as outliers. With this threshold, we were able to correctly identify 80/99 (81%) melt curves belonging a small test data set from a bacterial species (Staphylococcus) noval to our database as anomalies. Remarkably, 1352/1379 (98%) melt curves from Salmonella enterica serovars Typhimurium (not in our library) were not identified as outlier and later identified as either of two Salmonella labels present in our training label but with a high uncertainty score using methods described in the following section.

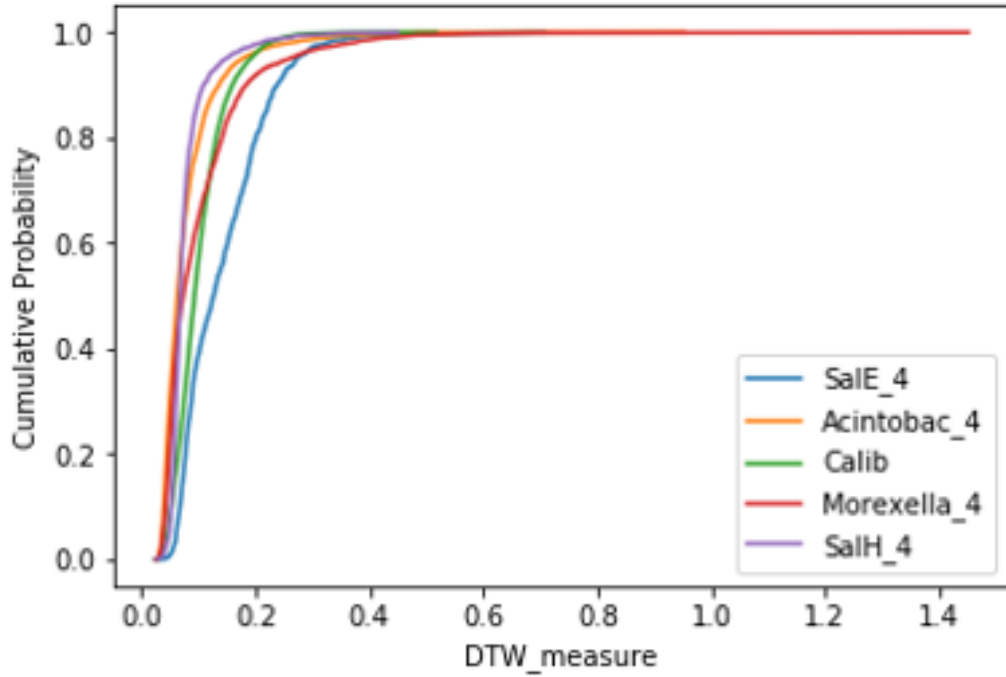


Figure 5.4: Estimated Cumulative density function for Dynamic Time warping measure for all classes

Table 5.1: Cut-offs calculated from statistical model for dynamic time warping to assign outlier

Bacteria	Cut-off Value
SalE_4	0.297476
Acintobac_4	0.217671
Calib	0.210845
Morexella_4	0.314864
SalH_4	0.181002

5.3.3 Classification Algorithm

Data from four bacteria DNA and one synthetic oligo generated at ramp rate of 0.2C/s was used to train the Gaussian NB, NB with Dynamic Time warping, multinomial LR, and MLP for classification. Table 5.2 shows the number of melt curves available per class. Our goal was to classify the bacteria from unknown sample using the posterior probabilities. Figure 5.5 shows the confusion matrices to compare the classification accuracy achieved by the different methods. Both the discriminative models (LR and MLP) outperform the generative models (Gaussian NB and classification with Dynamic Time Warping).

Table 5.2: Data set

Label	Number of curves
Acinetobacter	4095
Moraxella	3382
Calibrator (Synthetic Oligo)	4500
Salmonella enterica serovar Heidelberg	2612
Salmonella enterica serovars Enteritidis	1725

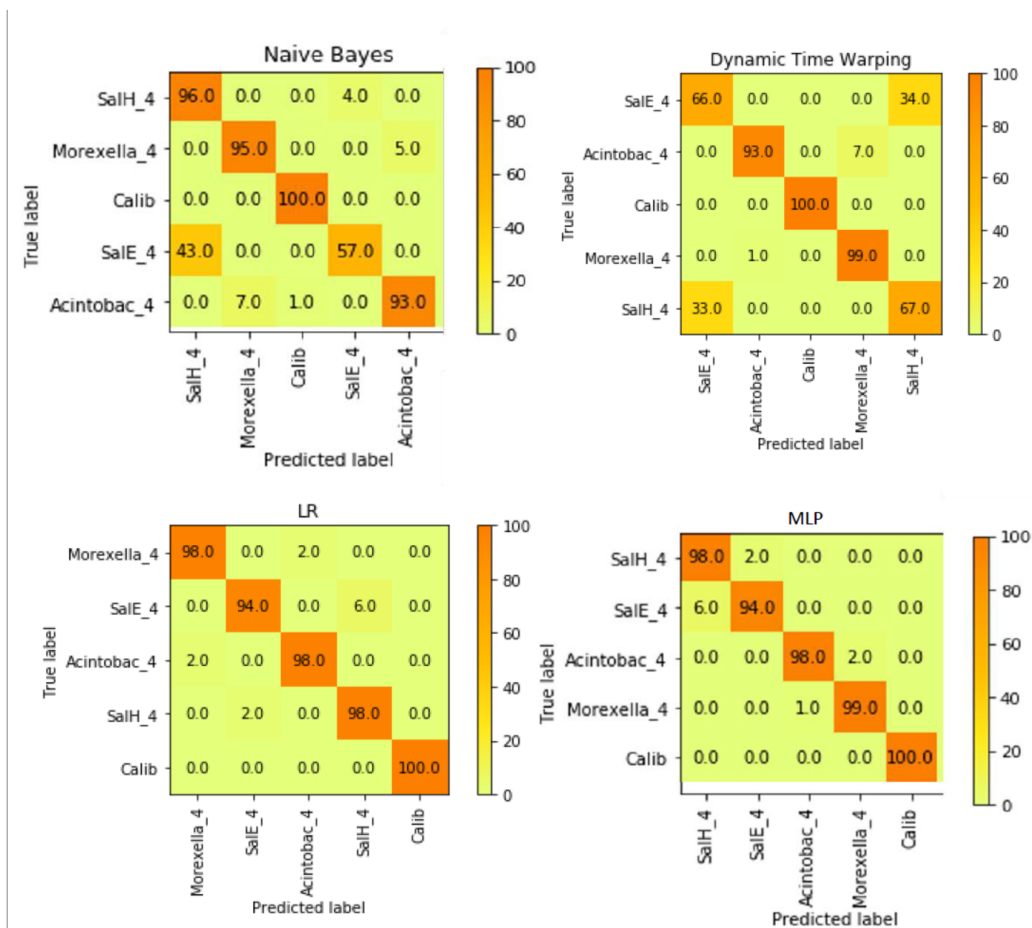


Figure 5.5: Confusion matrix for classifying melt curves from Salmonella, Acinetobacter and Moraxella and Caliberator sequences using (A) Nave Bayes (B) Dynamic Time Warping Metric (C) MLP (D) multinomial LR with 10-fold cross validation.

5.3.4 Uncertainty measure and outlier detection

Shannon entropy

To develop measures for uncertainty in classification, we selected the LR model. We calculated the Shannon entropy across the posterior probabilities as explained in the previous section. Figure 5.6 shows violin plots for the entropy values for each of the class (per row) that were classified incorrectly (Figure 5.6A) and correctly (Fig 5.6B). The misclassified melt curves have a higher entropy in comparison to the correctly classified melt curves. This suggests that Shannon

entropy measure of the posterior probability can be used along with the prediction class as measure of confidence of the classification. Interestingly, the entropy associated with Salmonella is higher. High degree of similarity between the two salmonella subspecies in our database does not allow classification of Salmonella melt curves to either class with high confidence. These preliminary results validate the usefulness of the uncertainty score.

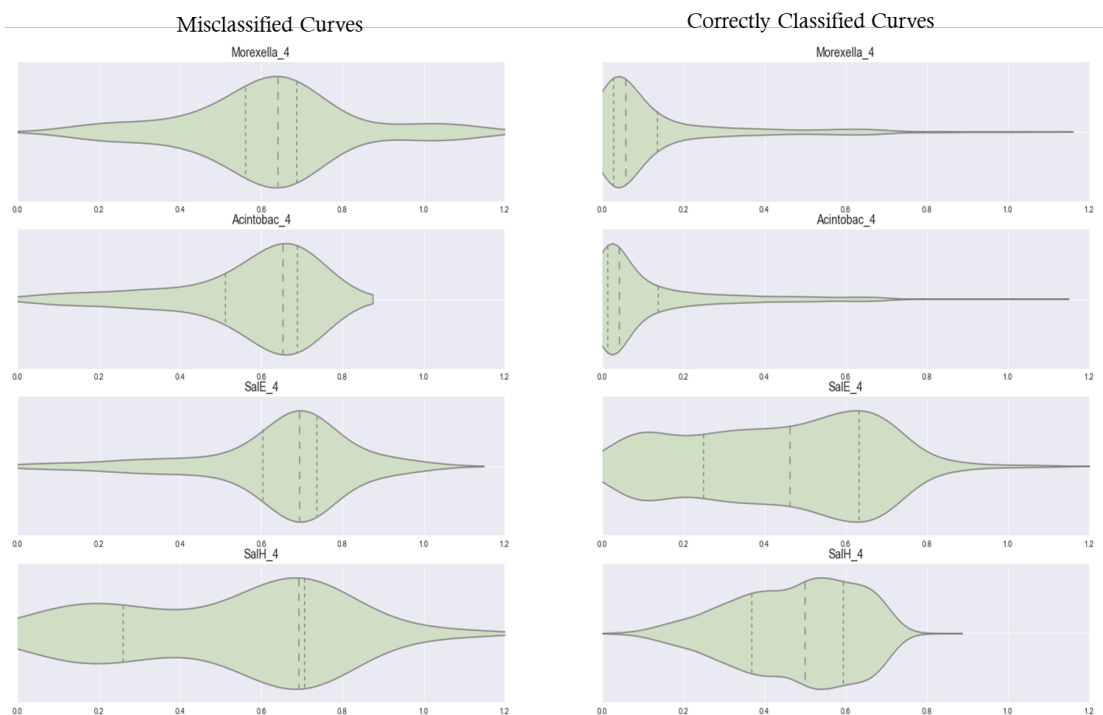


Figure 5.6: Shannon Entropy measure for melt curves that were (left) misclassified (right) classified correctly. The shape of the violin plot represents the probability density of data at different values. The dashed lines signify the lower percentile, median and upper percentile for each plot.

5.4 Materials and Methods

5.4.1 Data Generation and Signal Processing

The U-dHRM platform generates a curve of change in fluorescence versus temperature by sequentially melting conserved regions of the 16S gene at controlled temperatures and measuring the samples fluorescence. Images acquired

while melting the DNA are first aligned using normalized cross correlation (ImageJ Implementation) to remove any shifting throughout the melting process. Then custom software is used to correct salt and pepper noise from the image by applying median filtering. Binary masks are created for tracking the wells across the images in temperature. The mask is used to extract fluorescence data from the image for EvaGreen and ROX channels. The EvaGreen channel tracks the loss in fluorescence due to denaturing of DNA and the ROX channel tracks our control dye. Melt curves are generated by normalizing fluorescence in EvaGreen channel by ROX, followed by taking negative derivative with respect to temperature.

Measures for uncertainty and new species identification

Shannon Entropy

Entropy measures can estimate the amount of information produced. Here, we explore the use of Shannon entropy specified by:

$$H(P) = - \sum_{k=1}^M p_k \log(p_k) \quad (5.1)$$

Where p is the posterior probability estimated using previously defined classification methods. Higher magnitude of Shannon entropy is associated with more uncertainty with the classification decision made. This allows us to find empirical thresholds on the entropy measure to minimize the miss classifications. In other words the framework can abstain from making a decision for any classification with high associated entropy and instead provide information about the classes of pathogen that the curve is closest to.

Dynamic Time Warping(DTW) Measure

DTW is a measure for estimating the similarity between two temporal sequence. By sweeping one melt curve over the other, DTW tries to calculate the optimal match between the sequences, independent of any shifts and non-linearity along the temperature axis under certain constraints. It does so by trying to explain any fluctuations in the y axis of melt curve by warping the temperature axis.

We build a statistical model on the DTW measure for each class to identify melt curves with DTW measures that are unlikely.

For all classes in the training set $c = 1, 2, \dots, M$ we first generate μ_c which is the mean of all x_j in class c . Then we define $d(\mu_c, x_i)$ for all x_i that belong to class c . This is used to estimate the cumulative density function (CDF) for the dynamic time warping measure for each class c . To We try to estimate a τ_c associated with each class c so that:

$$P(X - \mu_c > \tau_c) = 0.03 \quad (5.2)$$

The threshold of 0.03 is empirically selected to minimize and type I and type II errors for all classes. To solve for τ we use the CDF:

$$P(X > \mu_c + \tau_c) = 0.03 \quad (5.3)$$

$$1 - F_x(\mu_c + \tau_c) = 0.03 \quad (5.4)$$

$$F_x(\mu_c + \tau_c) = 0.97 \quad (5.5)$$

$$\tau_c = F_x^{-1}(0.97) - \mu_c \quad (5.6)$$

The τ_c, μ_c is calculated for all classes $c = 1, 2, \dots, M$.

For an unlabeled x_j , $d(\mu_c, x_j)$ is calculated for $c = 1, \dots, M$. The observation is declared as an outlier if $P(X - \mu_c > \tau_c) \leq 0.03$ for all c . This framework labels observations as outliers if it is sufficiently farther way from the distribution mean.

5.5 Discussion

We anticipate the optimal framework will consist of first applying DTW to identify any melt curves that are highly anomalous followed by classification using LR or MLP modeled on our database, then calculation of SE as a confidence measure on the prediction. Previous work has demonstrated the use of OVO SVM. However, absence of a probabilistic model does not allow us to separate a weak yes from a strong yes. Available methods for generating probabilities from SVM, are typically very expensive for a large dataset. Moreover, the probabilities generated by mapping SVM to a probabilistic framework may not correlate with

the classification results. We are not surprised that Naive Bayes doesn't work as well in comparison to Logistic regression and MLP for classification. NB is a generative model that learns a likelihood function based only from the train data of the particular class, blinded to other data. On the other hand, LR is based on a discriminate model which optimizes the weights to be separate all the classes. Moreover, NB assumes independence and calculates the joint probability distribution across all features, where as LR can handle correlation among features. Typically, for a small number of data sets, Naive Bayes is expected to perform well. However, as the size of the training data increases, LR is expected to outperform NB for classification.

In conclusion, we demonstrate a promising framework for automatic anomaly detection and classification with confidence measure for detection and identification of meltcurves.

5.6 Acknowledgements

Chapter 5, in part is currently being prepared for submission for publication of the material. Sinha Mridu, Mack Hannah, Coleman Todd, Stephanie Fraley. The dissertation author was the primary investigator and author of this material.

This research was supported by UCSD FISP, and AIM pilot grants.

Chapter 6

Conclusion

Many advances have been made to improve neonatal care in the last two decades, yet significant gaps remain. A collaborative approach between sciences, engineering, medicine and sociology is needed to identify these gaps and tailor user centered solutions which can be effectively implemented in the clinics. The goal of this PhD was to identify challenges in the clinics pertaining to neonatal care in the first few hours of life and develop solutions that can be integrated into the work flow of providers.

First, careful user centered approach enabled development of decision support tools that can be integrated into the work-flow of community providers. This tool can assist the providers in skill building and supporting them to practice evidence based medicine in caring for infants with birth asphyxia. In this era of digital health, we leveraged computerized decision support to reduce inefficiencies and cost while improving the quality of care provided for a very niche undeserved population. In future, tools such as this can be integrated on to a single platform to enhance usability and encourage collaborative data sharing among providers and policy makers. Second, careful clinical needs assessment, and engineering design spanning across molecular biology, device development, machine learning allowed us to create a platform that can detect and identify pathogen in clinically relevant time-line to facilitate the diagnosis of sepsis and encourage targeted antibiotic treatment. Our hope is that both these platforms can be translated for use in the clinics in the near future.

References

- [1] “Global, regional, and national levels and trends in under-5 mortality between 1990 and 2015, with scenario-based projections to 2030: a systematic analysis by the UN Inter-agency Group for Child Mortality Estimation,” *The Lancet*, vol. 386, pp. 2275–2286, 12 2015.
- [2] J. E. Lawn, S. Cousens, J. Zupan, and Lancet Neonatal Survival Steering Team, “4 million neonatal deaths: When? Where? Why?,” *The Lancet*, vol. 365, pp. 891–900, 3 2005.
- [3] Aap, “Hypothermia and Neonatal Encephalopathy.,” *Pediatrics*, pp. 1146–1149, 2014.
- [4] R. P. Dellinger, M. M. Levy, J. M. Carlet, J. Bion, M. M. Parker, R. Jaeschke, K. Reinhart, D. C. Angus, C. Brun-Buisson, R. Beale, T. Calandra, J.-F. Dhainaut, H. Gerlach, M. Harvey, J. J. Marini, J. Marshall, M. Ranieri, G. Ramsay, J. Sevransky, B. T. Thompson, S. Townsend, J. S. Vender, J. L. Zimmerman, and J.-L. Vincent, “Surviving Sepsis Campaign: international guidelines for management of severe sepsis and septic shock: 2008.,” *Intensive care medicine*, vol. 34, pp. 17–60, 1 2008.
- [5] A. C. Lee, N. Kozuki, H. Blencowe, T. Vos, A. Bahalim, G. L. Darmstadt, S. Niermeyer, M. Ellis, N. J. Robertson, S. Cousens, and J. E. Lawn, “Intrapartum-related neonatal encephalopathy incidence and impairment at regional and global levels for 2010 with trends from 1990,” *Pediatric Research*, vol. 74, pp. 50–72, 12 2013.
- [6] H. B. Sarnat and M. S. Sarnat, “Neonatal encephalopathy following fetal distress. A clinical and electroencephalographic study.,” *Archives of neurology*, vol. 33, pp. 696–705, 10 1976.
- [7] J. J. Volpe, *Neurology of the Newborn E-Book*. Elsevier Health Sciences, 2008.
- [8] J. J. Kurinczuk, M. White-Koning, and N. Badawi, “Epidemiology of neonatal encephalopathy and hypoxicischaemic encephalopathy,” *Early Human Development*, vol. 86, pp. 329–338, 6 2010.

- [9] L. S. de Vries and M. J. Jongmans, “Long-term outcome after neonatal hypoxic-ischaemic encephalopathy,” *Archives of Disease in Childhood - Fetal and Neonatal Edition*, vol. 95, pp. F220–F224, 5 2010.
- [10] F. F. Gonzalez and S. P. Miller, “Does perinatal asphyxia impair cognitive function without cerebral palsy?,” *Archives of Disease in Childhood - Fetal and Neonatal Edition*, vol. 91, pp. F454–F459, 7 2006.
- [11] S. Jacobs, R. Hunt, W. Tarnow-Mordi, T. Inder, and P. Davis, “Cooling for Newborns with Hypoxic Ischaemic Encephalopathy,” *Pediatric Research*, vol. 58, no. 2, pp. 385–385, 2005.
- [12] S. E. Jacobs, M. Berg, R. Hunt, W. O. TarnowMordi, T. E. Inder, and P. G. Davis, “Cooling for newborns with hypoxic ischaemic encephalopathy,” *The Cochrane Library*, 2013.
- [13] B. Kracer, S. R. Hintz, K. P. Van Meurs, and H. C. Lee, “Hypothermia therapy for neonatal hypoxic ischemic encephalopathy in the state of California,” *Journal of Pediatrics*, vol. 165, no. 2, pp. 267–273, 2014.
- [14] J. Tu, J. Profit, K. Melsop, T. Brown, A. Davis, E. Main, and H. Lee, “Relationship of Hospital Staff Coverage and Delivery Room Resuscitation Practices to Birth Asphyxia,” *American Journal of Perinatology*, vol. 34, pp. 259–263, 8 2016.
- [15] R. D. Higgins, T. N. Raju, J. Perlman, D. V. Azzopardi, L. R. Blackmon, R. H. Clark, a. D. Edwards, D. M. Ferriero, P. D. Gluckman, a. J. Gunn, S. E. Jacobs, D. J. Eicher, a. H. Jobe, a. R. Laptook, M. H. LeBlanc, C. Palmer, S. Shankaran, R. F. Soll, a. R. Stark, M. Thoresen, and J. Wyatt, “Hypothermia and perinatal asphyxia: executive summary of the National Institute of Child Health and Human Development workshop,” *J Pediatr*, vol. 148, no. 2, pp. 170–175, 2006.
- [16] J. M. Perlman, “Pathogenesis of hypoxic-ischemic brain injury,” *Journal of Perinatology*, vol. 27, pp. S39–S46, 5 2007.
- [17] A. Lorek, Y. Takei, E. B. Cady, J. S. Wyatt, J. Penrice, A. D. Edwards, D. Peebles, M. Wylezinska, H. Owen-Reece, V. Kirkbride, C. E. Cooper, R. F. Aldridge, S. C. Roth, G. Brown, D. T. Delpy, and E. O. R. Reynolds, “Delayed (Secondary) Cerebral Energy Failure after Acute Hypoxia-Ischemia in the Newborn Piglet: Continuous 48-Hour Studies by Phosphorus Magnetic Resonance Spectroscopy,” *Pediatric Research*, vol. 36, pp. 699–706, 12 1994.
- [18] G. Natarajan, A. Pappas, S. Shankaran, A. R. Laptook, M. Walsh, S. A. McDonald, R. A. Ehrenkranz, J. E. Tyson, R. N. Goldberg, R. Bara, R. D. Higgins, A. Das, and B. Munoz, “Effect of inborn vs. outborn delivery on

- neurodevelopmental outcomes in infants with hypoxic-ischemic encephalopathy: secondary analyses of the NICHD whole-body cooling trial.,” *Pediatric research*, vol. 72, pp. 414–9, 10 2012.
- [19] B. Coburn, A. M. Morris, G. Tomlinson, and A. S. Detsky, “Does this adult patient with suspected bacteremia require blood cultures?,” *JAMA*, vol. 308, pp. 502–11, 8 2012.
- [20] D. W. Bates, E. F. Cook, L. Goldman, and T. H. Lee, “Predicting bacteremia in hospitalized patients. A prospectively validated model.,” *Annals of internal medicine*, vol. 113, pp. 495–500, 10 1990.
- [21] A. Roth, A. E. Wiklund, A. S. Pålsson, E. Z. Melander, M. Wullt, J. Cronqvist, M. Walder, and E. Sturegård, “Reducing blood culture contamination by a simple informational intervention.,” *Journal of clinical microbiology*, vol. 48, pp. 4552–8, 12 2010.
- [22] M. E. Stryjewski, Z. A. Kanafani, V. H. Chu, P. A. Pappas, T. Harding, L. A. Drew, D. K. Benjamin, L. B. Reller, B. A. Lee, G. R. Corey, and V. G. Fowler, “Staphylococcus aureus bacteremia among patients with health care-associated fever.,” *The American journal of medicine*, vol. 122, pp. 281–289, 3 2009.
- [23] S. S. Buehler, B. Madison, S. R. Snyder, J. H. Derzon, N. E. Cornish, M. A. Saubolle, A. S. Weissfeld, M. P. Weinstein, E. B. Liebow, and D. M. Wolk, “Effectiveness of Practices To Increase Timeliness of Providing Targeted Therapy for Inpatients with Bloodstream Infections: a Laboratory Medicine Best Practices Systematic Review and Meta-analysis.,” *Clinical microbiology reviews*, vol. 29, pp. 59–103, 1 2016.
- [24] L. Epstein, R. Dantes, S. Magill, and A. Fiore, “Varying Estimates of Sepsis Mortality Using Death Certificates and Administrative Codes—United States, 1999–2014.,” *MMWR. Morbidity and mortality weekly report*, vol. 65, pp. 342–345, 4 2016.
- [25] M. P. Weinstein, J. R. Murphy, L. B. Reller, and K. A. Lichtenstein, “The clinical significance of positive blood cultures: a comprehensive analysis of 500 episodes of bacteremia and fungemia in adults. II. Clinical observations, with special reference to factors influencing prognosis.,” *Reviews of infectious diseases*, vol. 5, no. 1, pp. 54–70, 1983.
- [26] C. C. Lee, W. J. Lin, H. I. Shih, C. J. Wu, P. L. Chen, H. C. Lee, N. Y. Lee, C. M. Chang, L. R. Wang, and W. C. Ko, “Clinical significance of potential contaminants in blood cultures among patients in a medical center.,” *Journal of microbiology, immunology, and infection = Wei mian yu gan ran za zhi*, vol. 40, pp. 438–444, 10 2007.

- [27] M. P. Weinstein, M. L. Towns, S. M. Quartey, S. Mirrett, L. G. Reimer, G. Parmigiani, and L. B. Reller, "The clinical significance of positive blood cultures in the 1990s: a prospective comprehensive evaluation of the microbiology, epidemiology, and outcome of bacteremia and fungemia in adults.," *Clinical infectious diseases : an official publication of the Infectious Diseases Society of America*, vol. 24, pp. 584–602, 4 1997.
- [28] R. M. Klevens, J. R. Edwards, and R. P. Gaynes, "The impact of antimicrobial-resistant, health care-associated infections on mortality in the United States.," *Clinical infectious diseases : an official publication of the Infectious Diseases Society of America*, vol. 47, pp. 927–930, 10 2008.
- [29] A. Elixhauser, B. Friedman, and E. Stranges, "Septicemia in US hospitals, 2009," *Agency for Healthcare Research and Quality*, vol. 348, no. 62, pp. 1–13, 2011.
- [30] S. A. Novosad, M. R. P. Sapiiano, C. Grigg, J. Lake, M. Robyn, G. Dumyati, C. Felsen, D. Blog, E. Dufort, S. Zansky, K. Wiedeman, L. Avery, R. B. Dantes, J. A. Jernigan, S. S. Magill, A. Fiore, and L. Epstein, "Vital Signs: Epidemiology of Sepsis: Prevalence of Health Care Factors and Opportunities for Prevention.," *MMWR. Morbidity and mortality weekly report*, vol. 65, no. 33, pp. 864–869, 2016.
- [31] C. M. Torio and B. J. Moore, "National Inpatient Hospital Costs: The Most Expensive Conditions by Pay, 2011," vol. 204, pp. 1–15, 2016.
- [32] C. Kiser, U. Nawab, K. McKenna, and Z. H. Aghai, "Role of guidelines on length of therapy in chorioamnionitis and neonatal sepsis.," *Pediatrics*, vol. 133, pp. 992–998, 6 2014.
- [33] S. J. Patel and L. Saiman, "Principles and strategies of antimicrobial stewardship in the neonatal intensive care unit.," *Seminars in perinatology*, vol. 36, pp. 431–436, 12 2012.
- [34] N. Tripathi, C. M. Cotten, and P. B. Smith, "Antibiotic use and misuse in the neonatal intensive care unit.," *Clinics in perinatology*, vol. 39, pp. 61–68, 3 2012.
- [35] S. J. Patel, A. Oshodi, P. Prasad, P. Delamora, E. Larson, T. Zaoutis, D. A. Paul, and L. Saiman, "Antibiotic use in neonatal intensive care units and adherence with Centers for Disease Control and Prevention 12 Step Campaign to Prevent Antimicrobial Resistance.," *The Pediatric infectious disease journal*, vol. 28, pp. 1047–1051, 12 2009.

- [36] J. R. Verani, L. McGee, and S. J. Schrag, "Prevention of perinatal group B streptococcal disease—revised guidelines from CDC, 2010.," *MMWR. Recommendations and reports : Morbidity and mortality weekly report. Recommendations and reports / Centers for Disease Control*, vol. 59, pp. 1–36, 11 2010.
- [37] O. Storro, E. Avershina, and K. Rudi, "Diversity of intestinal microbiota in infancy and the risk of allergic disease in childhood.," *Current opinion in allergy and clinical immunology*, vol. 13, pp. 257–262, 6 2013.
- [38] A. Saari, L. J. Virta, U. Sankilampi, L. Dunkel, and H. Saxen, "Antibiotic exposure in infancy and risk of being overweight in the first 24 months of life.," *Pediatrics*, vol. 135, pp. 617–626, 4 2015.
- [39] R. M. Blackburn, B. Muller-Pebody, T. Planche, A. Johnson, S. Hopkins, M. Sharland, N. Kennea, and P. T. Heath, "Neonatal sepsis—many blood samples, few positive cultures: implications for improving antibiotic prescribing.," 11 2012.
- [40] M. C. Ottolini, K. Lundgren, L. J. Mirkinson, S. Cason, and M. G. Ottolini, "Utility of complete blood count and blood culture screening to diagnose neonatal sepsis in the asymptomatic at risk newborn.," *The Pediatric infectious disease journal*, vol. 22, pp. 430–434, 5 2003.
- [41] E. J. Weston, T. Pondo, M. M. Lewis, P. Martell-Cleary, C. Morin, B. Jewell, P. Daily, M. Apostol, S. Petit, M. Farley, R. Lynfield, A. Reingold, N. I. Hansen, B. J. Stoll, A. L. Shane, E. Zell, and S. J. Schrag, "The burden of invasive early-onset neonatal sepsis in the United States, 2005-2008.," *The Pediatric infectious disease journal*, vol. 30, pp. 937–941, 11 2011.
- [42] K. Edmond and A. Zaidi, "New approaches to preventing, diagnosing, and treating neonatal sepsis," *PLoS Medicine*, vol. 7, no. 3, pp. 1–8, 2010.
- [43] C. Greenwood, A. L. Morrow, A. J. Lagomarcino, M. Altaye, D. H. Taft, Z. Yu, D. S. Newburg, D. V. Ward, and K. R. Schibler, "Early empiric antibiotic use in preterm infants is associated with lower bacterial diversity and higher relative abundance of *Enterobacter*.," *The Journal of pediatrics*, vol. 165, pp. 23–29, 7 2014.
- [44] M. K. Mwaniki, M. Atieno, J. E. Lawn, and C. R. Newton, "Long-term neurodevelopmental outcomes after intrauterine and neonatal insults: a systematic review," *The Lancet*, vol. 379, pp. 445–452, 2 2012.
- [45] S. A. Qazi and B. J. Stoll, "Neonatal sepsis: a major global public health challenge.," *The Pediatric infectious disease journal*, vol. 28, pp. 1–2, 1 2009.

- [46] S. L. Weiss, J. C. Fitzgerald, F. Balamuth, E. R. Alpern, J. Lavelle, M. Chialluti, R. Grundmeier, V. M. Nadkarni, and N. J. Thomas, "Delayed antimicrobial therapy increases mortality and organ dysfunction duration in pediatric sepsis," *Critical Care Medicine*, vol. 42, no. 11, pp. 2409–2417, 2014.
- [47] A. Kumar, P. Ellis, Y. Arabi, D. Roberts, B. Light, J. E. Parrillo, P. Dodek, G. Wood, A. Kumar, D. Simon, C. Peters, M. Ahsan, and D. Chateau, "Initiation of Inappropriate Antimicrobial Therapy Results in a Fivefold Reduction of Survival in Human Septic Shock," *Chest*, vol. 136, pp. 1237–1248, 11 2009.
- [48] W. E. Benitz, "Adjunct laboratory tests in the diagnosis of early-onset neonatal sepsis.," *Clinics in perinatology*, vol. 37, pp. 421–438, 6 2010.
- [49] M. H. Kollef, G. Sherman, S. Ward, and V. J. Fraser, "Inadequate antimicrobial treatment of infections: a risk factor for hospital mortality among critically ill patients.," *Chest*, vol. 115, pp. 462–474, 2 1999.
- [50] J. Garnacho-Montero, J. L. Garcia-Garmendia, A. Barrero-Almodovar, F. J. Jimenez-Jimenez, C. Perez-Paredes, and C. Ortiz-Leyba, "Impact of adequate empirical antibiotic therapy on the outcome of patients admitted to the intensive care unit with sepsis.," *Critical care medicine*, vol. 31, pp. 2742–2751, 12 2003.
- [51] J. Valles, J. Rello, A. Ochagavia, J. Garnacho, and M. A. Alcala, "Community-acquired bloodstream infection in critically ill adult patients: impact of shock and inappropriate antibiotic therapy on survival.," *Chest*, vol. 123, pp. 1615–1624, 5 2003.
- [52] S. M. Blevins and M. S. Bronze, "Robert Koch and the 'golden age' of bacteriology.," *International journal of infectious diseases : IJID : official publication of the International Society for Infectious Diseases*, vol. 14, pp. 744–51, 9 2010.
- [53] B. E. Kreger, D. E. Craven, P. C. Carling, and W. R. McCabe, "Gram-negative bacteremia. III. Reassessment of etiology, epidemiology and ecology in 612 patients.," *The American journal of medicine*, vol. 68, pp. 332–343, 3 1980.
- [54] A. Bacconi, G. S. Richmond, M. A. Baroldi, T. G. Laffler, L. B. Blyn, H. E. Carolan, M. R. Frinder, D. M. Toleno, D. Metzgar, J. R. Gutierrez, C. Masire, M. Rounds, N. J. Kennel, R. E. Rothman, S. Peterson, K. C. Carroll, T. Wakefield, D. J. Ecker, and R. Sampath, "Improved sensitivity for molecular detection of bacterial and Candida infections in blood.," *Journal of clinical microbiology*, vol. 52, pp. 3164–3174, 9 2014.

- [55] O. Opota, K. Jaton, and G. Greub, "Microbial diagnosis of bloodstream infection: Towards molecular diagnosis directly from blood," *Clinical Microbiology and Infection*, vol. 21, no. 4, pp. 323–331, 2015.
- [56] F. R. r. Cockerill, J. W. Wilson, E. A. Vetter, K. M. Goodman, C. A. Torgerson, W. S. Harmsen, C. D. Schleck, D. M. Ilstrup, J. A. n. Washington, and W. R. Wilson, "Optimal testing parameters for blood cultures.," *Clinical infectious diseases : an official publication of the Infectious Diseases Society of America*, vol. 38, pp. 1724–1730, 6 2004.
- [57] S. Riedel, P. Bourbeau, B. Swartz, S. Brecher, K. C. Carroll, P. D. Stamper, W. M. Dunne, T. McCardle, N. Walk, K. Fiebelkorn, D. Sewell, S. S. Richter, S. Beekmann, and G. V. Doern, "Timing of specimen collection for blood cultures from febrile patients with bacteremia.," *Journal of clinical microbiology*, vol. 46, pp. 1381–1385, 4 2008.
- [58] "Department for Evaluations, Standards and Training (DEST)."
- [59] M. L. Towns, W. R. Jarvis, and P.-R. Hsueh, "Guidelines on Blood Cultures," *Journal of Microbiology, Immunology and Infection*, vol. 43, pp. 347–349, 8 2010.
- [60] CLSI document M47-A, "Principles and Procedures for Blood Cultures; Approved Guideline," *Clinical and Laboratory Standards Institute*, no. May, p. Vol.27 No.17, 2007.
- [61] P. Tille, *Bailey & Scott's Diagnostic Microbiology*. St. Louis: Mosby Elsevier, 13th ed., 2015.
- [62] R. A. Garcia, E. D. Spitzer, J. Beaudry, C. Beck, R. Diblasi, M. Gilleeny-Blabac, C. Haugaard, S. Heuschneider, B. P. Kranz, K. McLean, K. L. Morales, S. Owens, M. E. Paciella, and E. Torregrosa, "Multidisciplinary team review of best practices for collection and handling of blood cultures to determine effective interventions for increasing the yield of true-positive bacteremias, reducing contamination, and eliminating false-positive central line-a," *American journal of infection control*, vol. 43, pp. 1222–1237, 11 2015.
- [63] D. M. Ilstrup and J. A. n. Washington, "The importance of volume of blood cultured in the detection of bacteremia and fungemia.," *Diagnostic microbiology and infectious disease*, vol. 1, pp. 107–110, 6 1983.
- [64] T. G. Connell, M. Rele, D. Cowley, J. P. Buttery, and N. Curtis, "How reliable is a negative blood culture result? Volume of blood submitted for culture in routine practice in a children's hospital.," *Pediatrics*, vol. 119, pp. 891–896, 5 2007.

- [65] L. A. Mermel and D. G. Maki, "Detection of bacteremia in adults: consequences of culturing an inadequate volume of blood.," *Annals of internal medicine*, vol. 119, pp. 270–272, 8 1993.
- [66] F. Fenollar and D. Raoult, "Molecular diagnosis of bloodstream infections caused by non-cultivable bacteria," *International Journal of Antimicrobial Agents*, vol. 30, no. SUPPL. 1, pp. 7–15, 2007.
- [67] S. Riedel and K. C. Carroll, "Blood cultures: key elements for best practices and future directions.," *Journal of infection and chemotherapy : official journal of the Japan Society of Chemotherapy*, vol. 16, pp. 301–316, 10 2010.
- [68] S. J. Schrag, E. R. Zell, R. Lynfield, A. Roome, K. E. Arnold, A. S. Craig, L. H. Harrison, A. Reingold, K. Stefonek, G. Smith, M. Gamble, and A. Schuchat, "A population-based comparison of strategies to prevent early-onset group B streptococcal disease in neonates.," *The New England journal of medicine*, vol. 347, pp. 233–239, 7 2002.
- [69] B. J. Stoll, N. I. Hansen, P. J. Sánchez, R. G. Faix, B. B. Poindexter, K. P. Van Meurs, M. J. Bizzarro, R. N. Goldberg, I. D. Frantz, E. C. Hale, S. Shankaran, K. Kennedy, W. A. Carlo, K. L. Watterberg, E. F. Bell, M. C. Walsh, K. Schibler, A. R. Lupton, A. L. Shane, S. J. Schrag, A. Das, R. D. Higgins, and Eunice Kennedy Shriver National Institute of Child Health and Human Development Neonatal Research Network, "Early onset neonatal sepsis: the burden of group B Streptococcal and E. coli disease continues.," *Pediatrics*, vol. 127, pp. 817–26, 5 2011.
- [70] C. M. Cotten, S. Taylor, B. Stoll, R. N. Goldberg, N. I. Hansen, P. J. Sanchez, N. Ambalavanan, and D. K. J. Benjamin, "Prolonged duration of initial empirical antibiotic treatment is associated with increased rates of necrotizing enterocolitis and death for extremely low birth weight infants.," *Pediatrics*, vol. 123, pp. 58–66, 1 2009.
- [71] L. Dethlefsen and D. A. Relman, "Incomplete recovery and individualized responses of the human distal gut microbiota to repeated antibiotic perturbation.," *Proceedings of the National Academy of Sciences of the United States of America*, vol. 108 Suppl, pp. 4554–4561, 3 2011.
- [72] L. G. Bekkeris, J. A. Tworek, M. K. Walsh, and P. N. Valenstein, "Trends in blood culture contamination: a College of American Pathologists Q-Tracks study of 356 institutions.," *Archives of pathology & laboratory medicine*, vol. 129, pp. 1222–1225, 10 2005.
- [73] O. Zwang and R. K. Albert, "Analysis of strategies to improve cost effectiveness of blood cultures.," *Journal of hospital medicine*, vol. 1, pp. 272–276, 9 2006.

- [74] Y. M. Alahmadi, M. A. Aldeyab, J. C. McElnay, M. G. Scott, F. W. Darwish Elhajji, F. A. Magee, M. Dowds, C. Edwards, L. Fullerton, A. Tate, and M. P. Kearney, "Clinical and economic impact of contaminated blood cultures within the hospital setting.," *The Journal of hospital infection*, vol. 77, pp. 233–236, 3 2011.
- [75] G. S. Segal and J. M. Chamberlain, "Resource utilization and contaminated blood cultures in children at risk for occult bacteremia.," *Archives of pediatrics & adolescent medicine*, vol. 154, pp. 469–473, 5 2000.
- [76] L. C. Thuler, M. Jenicek, J. P. Turgeon, M. Rivard, P. Lebel, and M. H. Lebel, "Impact of a false positive blood culture result on the management of febrile children.," *The Pediatric infectious disease journal*, vol. 16, pp. 846–851, 9 1997.
- [77] R. M. Gander, L. Byrd, M. DeCrescenzo, S. Hirany, M. Bowen, and J. Baughman, "Impact of blood cultures drawn by phlebotomy on contamination rates and health care costs in a hospital emergency department.," *Journal of clinical microbiology*, vol. 47, pp. 1021–1024, 4 2009.
- [78] B. C. Pien, P. Sundaram, N. Raoof, S. F. Costa, S. Mirrett, C. W. Woods, L. B. Reller, and M. P. Weinstein, "The clinical and prognostic importance of positive blood cultures in adults.," *The American journal of medicine*, vol. 123, pp. 819–828, 9 2010.
- [79] D. Souvenir, D. E. J. Anderson, S. Palpant, H. Mroch, S. Askin, J. Anderson, J. Claridge, J. Eiland, C. Malone, M. W. Garrison, P. Watson, and D. M. Campbell, "Blood cultures positive for coagulase-negative staphylococci: antisepsis, pseudobacteremia, and therapy of patients.," *Journal of clinical microbiology*, vol. 36, pp. 1923–1926, 7 1998.
- [80] G. N. Forrest, K. Mankes, M. A. Jabra-Rizk, E. Weekes, J. K. Johnson, D. P. Lincalis, and R. A. Venezia, "Peptide nucleic acid fluorescence in situ hybridization-based identification of *Candida albicans* and its impact on mortality and antifungal therapy costs.," *Journal of clinical microbiology*, vol. 44, pp. 3381–3383, 9 2006.
- [81] R. J. Cunney, E. B. McNamara, N. Alansari, B. Loo, and E. G. Smyth, "The impact of blood culture reporting and clinical liaison on the empiric treatment of bacteraemia.," *Journal of clinical pathology*, vol. 50, pp. 1010–1012, 12 1997.
- [82] C. Zhan and M. R. Miller, "Excess length of stay, charges, and mortality attributable to medical injuries during hospitalization.," *JAMA*, vol. 290, pp. 1868–1874, 10 2003.

- [83] W. C. Dunagan, R. S. Woodward, G. Medoff, J. L. r. Gray, E. Casabar, M. D. Smith, C. A. Lawrenz, and E. Spitznagel, "Antimicrobial misuse in patients with positive blood cultures.," *The American journal of medicine*, vol. 87, pp. 253–259, 9 1989.
- [84] C. J. Wusthoff, C. L. Clark, H. C. Glass, T. K. Shimotake, J. Schulman, and S. L. Bonifacio, "Cooling in neonatal hypoxic-ischemic encephalopathy: practices and opinions on minimum standards in the state of California," *Journal of Perinatology*, 10 2017.
- [85] C. Perinatal and Q. Care, "Early Screening and Identification of Candidates for Neonatal Therapeutic Hypothermia Toolkit," no. February, 2015.
- [86] M. M. Searl, L. Borgi, and Z. Chemali, "It is time to talk about people: a human-centered healthcare system.," *Health research policy and systems / BioMed Central*, vol. 8, p. 35, 12 2010.
- [87] S. Michie, M. M. van Stralen, and R. West, "The behaviour change wheel: a new method for characterising and designing behaviour change interventions," *Implementation science*, vol. 6, no. 1, p. 42, 2011.
- [88] S. Mridu, L. Henry, G. Hannah, W. Courtney, L. Shelly, V. Prachi, B. Roger, and Tom K Shimotake, "Web-Based Decision Support Tool to Screen Candidates for Potential Cooling," in *Pediatrics*, 2017.
- [89] A. Gawande, *Checklist Manifesto, The (HB)*. Penguin Books India, 2010.
- [90] C. Longhurst, S. Turner, and A. E. Burgos, "Development of a Web-based Decision Support Tool to Increase Use of Neonatal Hyperbilirubinemia Guidelines," *The Joint Commission Journal on Quality and Patient Safety*, vol. 35, pp. 256–262, 5 2009.
- [91] M. W. Kuzniewicz, E. M. Walsh, S. Li, A. Fischer, and G. J. Escobar, "Development and Implementation of an Early-Onset Sepsis Calculator to Guide Antibiotic Management in Late Preterm and Term Neonates.," *Joint Commission journal on quality and patient safety*, vol. 42, pp. 232–9, 5 2016.
- [92] S. Mehta, A. Joshi, B. Bajuk, N. Badawi, S. McIntyre, and K. Lui, "Eligibility criteria for therapeutic hypothermia: From trials to clinical practice," *Journal of Paediatrics and Child Health*, vol. 53, pp. 295–300, 3 2017.
- [93] A. R. Laptook, S. Shankaran, J. E. Tyson, B. Munoz, E. F. Bell, R. N. Goldberg, N. A. Parikh, N. Ambalavanan, C. Pedroza, A. Pappas, A. Das, A. S. Chaudhary, R. A. Ehrenkranz, A. M. Hensman, K. P. Van Meurs, L. F. Chalak, S. E. G. Hamrick, G. M. Sokol, M. C. Walsh, B. B. Poindexter, R. G. Faix, K. L. Watterberg, I. D. Frantz, R. Guillet, U. Devaskar, W. E. Truog,

- V. Y. Chock, M. H. Wyckoff, E. C. McGowan, D. P. Carlton, H. M. Harmon, J. E. Brumbaugh, C. M. Cotten, P. J. Sánchez, A. M. Hibbs, R. D. Higgins, and Eunice Kennedy Shriver National Institute of Child Health and Human Development Neonatal Research Network, “Effect of Therapeutic Hypothermia Initiated After 6 Hours of Age on Death or Disability Among Newborns With Hypoxic-Ischemic Encephalopathy,” *JAMA*, vol. 318, p. 1550, 10 2017.
- [94] E. Schump, T. Lancaster, D. Sparks, K. Weatherstone, and R. Holcomb, “Achieving Optimal Therapeutic Hypothermia on Transport,” *Advances in Neonatal Care*, vol. 16, pp. E3–E10, 10 2016.
- [95] A. M. Caliendo, D. N. Gilbert, C. C. Ginocchio, K. E. Hanson, L. May, T. C. Quinn, F. C. Tenover, D. Alland, A. J. Blaschke, R. A. Bonomo, K. C. Carroll, M. J. Ferraro, L. R. Hirschhorn, W. P. Joseph, T. Karchmer, A. T. MacIntyre, L. B. Reller, and A. F. Jackson, “Better Tests, Better Care: Improved Diagnostics for Infectious Diseases,” *Clinical Infectious Diseases*, vol. 57, pp. S139–S170, 12 2013.
- [96] C. D. Chin, V. Linder, and S. K. Sia, “Lab-on-a-chip devices for global health: Past studies and future opportunities,” *Lab Chip*, vol. 7, no. 1, pp. 41–57, 2007.
- [97] S. Bhattacharya, A. F. Rosenberg, D. R. Peterson, K. Grzesik, A. M. Baran, J. M. Ashton, S. R. Gill, A. M. Corbett, J. Holden-Wiltse, D. J. Topham, E. E. Walsh, T. J. Mariani, and A. R. Falsey, “Transcriptomic Biomarkers to Discriminate Bacterial from Nonbacterial Infection in Adults Hospitalized with Respiratory Illness,” *Scientific Reports*, vol. 7, p. 6548, 12 2017.
- [98] O. Ramilo, W. Allman, W. Chung, A. Mejias, M. Ardura, C. Glaser, K. M. Wittkowski, B. Piqueras, J. Banchereau, A. K. Palucka, and D. Chaussabel, “Gene expression patterns in blood leukocytes discriminate patients with acute infections,” *Blood*, vol. 109, pp. 2066–77, 3 2007.
- [99] O. Opota, A. Croxatto, G. Prod’hom, and G. Greub, “Blood culture-based diagnosis of bacteraemia: state of the art,” *Clinical Microbiology and Infection*, vol. 21, no. 4, pp. 313–322, 2015.
- [100] A. Kothari, M. Morgan, and D. A. Haake, “Emerging technologies for rapid identification of bloodstream pathogens,” *Clinical infectious diseases : an official publication of the Infectious Diseases Society of America*, vol. 59, pp. 272–278, 7 2014.
- [101] A. Afshari, J. Schrenzel, M. Ieven, S. Harbarth, G. C. Mda, A. Steigerwalt, R. Morey, D. Jackson, R. Davidson, R. Facklam, H. Wissing, A. Hoefft, D. Moore, S. Abbott, J. Janda, C. Whitehouse, K. Carroll, J. Takeda, S. Kamihira, K. Sugahara, S. Asari, M. Murata, Y. Kobayashi, H. Ginba,

- Y. Sumiyama, and M. Kitajima, "Bench-to-bedside review: Rapid molecular diagnostics for bloodstream infection - a new frontier?," *Critical care (London, England)*, vol. 16, no. 3, p. 222, 2012.
- [102] D. J. Ecker, R. Sampath, H. Li, C. Massire, H. E. Matthews, D. Toleno, T. A. Hall, L. B. Blyn, M. W. Eshoo, R. Ranken, S. A. Hofstadler, and Y. W. Tang, "New technology for rapid molecular diagnosis of bloodstream infections," *Expert.Rev.Mol.Diagn.*, vol. 10, no. 1744-8352 (Electronic), pp. 399-415, 2010.
- [103] "IRIDICA Technology."
- [104] E. Jordana-Lluch, M. Giménez, M. Dolores Quesada, B. Rivaya, C. Marcó, M. Jesus Domínguez, F. Arméstar, E. Martró, and V. Ausina, "Evaluation of the broad-range PCR/ESI-MS technology in blood specimens for the molecular diagnosis of bloodstream Infections," *PLoS ONE*, vol. 10, no. 10, pp. 1-13, 2015.
- [105] D. Metzgar, M. W. Frinder, R. E. Rothman, S. Peterson, K. C. Carroll, S. X. Zhang, G. D. Avornu, M. A. Rounds, H. E. Carolan, D. M. Toleno, D. Moore, T. A. Hall, C. Massire, G. S. Richmond, J. R. Gutierrez, R. Sampath, D. J. Ecker, and L. B. Blyn, "The IRIDICA BAC BSI Assay: Rapid, Sensitive and Culture-Independent Identification of Bacteria and Candida in Blood.," *PloS one*, vol. 11, no. 7, p. e0158186, 2016.
- [106] S. Desmet, J. Maertens, K. Bueselinck, and K. Lagrou, "Broad-Range PCR Coupled with Electrospray Ionization Time of Flight Mass Spectrometry for Detection of Bacteremia and Fungemia in Patients with Neutropenic Fever.," *Journal of clinical microbiology*, vol. 54, pp. 2513-20, 10 2016.
- [107] J.-L. Vincent, D. Brealey, N. Libert, N. E. Abidi, M. O'Dwyer, K. Zacharowski, M. Mikaszewska-Sokolewicz, J. Schrenzel, F. Simon, M. Wilks, M. Picard-Maureau, D. B. Chalfin, D. J. Ecker, R. Sampath, M. Singer, and t. R. D. o. I. i. t. C. I. Rapid Diagnosis of Infections in the Critically Ill Team, "Rapid Diagnosis of Infection in the Critically Ill, a Multicenter Study of Molecular Detection in Bloodstream Infections, Pneumonia, and Sterile Site Infections.," *Critical care medicine*, vol. 43, pp. 2283-91, 11 2015.
- [108] J. Dien Bard and E. McElvania TeKippe, "Diagnosis of Bloodstream Infections in Children," *Journal of Clinical Microbiology*, vol. 54, 6 2016.
- [109] "Roche Molecular Diagnostics - IVD Assays and Instruments."

- [110] L. E. Lehmann, K.-P. Hunfeld, T. Emrich, G. Haberhausen, H. Wissing, A. Hoeft, and F. Stüber, “A multiplex real-time PCR assay for rapid detection and differentiation of 25 bacterial and fungal pathogens from whole blood samples,” *Medical Microbiology and Immunology*, vol. 197, pp. 313–324, 9 2008.
- [111] B. Lucignano, S. Ranno, O. Liesenfeld, B. Pizzorno, L. Putignani, P. Bernaschi, and D. Menichella, “Multiplex PCR allows rapid and accurate diagnosis of bloodstream infections in newborns and children with suspected sepsis.,” *Journal of clinical microbiology*, vol. 49, pp. 2252–8, 6 2011.
- [112] P. Dark, B. Blackwood, S. Gates, D. McAuley, G. D. Perkins, R. McMullan, C. Wilson, D. Graham, K. Timms, and G. Warhurst, “Accuracy of LightCycler® SeptiFast for the detection and identification of pathogens in the blood of patients with suspected sepsis: a systematic review and meta-analysis,” *Intensive Care Medicine*, vol. 41, pp. 21–33, 1 2015.
- [113] S.-S. Chang, W.-H. Hsieh, T.-S. Liu, S.-H. Lee, C.-H. Wang, H.-C. Chou, Y. H. Yeo, C.-P. Tseng, and C.-C. Lee, “Multiplex PCR system for rapid detection of pathogens in patients with presumed sepsis - a systemic review and meta-analysis.,” *PloS one*, vol. 8, no. 5, p. e62323, 2013.
- [114] R. F. Louie, Z. Tang, T. E. Albertson, S. Cohen, N. K. Tran, and G. J. Kost, “Multiplex polymerase chain reaction detection enhancement of bacteremia and fungemia*,” *Critical Care Medicine*, vol. 36, pp. 1487–1492, 5 2008.
- [115] N. Mancini, D. Clerici, R. Diotti, M. Perotti, N. Ghidoli, D. De Marco, B. Pizzorno, T. Emrich, R. Burioni, F. Ciceri, and M. Clementi, “Molecular diagnosis of sepsis in neutropenic patients with haematological malignancies,” *Journal of Medical Microbiology*, vol. 57, pp. 601–604, 5 2008.
- [116] A. Vince, S. . Lepej, B. Baršić, D. Dušek, Z. Mitrović, R. Serventi-Seiwerth, and B. Labar, “LightCycler SeptiFast assay as a tool for the rapid diagnosis of sepsis in patients during antimicrobial therapy,” *Journal of medical microbiology*, vol. 57, no. 10, pp. 1306–1307, 2008.
- [117] C. Dierkes, B. Ehrenstein, S. Siebig, H.-J. Linde, U. Reischl, and B. Salzberger, “Clinical impact of a commercially available multiplex PCR system for rapid detection of pathogens in patients with presumed sepsis,” *BMC Infectious Diseases*, vol. 9, p. 126, 12 2009.
- [118] M. von Lilienfeld-Toal, L. E. Lehmann, A. D. Raadts, C. Hahn-Ast, K. S. Orlopp, G. Marklein, I. Purr, G. Cook, A. Hoeft, A. Glasmacher, and F. Stüber, “Utility of a commercially available multiplex real-time PCR assay to detect bacterial and fungal pathogens in febrile neutropenia.,” *Journal of clinical microbiology*, vol. 47, pp. 2405–10, 8 2009.

- [119] S. Varani, M. Stanzani, M. Paolucci, F. Melchionda, G. Castellani, L. Nardi, M. P. Landini, M. Baccarani, A. Pession, and V. Sambri, "Diagnosis of bloodstream infections in immunocompromised patients by real-time PCR," *Journal of Infection*, vol. 58, no. 5, pp. 346–351, 2009.
- [120] H. Westh, G. Lisby, F. Breysse, B. Böddinghaus, M. Chomarat, V. Gant, A. Goglio, A. Raglio, H. Schuster, F. Stuber, H. Wissing, and A. Hoeft, "Multiplex real-time PCR and blood culture for identification of bloodstream pathogens in patients with suspected sepsis," *Clinical Microbiology and Infection*, vol. 15, pp. 544–551, 6 2009.
- [121] M. Avolio, P. Diamante, S. Zamparo, M. L. Modolo, S. Grosso, P. Zigante, N. Tosoni, R. De Rosa, P. Stano, and A. Camporese, "MOLECULAR IDENTIFICATION OF BLOODSTREAM PATHOGENS IN PATIENTS PRESENTING TO THE EMERGENCY DEPARTMENT WITH SUSPECTED SEPSIS," *Shock*, vol. 34, pp. 27–30, 7 2010.
- [122] F. Bloos, F. Hinder, K. Becker, S. Sachse, A. M. Dessap, E. Straube, V. Cattoir, C. Brun-Buisson, K. Reinhart, and G. Peters, "A multicenter trial to compare blood culture with polymerase chain reaction in severe human sepsis," *Intensive care medicine*, vol. 36, no. 2, pp. 241–247, 2010.
- [123] L. E. Lehmann, K.-P. Hunfeld, M. Steinbrucker, V. Brade, M. Book, H. Seifert, T. Bingold, A. Hoeft, H. Wissing, and F. Stüber, "Improved detection of blood stream pathogens by real-time PCR in severe sepsis," *Intensive care medicine*, vol. 36, no. 1, pp. 49–56, 2010.
- [124] D. Maubon, R. Hamidfar-Roy, S. Courby, A. Vesin, M. Maurin, P. Pavese, N. Ravanel, C.-E. Bulabois, J.-P. Brion, H. Pelloux, and J.-F. Timsit, "Therapeutic impact and diagnostic performance of multiplex PCR in patients with malignancies and suspected sepsis," *Journal of Infection*, vol. 61, no. 4, pp. 335–342, 2010.
- [125] H. Obara, M. Tanabe, M. Kitajima, Y. Kitagawa, M. Kitajima, N. Aikawa, S. Hori, N. Hasegawa, Y. Ikeda, S. Okamoto, Y. Kobayashi, M. Murata, J. Takeda, Y. Sakakura, and H. Ginba, "The role of a real-time PCR technology for rapid detection and identification of bacterial and fungal pathogens in whole-blood samples," *Journal of Infection and Chemotherapy*, vol. 17, no. 3, pp. 327–333, 2011.
- [126] B. J. Regueiro, E. Varela-Ledo, L. Martinez-Lamas, J. Rodriguez-Calviño, A. Aguilera, A. Santos, A. Gomez-Tato, and J. Alvarez-Escudero, "Automated Extraction Improves Multiplex Molecular Detection of Infection in Septic Patients," *PLoS ONE*, vol. 5, p. e13387, 10 2010.

- [127] E. L. Tsalik, D. Jones, B. Nicholson, L. Waring, O. Liesenfeld, L. P. Park, S. W. Glickman, L. B. Caram, R. J. Langley, J. C. van Velkinburgh, C. B. Cairns, E. P. Rivers, R. M. Otero, S. F. Kingsmore, T. Lalani, V. G. Fowler, and C. W. Woods, "Multiplex PCR to diagnose bloodstream infections in patients admitted from the emergency department with sepsis.," *Journal of clinical microbiology*, vol. 48, pp. 26–33, 1 2010.
- [128] F. Wallet, S. Nseir, L. Baumann, S. Herwegh, B. Sendid, M. Boulo, M. Roussel-Delvallez, A. Durocher, and R. Courcol, "Preliminary clinical study using a multiplex real-time PCR test for the detection of bacterial and fungal DNA directly in blood," *Clinical Microbiology and Infection*, vol. 16, pp. 774–779, 6 2010.
- [129] K. Yanagihara, Y. Kitagawa, M. Tomonaga, K. Tsukasaki, S. Kohno, M. Seki, H. Sugimoto, T. Shimazu, O. Tasaki, and A. Matsushima, "Evaluation of pathogen detection from clinical samples by real-time polymerase chain reaction using a sepsis pathogen DNA detection kit," *Critical care*, vol. 14, no. 4, p. R159, 2010.
- [130] D. Bravo, J. Blanquer, M. Tormo, G. Aguilar, R. Borrás, C. Solano, M. A. Clari, E. Costa, B. Muñoz-Cobo, M. Argüeso, J. R. Pineda, and D. Navarro, "Diagnostic accuracy and potential clinical value of the LightCycler SeptiFast assay in the management of bloodstream infections occurring in neutropenic and critically ill patients," *International Journal of Infectious Diseases*, vol. 15, pp. e326–e331, 5 2011.
- [131] P. Josefson, K. Strålin, A. Ohlin, T. Ennefors, B. Dragsten, L. Andersson, H. Fredlund, P. Mölling, and P. Olcén, "Evaluation of a commercial multiplex PCR test (SeptiFast) in the etiological diagnosis of community-onset bloodstream infections," *European Journal of Clinical Microbiology & Infectious Diseases*, vol. 30, pp. 1127–1134, 9 2011.
- [132] U. Lodes, B. Bohmeier, H. Lippert, B. König, and F. Meyer, "PCR-based rapid sepsis diagnosis effectively guides clinical treatment in patients with new onset of SIRS," *Langenbeck's Archives of Surgery*, vol. 397, pp. 447–455, 3 2012.
- [133] K. Grif, M. Fille, R. Würzner, G. Weiss, I. Lorenz, G. Gruber, S. Eschertzhuber, D. Nachbaur, C. Lass-Flörl, and D. Orth, "Rapid detection of bloodstream pathogens by real-time PCR in patients with sepsis," *Wiener klinische Wochenschrift*, vol. 124, pp. 266–270, 4 2012.
- [134] M. Guido, M. Quattrocchi, A. Zizza, G. Pasanisi, V. Pavone, G. Lobreglio, G. Gabutti, and M. A. De Donno, "Molecular approaches in the diagnosis of sepsis in neutropenic patients with haematological malignances," *Journal of Preventive Medicine and Hygiene*, vol. 53, 1 2012.

- [135] S. Hettwer, J. Wilhelm, M. Schürmann, H. Ebelt, D. Hammer, M. Amoury, F. Hofmann, A. Oehme, D. Wilhelms, A. Kekulé, T. Klöss, and K. Werdan, “Microbial diagnostics in patients with presumed severe infection in the emergency department,” *Medizinische Klinik - Intensivmedizin und Notfallmedizin*, vol. 107, pp. 53–62, 2 2012.
- [136] M. Mauro, P. Cavalcanti, D. Perugini, A. Noto, D. Sperli, and C. Giraldi, “Diagnostic utility of LightCycler SeptiFast and procalcitonin assays in the diagnosis of bloodstream infection in immunocompromised patients,” *Diagnostic Microbiology and Infectious Disease*, vol. 73, no. 4, pp. 308–311, 2012.
- [137] L. Pasqualini, A. Mencacci, C. Leli, P. Montagna, A. Cardaccia, E. Cenci, I. Montecarlo, M. Pirro, F. di Filippo, E. Cistaro, G. Schillaci, F. Bistoni, and E. Mannarino, “Diagnostic performance of a multiple real-time PCR assay in patients with suspected sepsis hospitalized in an internal medicine ward.,” *Journal of clinical microbiology*, vol. 50, pp. 1285–8, 4 2012.
- [138] P.-M. Rath, F. Saner, A. Paul, N. Lehmann, E. Steinmann, J. Buer, and J. Steinmann, “Multiplex PCR for rapid and improved diagnosis of bloodstream infections in liver transplant recipients.,” *Journal of clinical microbiology*, vol. 50, pp. 2069–71, 6 2012.
- [139] E. Tschiedel, J. Steinmann, J. Buer, J. Onnebrink, U. Felderhoff-Müser, P.-M. Rath, and C. Dohna-Schwake, “Results and Relevance of Molecular Detection of Pathogens by SeptiFast A Retrospective Analysis in 75 Critically Ill Children,” *Klinische Pädiatrie*, vol. 224, pp. 12–16, 1 2012.
- [140] V. Herne, A. Nelovkov, M. Kütt, and M. Ivanova, “Diagnostic performance and therapeutic impact of LightCycler SeptiFast assay in patients with suspected sepsis.,” *European journal of microbiology & immunology*, vol. 3, pp. 68–76, 3 2013.
- [141] E. Leitner, H. H. Kessler, W. Spindelboeck, M. Hoenigl, C. Putz-Bankuti, V. Stadlbauer-Köllner, R. Krause, A. J. Grisold, G. Feierl, and R. E. Stauber, “Comparison of two molecular assays with conventional blood culture for diagnosis of sepsis,” *Journal of Microbiological Methods*, vol. 92, pp. 253–255, 3 2013.
- [142] M. Avolio, P. Diamante, M. L. Modolo, R. De Rosa, P. Stano, and A. Camporese, “Direct Molecular Detection of Pathogens in Blood as Specific Rule-In Diagnostic Biomarker in Patients With Presumed Sepsis,” *Shock*, vol. 42, pp. 86–92, 8 2014.
- [143] E. Burdino, T. Ruggiero, T. Alice, M. G. Milia, G. Gregori, R. Milano, F. Cerutti, F. G. De Rosa, E. Manno, P. Caramello, G. Di Perri, and

- V. Ghisetti, "Combination of conventional blood cultures and the SeptiFast molecular test in patients with suspected sepsis for the identification of bloodstream pathogens," *Diagnostic Microbiology and Infectious Disease*, vol. 79, no. 3, pp. 287–292, 2014.
- [144] J. Ortiz Ibarra, P. Trevino Valdez, E. Valenzuela Mendez, A. Limon Rojas, G. Lara Flores, A. Ceballos Bocanegra, I. Morales Mendez, L. Fernandez Carrocera, E. Covian Molina, and J. Reyna Figueroa, "Evaluation of the Light-Cycler® SeptiFast Test in Newborns With Suspicion of Nosocomial Sepsis.," *Iranian journal of pediatrics*, vol. 25, p. e253, 2 2015.
- [145] S. Stefani, G. Mongelli, M. A. Romeo, C. Denaro, M. Gennaro, and F. Fraggetta, "Added value of multi-pathogen probe-based real-time PCR SeptiFast in the rapid diagnosis of bloodstream infections in patients with bacteraemia," *Journal of Medical Microbiology*, vol. 64, pp. 670–675, 7 2015.
- [146] S. Tafelski, I. Nachtigall, T. Adam, S. Bereswill, J. Faust, A. Tamarkin, T. Trefzer, M. Deja, E. A. Idelevich, K.-D. Wernecke, K. Becker, and C. Spies, "Randomized controlled clinical trial evaluating multiplex polymerase chain reaction for pathogen identification and therapy adaptation in critical care patients with pulmonary or abdominal sepsis," *Journal of International Medical Research*, vol. 43, pp. 364–377, 6 2015.
- [147] F. Dinç, H. Akalin, C. Özakin, M. Sinirtaş, N. Kebabçi, R. Işçimen, N. Kelebek Girgin, and F. Kahveci, "Comparison of blood culture and multiplex real-time PCR for the diagnosis of nosocomial sepsis.," *Minerva anesthesiologica*, vol. 82, pp. 301–9, 3 2016.
- [148] F. Ratzinger, I. Tsirkinidou, H. Haslacher, T. Perkmann, K. G. Schmetterer, D. Mitteregger, A. Makrithathis, and H. Burgmann, "Evaluation of the Septifast MGrade Test on Standard Care WardsA Cohort Study," *PLOS ONE*, vol. 11, p. e0151108, 3 2016.
- [149] B. Suberviola, A. Márquez-López, A. Castellanos-Ortega, C. Fernández-Mazarrasa, M. Santibáñez, and L. M. Martínez, "Microbiological diagnosis of sepsis: polymerase chain reaction system versus blood cultures," *American Journal of Critical Care*, vol. 25, no. 1, pp. 68–75, 2016.
- [150] B. Tröger, C. Härtel, J. Buer, M. Dördelmann, U. Felderhoff-Müser, T. Höhn, N. Hepping, G. Hillebrand, A. Kribs, J. Marissen, D. Olbertz, P.-M. Rath, S. Schmidtke, J. Siegel, E. Herting, W. Göpel, J. Steinmann, and A. Stein, "Clinical Relevance of Pathogens Detected by Multiplex PCR in Blood of Very-Low-Birth Weight Infants with Suspected Sepsis - Multicentre Study of the German Neonatal Network.," *PloS one*, vol. 11, no. 7, p. e0159821, 2016.

- [151] F. Korber, I. Zeller, M. Grünstäudl, B. Willinger, P. Apfalter, A. M. Hirschl, and A. Makristathis, “SeptiFast versus blood culture in clinical routine A report on 3 years experience,” *Wiener klinische Wochenschrift*, pp. 1–8, 2 2017.
- [152] F. Gies, E. Tschiedel, U. Felderhoff-Müser, P.-M. Rath, J. Steinmann, and C. Dohna-Schwake, “Prospective evaluation of SeptiFast Multiplex PCR in children with systemic inflammatory response syndrome under antibiotic treatment,” *BMC Infectious Diseases*, vol. 16, p. 378, 12 2016.
- [153] K. Reinhart, M. Bauer, N. C. Riedemann, and C. S. Hartog, “New approaches to sepsis: molecular diagnostics and biomarkers.,” *Clinical microbiology reviews*, vol. 25, pp. 609–34, 10 2012.
- [154] U. Lodes, F. Meyer, B. König, and H. Lippert, “[Microbiological sepsis screening in surgical ICU patients with the ‘lightCycler’; Septifast test—a pilot study].,” *Zentralblatt für Chirurgie*, vol. 134, pp. 249–53, 6 2009.
- [155] N. Mancini, S. Carletti, N. Ghidoli, P. Cichero, C. M. Ossi, R. Ieri, E. Poli, R. Burioni, and M. Clementi, “Molecular diagnosis of polymicrobial sepsis.,” *Journal of clinical microbiology*, vol. 47, pp. 1274–5, 4 2009.
- [156] G. Vrioni, I. Daniil, M. Drogari-Apiranthitou, M. Kimouli, M. Papadopoulou, and A. Tsakris, “Molecular diagnosis of polymicrobial newborn sepsis by multiplex real-time PCR using a small volume of blood sample,” *Journal of medical microbiology*, vol. 61, no. 8, pp. 1177–1178, 2012.
- [157] A. Fernandez-Cruz, M. Marin, M. Kestler, L. Alcala, M. Rodriguez-Creixems, and E. Bouza, “The Value of Combining Blood Culture and SeptiFast Data for Predicting Complicated Bloodstream Infections Caused by Gram-Positive Bacteria or Candida Species,” *Journal of Clinical Microbiology*, vol. 51, pp. 1130–1136, 4 2013.
- [158] G. Warhurst, S. Maddi, G. Dunn, M. Ghrew, P. Chadwick, P. Alexander, A. Bentley, J. Moore, M. Sharman, G. L. Carlson, D. Young, and P. Dark, “Diagnostic accuracy of SeptiFast multi-pathogen real-time PCR in the setting of suspected healthcare-associated bloodstream infection,” *Intensive Care Medicine*, vol. 41, pp. 86–93, 1 2015.
- [159] “SepsiTest-UMD.”
- [160] H.-P. Horz, S. Scheer, M. E. Vianna, and G. Conrads, “New methods for selective isolation of bacterial DNA from human clinical specimens,” *Anaerobe*, vol. 16, no. 1, pp. 47–53, 2010.

- [161] H. Mühl, A.-J. Kochem, C. Disqué, and S. G. Sakka, "Activity and DNA contamination of commercial polymerase chain reaction reagents for the universal 16S rDNA real-time polymerase chain reaction detection of bacterial pathogens in blood," *Diagnostic Microbiology and Infectious Disease*, vol. 66, no. 1, pp. 41–49, 2010.
- [162] S. G. Sakka, A.-J. Kochem, C. Disqué, and N. Wellinghausen, "Blood Infection Diagnosis by 16S rDNA Broad-Spectrum Polymerase Chain Reaction: The Relationship Between Antibiotic Treatment and Bacterial DNA Load," *Anesthesia & Analgesia*, vol. 109, pp. 1707–1708, 11 2009.
- [163] N. Wellinghausen, A.-J. Kochem, C. Disqué, H. Mühl, S. Gebert, J. Winter, J. Matten, and S. G. Sakka, "Diagnosis of bacteremia in whole-blood samples by use of a commercial universal 16S rRNA gene-based PCR and sequence analysis.," *Journal of clinical microbiology*, vol. 47, pp. 2759–65, 9 2009.
- [164] P. Orszag, C. Disque, S. Keim, M. G. Lorenz, O. Wiesner, J. Hadem, M. Stiesch, A. Haverich, and C. Kuhn, "Monitoring of Patients Supported by Extracorporeal Membrane Oxygenation for Systemic Infections by Broad-Range rRNA Gene PCR Amplification and Sequence Analysis," *Journal of Clinical Microbiology*, vol. 52, pp. 307–311, 1 2014.
- [165] A. E. Nieman, P. H. M. Savelkoul, A. Beishuizen, B. Henrich, B. Lamik, C. R. MacKenzie, D. Kindgen-Milles, A. Helmers, C. Diaz, S. G. Sakka, and R. P. Schade, "A prospective multicenter evaluation of direct molecular detection of blood stream infection from a clinical perspective.," *BMC infectious diseases*, vol. 16, p. 314, 6 2016.
- [166] C. Kühn, C. Disqué, H. Mühl, P. Orszag, M. Stiesch, and A. Haverich, "Evaluation of Commercial Universal rRNA Gene PCR plus Sequencing Tests for Identification of Bacteria and Fungi Associated with Infectious Endocarditis," *Journal of Clinical Microbiology*, vol. 49, no. 8, pp. 2919–2923, 2011.
- [167] Y. Wang, Q. Yang, and Z. Wang, "The evolution of nanopore sequencing," *Frontiers in Genetics*, vol. 5, no. JAN, p. 449, 2015.
- [168] "Oxford Nanopore Technologies 2017."
- [169] K. Schmidt, S. Mwaigwisya, L. C. Crossman, M. Doumith, D. Munroe, C. Pires, A. M. Khan, N. Woodford, N. J. Saunders, J. Wain, J. O'Grady, and D. M. Livermore, "Identification of bacterial pathogens and antimicrobial resistance directly from clinical urines by nanopore-based metagenomic sequencing," *Journal of Antimicrobial Chemotherapy*, p. dkw397, 2016.
- [170] "DNA extraction and library preparation for rapid genus- and species-level identification, with or without PCR."

- [171] J. Quick, P. Ashton, S. Calus, C. Chatt, S. Gossain, J. Hawker, S. Nair, K. Neal, K. Nye, T. Peters, E. D. Pinna, E. Robinson, K. Struthers, M. Webber, A. Catto, T. J. Dallman, P. Hawkey, and N. J. Loman, "Rapid draft sequencing and real-time nanopore sequencing in a hospital outbreak of Salmonella," *Genome Biology*, pp. 1–14, 2015.
- [172] A. Benitez-Paez, K. Portune, and Y. Sanz, "Species-level resolution of 16S rRNA gene amplicons sequenced through MinION™ portable nanopore sequencer," *GigaScience*, vol. 5, p. 4, 2015.
- [173] S. Mitsuhashi, K. Kryukov, S. Nakagawa, J. S. Takeuchi, Y. Shiraishi, K. Asano, and T. Imanishi, "A portable system for metagenomic analyses using nanopore-based sequencer and laptop computers can realize rapid on-site determination of bacterial compositions," *bioRxiv*, 1 2017.
- [174] "BEI Resources Web Portal > Home."
- [175] A. L. Greninger, S. N. Naccache, S. Federman, G. Yu, P. Mbala, V. Bres, D. Stryke, J. Bouquet, S. Somasekar, J. M. Linnen, R. Dodd, P. Mulembakani, B. S. Schneider, J.-J. Muyembe-Tamfum, S. L. Stramer, and C. Y. Chiu, "Rapid metagenomic identification of viral pathogens in clinical samples by real-time nanopore sequencing analysis," *Genome medicine*, vol. 7, no. 1, p. 99, 2015.
- [176] P. M. Ashton, S. Nair, T. Dallman, S. Rubino, W. Rabsch, S. Mwaigwisya, J. Wain, and J. O'Grady, "MinION nanopore sequencing identifies the position and structure of a bacterial antibiotic resistance island," *Nat Biotech*, vol. 33, pp. 296–300, 3 2015.
- [177] P. Bradley, N. C. Gordon, T. M. Walker, L. Dunn, S. Heys, B. Huang, S. Earle, L. J. Pankhurst, L. Anson, M. de Cesare, P. Piazza, A. A. Votintseva, T. Golubchik, D. J. Wilson, D. H. Wyllie, R. Diel, S. Niemann, S. Feuerriegel, T. A. Kohl, N. Ismail, S. V. Omar, E. G. Smith, D. Buck, G. McVean, A. S. Walker, T. Peto, D. Crook, and Z. Iqbal, "Rapid antibiotic resistance predictions from genome sequence data for *S. aureus* and *M. tuberculosis*," *bioRxiv*, vol. 6, p. 018564, 2015.
- [178] S. I. Fraley, J. Hardick, B. Jo Masek, P. Athamanolap, R. E. Rothman, C. A. Gaydos, K. C. Carroll, T. Wakefield, T.-H. T.-H. H. Wang, S. Yang, B. J. Masek, P. Athamanolap, R. E. Rothman, C. A. Gaydos, K. C. Carroll, T. Wakefield, T.-H. T.-H. H. Wang, and S. Yang, "Universal digital high-resolution melt: a novel approach to broad-based profiling of heterogeneous biological samples," *Nucleic Acids Research*, vol. 44, p. 508, 1 2016.
- [179] D. O. Velez, H. Mack, J. Jupe, S. Hawker, N. Kulkarni, B. Hedayatnia, Y. Zhang, S. Lawrence, and S. I. Fraley, "Massively parallel digital high

- resolution melt for rapid and absolutely quantitative sequence profiling,” *Scientific Reports*, vol. 7, p. 42326, 2 2017.
- [180] M. Erali, R. Palais, and C. Wittwer, “SNP genotyping by unlabeled probe melting analysis,” *Methods in Molecular Biology (Clifton, N.J.)*, vol. 429, pp. 199–206, 2008.
- [181] M. Erali, K. V. Voelkerding, and C. T. Wittwer, “High resolution melting applications for clinical laboratory medicine.,” *Experimental and molecular pathology*, vol. 85, pp. 50–58, 8 2008.
- [182] C. N. Gundry, J. G. Vandersteen, G. H. Reed, R. J. Pryor, J. Chen, and C. T. Wittwer, “Amplicon melting analysis with labeled primers: a closed-tube method for differentiating homozygotes and heterozygotes.,” *Clinical chemistry*, vol. 49, pp. 396–406, 3 2003.
- [183] Z. Dwight, R. Palais, and C. T. Wittwer, “uMELT: prediction of high-resolution melting curves and dynamic melting profiles of PCR products in a rich web application,” vol. 27, pp. 1019–1020, 4 2011.
- [184] S. D. Vernon, S. K. Shukla, J. Conradt, E. R. Unger, and W. C. Reeves, “Analysis of 16S rRNA gene sequences and circulating cell-free DNA from plasma of chronic fatigue syndrome and non-fatigued subjects,” *BMC microbiology*, vol. 2, no. 1, p. 39, 2002.
- [185] I. Ziegler, P. Josefson, P. Olcén, P. Mölling, and K. Strålin, “Quantitative data from the SeptiFast real-time PCR is associated with disease severity in patients with sepsis,” *BMC infectious diseases*, vol. 14, no. 1, p. 155, 2014.
- [186] Y. Reers, E. A. Idelevich, H. Pätkau, M. C. Sauerland, S. Tafelski, I. Nachtigall, W. E. Berdel, G. Peters, G. Silling, and K. Becker, “Multiplex PCR assay underreports true bloodstream infections with coagulase-negative staphylococci in hematological patients with febrile neutropenia,” *Diagnostic Microbiology and Infectious Disease*, vol. 85, no. 4, pp. 413–415, 2016.
- [187] P. Rogina, M. Skvarc, D. Stubljär, R. Kofol, and A. Kaasch, “Diagnostic utility of broad range bacterial 16S rRNA gene PCR with degradation of human and free bacterial DNA in bloodstream infection is more sensitive than an in-house developed PCR without degradation of human and free bacterial DNA.,” *Mediators of inflammation*, vol. 2014, p. 108592, 2014.
- [188] D. Mihajlovic, S. Brkic, A. Uvelin, B. Draskovic, and V. Vrsajkov, “Use of presepsin and procalcitonin for prediction of SeptiFast results in critically ill patients,” *Journal of Critical Care*, vol. 40, pp. 197–201, 8 2017.

- [189] A. J. M. Loonen, C. P. C. de Jager, J. Tosserams, R. Kusters, M. Hilbink, P. C. Wever, and A. J. C. van den Brule, “Biomarkers and Molecular Analysis to Improve Bloodstream Infection Diagnostics in an Emergency Care Unit,” *PLoS ONE*, vol. 9, p. e87315, 1 2014.
- [190] S. I. Fraley, J. Hardick, B. Jo Masek, P. Athamanolap, R. E. Rothman, C. A. Gaydos, K. C. Carroll, T. Wakefield, T.-H. Wang, and S. Yang, “Universal digital high-resolution melt: a novel approach to broad-based profiling of heterogeneous biological samples,” *Nucleic Acids Research*, vol. 41, pp. e175–e175, 10 2013.
- [191] J. Schreiber, A. Nierhaus, S. Braune, G. de Heer, and S. Kluge, “Comparison of three different commercial PCR assays for the detection of pathogens in critically ill sepsis patients,” *Medizinische Klinik - Intensivmedizin und Notfallmedizin*, vol. 108, pp. 311–318, 5 2013.
- [192] I. G. Wilson, “Inhibition and facilitation of nucleic acid amplification.,” *Applied and environmental microbiology*, vol. 63, pp. 3741–51, 10 1997.
- [193] P. Morata, M. I. Queipo-Ortuño, and J. de Dios Colmenero, “Strategy for optimizing DNA amplification in a peripheral blood PCR assay used for diagnosis of human brucellosis.,” *Journal of clinical microbiology*, vol. 36, pp. 2443–6, 9 1998.
- [194] “Immunexpress Inc..”
- [195] L. Mchugh, T. A. Seldon, R. A. Brandon, J. T. Kirk, A. Rapisarda, A. J. Sutherland, J. J. Presneill, D. J. Venter, J. Lipman, M. R. Thomas, P. M. C. K. Klouwenberg, and L. Van, “RESEARCH ARTICLE A Molecular Host Response Assay to Discriminate Between Sepsis and Infection- Negative Systemic Inflammation in Critically Ill Patients : Discovery and Validation in Independent Cohorts,” no. 3, pp. 1–35, 2015.
- [196] J. J. Zimmerman, E. Sullivan, T. D. Yager, C. Cheng, L. Permut, S. Cermelli, L. Mchugh, D. Sampson, T. Seldon, R. B. Brandon, and R. A. Brandon, “Diagnostic Accuracy of a Host Gene Expression Signature That Discriminates Clinical Severe Sepsis Syndrome and Infection-Negative Systemic Inflammation Among Critically Ill Children,” *Critical Care Medicine*, vol. 45, no. 4, 2017.
- [197] J. Zimmerman, E. Sullivan, D. Sampson, L. McHugh, T. Yager, and T. Seldon, “SENSITIVE AND SPECIFIC DIAGNOSIS OF SEPSIS IN CRITICALLY ILL CHILDREN UTILIZING HOST GENE EXPRESSION,” *Critical Care Medicine*, vol. 43, p. 258, 12 2015.

- [198] R. Miller, B. Lopansri, L. McHugh, A. Rapisarda, T. Seldon, and J. Burke, "VALIDATION OF A NOVEL HOST RESPONSE ASSAY TO DISTINGUISH SIRS AND SEPSIS IN CRITICALLY ILL PATIENTS," *Critical Care Medicine*, vol. 43, p. 252, 12 2015.
- [199] D.-K. Kang, M. M. Ali, K. Zhang, S. S. Huang, E. Peterson, M. a. Digman, E. Gratton, and W. Zhao, "Rapid detection of single bacteria in unprocessed blood using Integrated Comprehensive Droplet Digital Detection.," *Nature communications*, vol. 5, p. 5427, 2014.
- [200] "UC Irvine News: November 13, 2014."
- [201] "Medical Predictive Science Corporation (MPSC)."
- [202] J. R. Moorman, W. A. Carlo, J. Kattwinkel, R. L. Schelonka, P. J. Porcelli, C. T. Navarrete, E. Bancalari, J. L. Aschner, M. W. Walker, J. A. Perez, C. Palmer, G. J. Stukenborg, D. E. Lake, and T. M. OShea, "Mortality reduction by heart rate characteristic monitoring in very low birth weight neonates: a randomized trial," *The Journal of pediatrics*, vol. 159, pp. 900–906, 12 2011.
- [203] B. A. Sullivan, S. M. Grice, D. E. Lake, J. R. Moorman, and K. D. Fairchild, "INFECTION AND OTHER CLINICAL CORRELATES OF ABNORMAL HEART RATE CHARACTERISTICS IN PRETERM INFANTS," *The Journal of pediatrics*, vol. 164, pp. 775–780, 4 2014.
- [204] S. A. Coggins, J.-H. Weitkamp, L. Grunwald, A. R. Stark, J. Reese, W. Walsh, and J. L. Wynn, "Heart rate characteristic index monitoring for bloodstream infection in an NICU: a 3-year experience.," *Archives of disease in childhood. Fetal and neonatal edition*, vol. 101, pp. 329–32, 7 2016.
- [205] K. Wang, V. Bhandari, S. Chepustanova, G. Huber, S. O'Hara, C. S. O'Hern, M. D. Shattuck, and M. Kirby, "Which biomarkers reveal neonatal sepsis?," *PloS one*, vol. 8, no. 12, p. e82700, 2013.
- [206] S. Mani, A. Ozdas, C. Aliferis, H. A. Varol, Q. Chen, R. Carnevale, Y. Chen, J. Romano-Keeler, H. Nian, and J.-H. Weitkamp, "Medical decision support using machine learning for early detection of late-onset neonatal sepsis.," *Journal of the American Medical Informatics Association : JAMIA*, vol. 21, no. 2, pp. 326–336, 2014.
- [207] K. E. Henry, D. N. Hager, P. J. Pronovost, and S. Saria, "A targeted real-time early warning score (TREWScore) for septic shock.," *Science translational medicine*, vol. 7, no. 299, p. 299ra122, 2015.

- [208] J. Kwong, N. McCallum, V. Sintchenko, and B. Howden, "Whole genome sequencing in clinical and public health microbiology," *Pathology*, vol. 47, pp. 199–210, 4 2015.
- [209] R. H. Deurenberg, E. Bathoorn, M. A. Chlebowicz, N. Couto, M. Ferdous, S. García-Cobos, A. M. Kooistra-Smid, E. C. Raangs, S. Rosema, A. C. Veloo, K. Zhou, A. W. Friedrich, and J. W. Rossen, "Application of next generation sequencing in clinical microbiology and infection prevention," *Journal of Biotechnology*, vol. 243, pp. 16–24, 2 2017.
- [210] S. J. Salter, M. J. Cox, E. M. Turek, S. T. Calus, W. O. Cookson, M. F. Moffatt, P. Turner, J. Parkhill, N. J. Loman, and A. W. Walker, "Reagent and laboratory contamination can critically impact sequence-based microbiome analyses," *BMC Biology*, 2014.
- [211] G. H. Reed and C. T. Wittwer, "Sensitivity and Specificity of Single-Nucleotide Polymorphism Scanning by High-Resolution Melting Analysis," *Clinical Chemistry*, vol. 50, no. 10, 2004.
- [212] M. Liew, R. Pryor, R. Palais, C. Meadows, M. Erali, E. Lyon, and C. Wittwer, "Genotyping of Single-Nucleotide Polymorphisms by High-Resolution Melting of Small Amplicons," *Clinical Chemistry*, vol. 50, no. 7, 2004.
- [213] C. T. Wittwer, "High-resolution DNA melting analysis: advancements and limitations," *Human Mutation*, vol. 30, pp. 857–859, 6 2009.
- [214] I. L. M. Candiloro, T. Mikeska, P. Hokland, and A. Dobrovic, "Rapid analysis of heterogeneously methylated DNA using digital methylation-sensitive high resolution melting: application to the CDKN2B (p15) gene," *Epigenetics & Chromatin*, vol. 1, p. 7, 2008.
- [215] A. Y. Golovina, M. M. Dzama, K. S. Petriukov, T. S. Zatsepin, P. V. Sergiev, A. A. Bogdanov, and O. A. Dontsova, "Method for site-specific detection of m6A nucleoside presence in RNA based on high-resolution melting (HRM) analysis," *Nucleic Acids Research*, vol. 42, pp. e27–e27, 2 2014.
- [216] H. Zou, W. R. Taylor, J. J. Harrington, F. T. N. Hussain, X. Cao, C. L. Loprinzi, T. R. Levine, D. K. Rex, D. Ahnen, K. L. Knigge, P. Lance, X. Jiang, D. I. Smith, and D. A. Ahlquist, "High Detection Rates of Colorectal Neoplasia by Stool DNA Testing With a Novel Digital Melt Curve Assay," *Gastroenterology*, vol. 136, no. 2, pp. 459–470, 2009.
- [217] C. J. Wienken, P. Baaske, S. Duhr, and D. Braun, "Thermophoretic melting curves quantify the conformation and stability of RNA and DNA," *Nucleic Acids Research*, vol. 39, pp. e52–e52, 4 2011.

- [218] S. Yang, P. Ramachandran, R. Rothman, Y.-H. Hsieh, A. Hardick, H. Won, A. Kecojevic, J. Jackman, and C. Gaydos, "Rapid identification of bioterror and other clinically relevant bacterial species by use of universal PCR coupled with high-resolution melting analysis.," *Journal of clinical microbiology*, vol. 47, pp. 2252–5, 7 2009.
- [219] H. Won, R. Rothman, P. Ramachandran, Y.-H. Hsieh, A. Kecojevic, K. C. Carroll, D. Aird, C. Gaydos, and S. Yang, "Rapid Identification of Bacterial Pathogens in Positive Blood Culture Bottles by Use of a Broad-Based PCR Assay Coupled with High-Resolution Melt Analysis," *Journal of Clinical Microbiology*, vol. 48, pp. 3410–3413, 9 2010.
- [220] S. Y. C. Tong and P. M. Giffard, "Microbiological applications of high-resolution melting analysis.," *Journal of clinical microbiology*, vol. 50, pp. 3418–21, 11 2012.
- [221] S. O. Sundberg, C. T. Wittwer, R. M. Howell, J. Huuskonen, R. J. Pryor, J. S. Farrar, H. M. Stiles, R. A. Palais, and I. T. Knight, "Microfluidic Genotyping by Rapid Serial PCR and High-Speed Melting Analysis," *Clinical Chemistry*, vol. 60, pp. 1306–1313, 10 2014.
- [222] J.-B. Fan, M. S. Chee, and K. L. Gunderson, "Highly parallel genomic assays," *Nature Reviews Genetics*, vol. 7, pp. 632–644, 8 2006.
- [223] R. H. Vossen, E. Aten, A. Roos, and J. T. den Dunnen, "High-Resolution Melting Analysis (HRMA)-More than just sequence variant screening," *Human Mutation*, vol. 30, pp. 860–866, 6 2009.
- [224] S. I. Fraley, P. Athamanolap, B. J. Masek, J. Hardick, K. C. Carroll, Y.-H. Hsieh, R. E. Rothman, C. A. Gaydos, T.-H. Wang, and S. Yang, "Nested Machine Learning Facilitates Increased Sequence Content for Large-Scale Automated High Resolution Melt Genotyping," *Scientific Reports*, vol. 6, p. 19218, 2016.
- [225] P. Athamanolap, V. Parekh, S. I. Fraley, V. Agarwal, D. J. Shin, M. A. Jacobs, T.-H. Wang, and S. Yang, "Trainable High Resolution Melt Curve Machine Learning Classifier for Large-Scale Reliable Genotyping of Sequence Variants," *PLOS ONE*, vol. 9, no. 10, p. e109094, 2014.
- [226] M. Baker, "Digital PCR hits its stride," *Nat Meth*, vol. 9, pp. 541–544, 6 2012.
- [227] R. H. Sedlak and K. R. Jerome, "Viral diagnostics in the era of digital polymerase chain reaction.," *Diagnostic microbiology and infectious disease*, vol. 75, pp. 1–4, 1 2013.

- [228] M. Li, L. Zhou, R. A. Palais, and C. T. Wittwer, "Genotyping Accuracy of High-Resolution DNA Melting Instruments," *Clinical Chemistry*, vol. 60, no. 6, 2014.
- [229] M. G. Herrmann, J. D. Durtschi, C. T. Wittwer, and K. V. Voelkerding, "Expanded Instrument Comparison of Amplicon DNA Melting Analysis for Mutation Scanning and Genotyping," *Clinical Chemistry*, 2007.
- [230] J. Montgomery, C. T. Wittwer, R. Palais, and L. Zhou, "Simultaneous mutation scanning and genotyping by high-resolution DNA melting analysis," *Nature protocols*, vol. 2, no. 1, p. 59, 2007.
- [231] C. N. Gundry, S. F. Dobrowolski, Y. R. Martin, T. C. Robbins, L. M. Nay, N. Boyd, T. Coyne, M. D. Wall, C. T. Wittwer, and D. H.-F. Teng, "Base-pair neutral homozygotes can be discriminated by calibrated high-resolution melting of small amplicons," *Nucleic Acids Research*, vol. 36, pp. 3401–3408, 4 2008.
- [232] A. Panjkovich and F. Melo, "Comparison of different melting temperature calculation methods for short DNA sequences," *Bioinformatics*, vol. 21, pp. 711–722, 3 2005.
- [233] C. Schildkraut and S. Lifson, "Dependence of the melting temperature of DNA on salt concentration," *Biopolymers*, vol. 3, no. 2, pp. 195–208, 1965.
- [234] N. von Ahsen, C. T. Wittwer, and E. Schütz, "Oligonucleotide Melting Temperatures under PCR Conditions: Nearest-Neighbor Corrections for Mg²⁺, Deoxynucleotide Triphosphate, and Dimethyl Sulfoxide Concentrations with Comparison to Alternative Empirical Formulas," *Clinical Chemistry*, vol. 47, no. 11, 2001.
- [235] C. N. Gundry, J. G. Vandersteen, G. H. Reed, R. J. Pryor, J. Chen, and C. T. Wittwer, "No Title," vol. 49, pp. 396–406, 3 2003.
- [236] J. G. Wetmur, "DNA Probes: Applications of the Principles of Nucleic Acid Hybridization," *Critical Reviews in Biochemistry and Molecular Biology*, vol. 26, pp. 227–259, 1 1991.
- [237] F. Mao, W.-Y. Leung, and X. Xin, "Characterization of EvaGreen and the implication of its physicochemical properties for qPCR applications," *BMC biotechnology*, vol. 7, p. 76, 11 2007.
- [238] M. W. Pfaffl, J. Vandesompele, and M. Kubista, "Data analysis software," *Real-time PCR: current technology and applications*. Caister Academic Press Norfolk, UK, pp. 65–83, 2009.

- [239] T. E. Ouldridge, P. Sulc, F. Romano, J. P. K. Doye, and A. A. Louis, “DNA hybridization kinetics: zippering, internal displacement and sequence dependence.” *Nucleic acids research*, vol. 41, pp. 8886–95, 10 2013.